

An eight-state molecular sequential switch featuring a dual single-bond rotation photoreaction

Aaron Gerwien,[§] Benjamin Jehle,[§] Marvin Irmeler,[§] Peter Mayer,[§] Henry Dube^{†}*

[§]Ludwig-Maximilians Universität München, Department of Chemistry and Center for Integrated Protein Science CIPSM, Butenandtstr. 5–13, 81377 Munich, Germany

[†]Friedrich-Alexander Universität Erlangen-Nürnberg, Department of Chemistry and Pharmacy, Nikolaus-Fiebiger-Str. 10, 91058 Erlangen, Germany

* E-mail: henry.dube@fau.de

Supporting Information

Table of contents

Experimental Section.....	3
Synthesis	3
General experimental	3
Synthesis of HTI 1	5
Determination of constitution and conformation in the crystalline state and in solution.....	12
Physical and photophysical properties	22
Thermal atropisomerizations <i>rac</i> -A to <i>rac</i> -B and <i>rac</i> -D to <i>rac</i> -C.....	22
Molar extinction coefficients.....	28
Photoconversion of <i>rac</i> -A, <i>rac</i> -B, <i>rac</i> -C, and <i>rac</i> -D followed by NMR-spectroscopy.....	30
Photoconversion of <i>rac</i> -B, <i>rac</i> -C, and <i>rac</i> -D determined by quantum yield measurements	33
Photo and thermal conversions of the enantiomers determined by chiral HPLC and Markov matrix analysis.....	37
Cycle processes in the photoisomerization of HTI 1	59
NMR-Spectra.....	63
Crystal structure analysis	68
Calculated Ground State Energy Profile of Compound 1	72
Calculated Ground state geometries - xyz coordinates	76
References	88

Experimental Section

Synthesis

General experimental

Reagents and solvents were obtained from *abcr*, *Acros*, *Fluka*, *Merck*, *Sigma-Aldrich* or *TCl* in the qualities *puriss.*, *p.a.*, or *purum* and used as received. Technical solvents were distilled before use for column chromatography and extraction on a rotary evaporator (*Heidolph Hei-VAP Value*, *vacuubrand CVC 3000*). Reactions were monitored on *Merck Silica 60 F254* TLC plates. Detection was done by irradiation with UV light (254 nm or 366 nm).

Flash column chromatography (FCC) was performed with silica gel 60 (*Merck*, particle size 0.063- 0.200 mm) and distilled technical solvents.

¹H NMR and ¹³C NMR spectra were measured on a *Varian Mercury 200 VX*, *Varian 300*, *Inova 400*, *Varian 600 NMR* or *Bruker Avance III HD 800 MHz* spectrometer at different indicated temperatures. Deuterated solvents were obtained from *Cambridge Isotope Laboratories* or *Eurisotop* and used without further purification. Chemical shifts (δ) are given relative to tetramethylsilane as external standard. Residual solvent signals in the ¹H and ¹³C NMR spectra were used as internal reference. For ¹H NMR: CDCl₃ = 7.26 ppm, CD₂Cl₂ = 5.32 ppm, toluene-*d*₈ = 2.08 ppm, MeCN-*d*₃ = 1.94 ppm. For ¹³C NMR: CDCl₃ = 77.16 ppm, CD₂Cl₂ = 53.84 ppm, toluene-*d*₈ = 20.43, MeCN-*d*₃ = 118.26 ppm. The resonance multiplicity is indicated as *s* (singlet), *d* (doublet), *t* (triplet), *q* (quartet) and *m* (multiplet). The chemical shifts are given in parts per million (ppm) on the delta scale (δ). The coupling constant values (*J*) are given in hertz (Hz).

Electron Impact (EI) mass spectra were measured on a *Finnigan MAT95Q* or on a *Finnigan MAT90* mass spectrometer. **Electrospray ionisation (ESI) mass spectra** were measured on a *Thermo Finnigan LTQ-FT*. The most important signals are reported in *m/z* units with *M* as the molecular ion.

Elemental analysis was performed in the micro analytical laboratory of the LMU department of chemistry on an *Elementar Vario EL* apparatus.

Infrared spectra were recorded on a *Perkin Elmer Spectrum BX-FT-IR* instrument equipped with a *Smith DuraSamplIR II ATR*-device. Transmittance values are qualitatively described by wavenumber (cm⁻¹) as very strong (vs), strong (s), medium (m) and weak (w).

Isomerization experiments: Irradiations of the HTI solutions were conducted in NMR tubes at concentrations in the range of 1x10⁻³ mol/L in deuterated solvents or in UV/vis cuvettes at concentrations in

the range of 1×10^{-5} mol/L in *spectroscopic grade* solvents. For irradiation, LEDs from *Roithner Lasertechnik GmbH* (365 nm, 385 nm, 405 nm, 420 nm, 435 nm) were used.

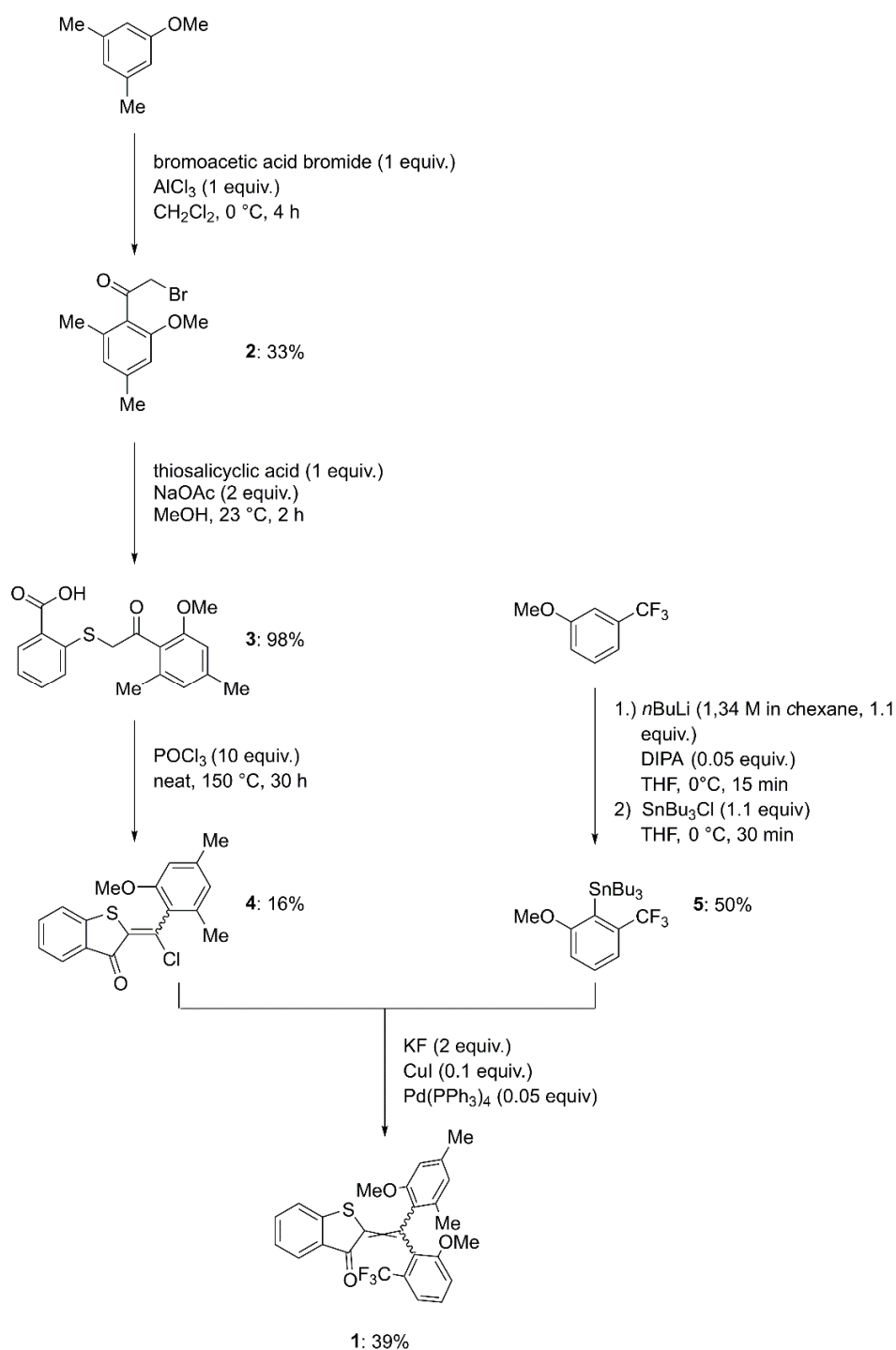
UV/vis spectra were measured on a *Varian Cary 5000* spectrophotometer. The spectra were recorded in a quartz cuvette ($l = 1$ cm). Solvents for spectroscopy were obtained from *VWR* and *Merck*. Absorption wavelength (λ) are reported in nm and the molar extinction coefficient (ϵ) $\text{L mol}^{-1} \text{cm}^{-1}$ in brackets. Shoulders are declared as sh.

Quantum yields at a given temperature were measured on a *Varian Cary® 50* spectrophotometer with an *Oxford DN 1704* optical cryostat controlled by an *Oxford ITC 4* device. Low temperatures were reached by cooling slowly with liquid nitrogen. The spectra were recorded in a quartz cuvette ($l = 1$ cm). Solvents for spectroscopy were obtained from *VWR*, *Merck* and *Sigma Aldrich* and were dried, degassed prior use. For irradiation studies a *Prizmatix UHP-T-LED-450* (450 nm) was used as light source.

Melting points (M.p.) were measured on a *Stuart SMP10* melting point apparatus in open capillaries and are not corrected.

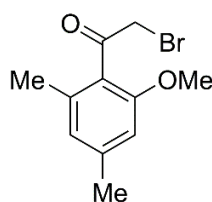
High Performance Liquid Chromatography (HPLC) was performed on a Shimadzu HPLC system consisting of a LC-20AP solvent delivery module, a CTO-20A column oven, a SPD-M20A photodiode array UV/vis detector and a CBM-20A system controller using a preparative or analytical CHIRALPAK® ID column (particle size $5 \mu\text{m}$) from *Daicel* and HPLC grade solvents (*n*-heptane and ethyl acetate) from *Sigma-Aldrich*, *VWR*, and *ROTH*.

Synthesis of HTI 1



Supplementary Scheme 1. Synthesis of HTI 1. Compounds **2**¹ and **3**² were prepared following published procedures.

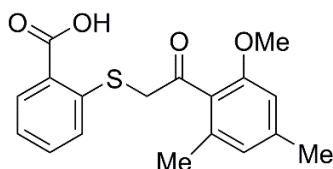
2-Bromo-1-(2-methoxy-4,6-dimethylphenyl)ethan-1-one (2) ¹



3,5-Dimethylanisole (9.55 mL, 9.20 g, 67.5 mmol, 1 equiv.) and bromoacetyl bromide (5.88 mL, 13.6 g, 67.4 mmol, 1 equiv.) were dissolved in CH₂Cl₂ (50 mL) and AlCl₃ (9.00 g, 67.5 mmol, 1 equiv.) was added portion-wise at 0 °C. The reaction mixture was stirred for 4 h while reaching 23 °C and was then completed by adding HCl (2 M aq. solution, 50 mL) carefully under cooling with an ice bath (0 °C). The aqueous phase was extracted with CH₂Cl₂ (3 x 50 mL) the combined organic phases were dried over Na₂SO₄ and the solvent was removed *in vacuo*. The crude product was purified via FCC (SiO₂, *i*Hex:EtOAc = 99:1) yielding the title compound as colorless solid (5.73 g, 22.3 mmol, 33%).

¹H NMR (200 MHz, CDCl₃) δ (ppm) = 6.67 (s, 1H), 6.59 (s, 1H), 4.36 (s, 2H), 3.83 (s, 3H), 2.33 (s, 3H), 2.25 (s, 3H).

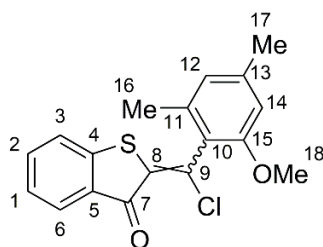
2-((2-(2-Methoxy-4,6-dimethylphenyl)-2-oxoethyl)thio)benzoic acid (3) ²



Thiosalicylic acid (7.58 g, 50.9 mmol, 1 equiv.), bromide **2** (13.1 g, 50.9 mmol, 1 equiv.) and sodium acetate (8.56 g, 102 mmol, 2.00 equiv.) were dissolved in MeOH (100 mL) and stirred for 30 min at 60 °C. The reaction was terminated by adding a mixture of HCl (2 M aq. solution) and ice water (100 mL) upon which a precipitate formed. The precipitate was filtered, washed with H₂O and hexanes and dried *in vacuo*. The thus obtained pure compound **3** was isolated as colorless solid (16.5 g, 49.9 mmol, 98 %).

¹H NMR (200 MHz, CDCl₃) δ (ppm) = 8.07 (dt, *J* = 7.8, 1.2, 1H), 7.55 – 7.40 (m, 2H), 7.21 (ddd, *J* = 8.4, 6.1, 2.3, 1H), 6.65 – 6.51 (m, , 2H), 4.27 (s, 2H), 3.83 (s, 3H), 2.31 (s, 3H), 2.06 (s, 3H).

2-(Chloro(2-methoxy-4,6-dimethylphenyl)methylene)benzo[*b*]thiophen-3(2*H*)-one (4)³



Thioether **3** (15.3 g, 46.3 mmol, 1 equiv.) was dissolved in POCl₃ (42.3 mL, 71.9 g, 463 mmol, 10.0 equiv.) and the reaction mixture was immediately heated up to 150 °C. After stirring for 30 min at that temperature the reaction was stopped by carefully adding water (250 mL). The aqueous phase was extracted with CH₂Cl₂ (3 x 80 mL) the combined organic phases were dried over Na₂SO₄ and the solvent was removed *in vacuo*. The crude product was purified via FCC (SiO₂, *i*Hex:EtOAc = 98:2 → 93:7) yielding the title compound as mixture of *E/Z* isomers in a ratio of 1:5 as yellow solid (2.40 g, 7.25 mmol, 16%).

HR-MS (EI) for C₁₈H₁₅ClO₂S⁺, [M]⁺, calcd. 330.0476, found 330.0474.

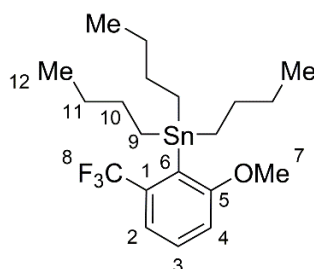
¹H-NMR (600 MHz, CDCl₃) δ = 7.90 (d, *J* = 7.6 Hz, 1H, H-C(6)_{*E*}), 7.67 (d, *J* = 8.3 Hz, 1H, H-C(6)_{*Z*}), 7.57 – 7.52 (m, 1H, H-C(2)_{*Z*}), 7.51 (t, *J* = 7.6 Hz, 1H, H-C(2)_{*E*}), 7.44 (d, *J* = 7.9 Hz, 1H, H-C(6)_{*Z*}), 7.28 – 7.24 (m, 2H, H-C(1)_{*E*}, H-C(3)_{*E*}), 7.21 (t, *J* = 7.8 Hz, 1H, H-C(1)_{*Z*}), 6.71 (s, 1H, H-C(12)_{*Z*}), 6.66 (s, 1H, H-C(12)_{*E*}), 6.63 (s, 1H, H-C(14)_{*E*}), 6.62 (s, 1H, H-C(14)_{*Z*}), 3.79 (s, 3H, H-C(18)_{*E*}), 3.76 (s, 3H, H-C(18)_{*E*}), 2.36 (s, 3H, H-C(17)_{*E*}), 2.36 (s, 3H, H-C(17)_{*E*}), 2.25 (s, 3H, H-C(17)_{*E*}), 2.19 (s, 3H, H-C(17)_{*Z*}) ppm.

¹³C-NMR (151 MHz, CDCl₃) δ = 185.2 (C(7)_{*E*}), 183.7 (C(7)_{*Z*}), 156.5 (C(15)_{*Z*}), 156.1 (C(15)_{*E*}), 144.5 (C(4)_{*Z*}), 144.0 (C(4)_{*E*}), 141.5 (C(13)_{*E*}), 140.9 (C(13)_{*Z*}), 140.2 (C(8/9)_{*Z*}), 140.2 (C(8/9)_{*E*}), 137.2 (C(11)_{*Z*}), 136.8 (C(11)_{*E*}), 135.2 (C(2)_{*Z*}), 135.1 (C(2)_{*E*}), 134.2 (C(8/9)_{*Z*}), 133.7 (C(8/9)_{*E*}), 132.6 (C(5)_{*Z*}), 132.5 (C(5)_{*E*}), 127.1 (C(6)_{*E*}), 127.0 (C(6)_{*Z*}), 125.4 (C(1)_{*Z*}), 125.2 (C(1)_{*E*}), 124.4 (C(10)_{*E*}), 123.6 (C(3)_{*Z*}), 123.4 (C(12)_{*Z*}), 123.1 (C(3)_{*E*}), 122.4 (C(10)_{*Z*}), 109.8 (C(14)_{*E*}), 109.6 (C(14)_{*Z*}), 56.0 (C(18)_{*E*}), 55.8 (C(18)_{*Z*}), 21.9 (C(17)_{*Z*}), 21.8 (C(17)_{*E*}), 19.0 (C(16)_{*Z*}), 18.8 (C(16)_{*E*}) ppm.

IR (ATR): $\tilde{\nu}/\text{cm}^{-1}$ = 2915 (w), 2832 (w), 1728 (m), 1679 (vs), 1591 (vs), 1565 (vs), 1446 (vs), 1408 (m), 1375 (w), 1311 (vs), 1279 (vs), 1249 (m), 1222 (s), 1185 (m), 1157 (vs), 1093 (vs), 1056 (m), 1020 (m), 1002 (m), 948 (m), 921 (m), 893 (w), 876 (w), 860 (m), 845 (m), 828 (vs), 789 (m), 733 (vs), 702 (m), 687 (m), 663 (m).

R_f(SiO₂, *i*hexane:EtOAc = 95:5) = 0.37.

Tributyl(2-methoxy-6-(trifluoromethyl)phenyl)stannane (5)



In a flame dried round bottom flask 1-methoxy-3-(trifluoromethyl)benzene (5.00 mL, 4.11 g, 23.3 mmol, 1 equiv.) was dissolved in THF (20 mL) and the solution was cooled to 0 °C. Diisopropylamine (0.16 mL, 118 mg, 1.17 mmol, 0.05 equiv.) and *n*BuLi (1.43 M in hexane, 17.9 mL, 25.7 mmol, 1.1 equiv.) were added at 0 °C and the reaction was stirred for 15 min at that temperature. Tributyltin chloride (6.96 mL, 8.35 g, 25.7 mmol, 1.1 equiv.) was added and stirring was continued for 30 min at 0 °C. After completion the reaction was quenched by adding a sat. aq. NaHCO₃ solution (50 mL), the aqueous phase was extracted with CH₂Cl₂ (3 x 50 mL) and the combined organic phases were dried over Na₂SO₄. After removing the solvent *in vacuo* the crude product was purified via FCC (SiO₂, *i*Hex:EtOAc = 99:1) and the product was obtained as colorless liquid (5.45 g, 11.7 mmol, 50%).

HR-MS (EI) for C₂₀H₃₃F₃O₂Sn⁺, [M]⁺, calcd. 466.1500, found 466.1456.

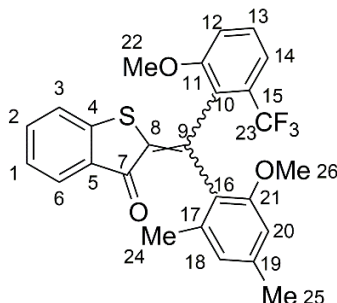
¹H-NMR (400 MHz, CDCl₃) δ = 7.40 (t, *J* = 7.7 Hz, 1H), 7.34 (d, *J* = 7.7 Hz, 1H), 6.98 (d, *J* = 8.0 Hz, 1H), 3.83 (s, 3H), 1.52 – 1.44 (m, 2H), 1.33 (tq, *J* = 7.3, 7.2 Hz, 2H), 1.14 – 1.08 (m, 2H), 0.89 (t, *J* = 7.3 Hz, 3H) ppm.

¹³C-NMR (101 MHz, CDCl₃) δ = 164.2 (C(5)), 137.7 (q, *J* = 30.2 Hz, C(1)), 130.4 (q, *J* = 3.9 Hz, C(6)), 129.6 (C(3)), 124.4 (q, *J* = 273.4 Hz, C(8)), 118.3 (q, *J* = 5.4 Hz, C(2)), 111.9 (q, *J* = 1.3 Hz, C(4)), 55.5 (C(7)), 28.9 (C(10)), 27.3 (C(11)), 13.7 (C(12)), 11.9 (q, *J* = 2.1 Hz, C(9)) ppm.

IR (ATR): $\tilde{\nu}/\text{cm}^{-1}$ = 2955 (w), 2921 (w), 2871 (w), 2853 (w), 1462 (m), 1444 (w), 1425 (m), 1376 (w), 1317 (vs), 1289 (w), 1244 (s), 1188 (m), 1163 (s), 1096 (s), 1071 (w), 1041 (vs), 960 (w), 857 (w), 790 (s), 748 (m), 720 (m), 675 (m).

R_f(SiO₂, *i*hexane:EtOAc = 99:1) = 0.86.

2-((2-Methoxy-4,6-dimethylphenyl)(2-methoxy-6-(trifluoromethyl)phenyl)methylene)benzo[*b*]thiophen-3(2*H*)-one (1)



HTI-chloride **4** (750 mg, 2.27 mmol, 1.00 equiv.), tributyl stannane **5** (1.06 g, 2.27 mmol, 1.00 equiv.), potassium fluoride (264 mg, 4.54 mmol, 2.00 equiv.), and copper(I) iodide (43.8 mg, 0.23 mmol, 0.10 equiv.) were added to dioxane (10 mL) and N₂ was bubbled through the suspension for 15 min under continuous stirring. Under N₂ atmosphere Pd(PPh₃)₄ (127 mg, 0.11 mmol, 0.05 equiv.) was added and the reaction mixture was heated to 100 °C. After stirring the reaction mixture at that temperature for 12 h N₂ was bubbled through the solution again for 5 min. Subsequently tributyl stannane **5** (528 mg, 1.14 mmol, 0.50 equiv.) and Pd(PPh₃)₄ (127 mg, 0.11 mmol, 0.05 equiv.) were added again and the resulting mixture was further stirred for 2 d at 100 °C. The reaction was terminated by addition of a sat. aq. NaHCO₃ solution (30 mL), the aqueous phase was extracted with CH₂Cl₂ (3 x 50 mL) and the combined organic phases were dried over Na₂SO₄. After removing the solvent *in vacuo* the crude product was purified via FCC (SiO₂, *i*Hex:EtOAc = 95:5 → 9:1) yielding three fractions containing different diastereoisomers of the title compound: fraction 1 with **1-B** (120 mg, 0.26 mmol, 11%), fraction 2 containing both *E* isomers (**1-C**, **1-D**, 223 mg, 0.48 mmol, 21%) and fraction 3 containing **1-A** (74.4 mg, 0.16 mmol, 7%); overall yield of **1** = 39%. All isomers were obtained as yellow to orange crystals after crystallization from *n*heptane/CH₂Cl₂.

rac-A-I

¹H-NMR (800 MHz, CDCl₃) δ = 7.77 (dd, *J* = 7.8, 1.4 Hz, 1H, H-C(6)), 7.48 (ddd, *J* = 8.3, 7.2, 1.3 Hz, 1H, H-C(2)), 7.43 (t, *J* = 8.2 Hz, 1H, H-C(13)), 7.30 (d, *J* = 7.9 Hz, 1H, H-C(3)), 7.25 (dd, *J* = 8.0, 1.1 Hz, 1H, H-C(14)), 7.20 (t, *J* = 7.9 Hz, 1H, H-C(1)), 7.15 (d, *J* = 8.4 Hz, 1H, H-C(12)), 6.73 (s, 1H, H-C(18)), 6.42 (s, 1H, H-C(20)), 3.84 (s, 3H, H-C(22)), 3.36 (s, 3H, H-C(26)), 2.29 (s, 6H, H-C(24), H-C(25)) ppm.

¹³C-NMR (200 MHz, CDCl₃) δ = 185.8 (C(7)), 158.6 (C(11)), 158.0 (C(21)), 145.3 (C(4)), 141.2 (C(19)), 139.8 (C(17)), 137.8 (C(8/9)), 134.6 (C(2)), 132.8 (C(5)), 129.5 (C(13)), 129.4 (C(10)), 128.9 (q, *J* = 30.8 Hz, (C(11))), 127.0 (C(6)), 124.8 (C(1)), 124.3 (C(18)), 124.0 (C(16)), 123.7 (q, *J* = 274.3 Hz, (C(23))), 123.3 (C(3)), 118.1 (q, *J* = 6.6 Hz, (C(14))), 114.2 (C(12)), 110.0 (C(20)), 56.6 (C(22)), 55.6 (C(26)), 21.8 (C(25)), 20.3 (q, *J* = 3.1 Hz, (C(24))) ppm.

IR (ATR): $\tilde{\nu}/\text{cm}^{-1}$ = 1669 (m), 1584 (m), 1457 (m), 1315 (vs), 1266 (s), 1171 (s), 1137 (vs), 1094 (s), 1032 (vs), 870 (m), 829 (s), 785 (m), 748 (vs), 735 (vs), 707 (m), 676 (m).

Melting point: 158 – 162 °C.

R_f (SiO₂, *i*Hex/EtOAc = 9/1) = 0.10.

rac-B-1

¹H-NMR (600 MHz, CDCl₃) δ = 7.76 (d, J = 8.3 Hz, 1H, H-C(6)), 7.48 (td, J = 7.7, 1.3 Hz, 2H, H-C(2)), 7.43 (t, J = 8.1 Hz, 1H, H-C(13)), 7.31 (d, J = 4.5 Hz, 1H, H-C(3)), 7.30 (d, J = 4.5 Hz, 1H, H-C(14)), 7.20 (t, J = 7.5 Hz, 1H, H-C(1)), 7.03 (d, J = 8.3 Hz, 1H, H-C(12)), 6.68 (s, 1H, H-C(18)), 6.50 (s, 2H, H-C(20)), 3.67 (s, 3H, H-C(22)), 3.56 (s, 5H, H-C(26)), 2.30 (s, 3H, H-C(25)), 2.29 (s, 3H, H-C(24)) ppm.

¹³C-NMR (150 MHz, CDCl₃) δ = 186.0 (C(7)), 157.6 (C(11)), 157.5 (C(21)), 145.2 (C(4)), 140.6 (C(17)), 140.3 (C(8/9)), 139.5 (C(19)), 136.9 (C(8/9)), 134.8 (C(2)), 132.8 (C(5)), 131.6 (q, J = 30.8 Hz, (C(15))), 129.8 (C(13)), 128.3 (C(10)), 127.0 (C(6)), 125.0 (C(1)), 124.4 (q, J = 274.5 Hz, (C(23))), 123.8 (C(3)), 123.5 (C(18)), 122.8 (C(16)), 119.9 (C(14)), 114.5 (C(12)), 109.7 (C(20)), 56.2 (C(22)), 55.1 (C(26)), 21.8 (C(25)), 20.0 (C(24)) ppm.

IR (ATR): $\tilde{\nu}/\text{cm}^{-1}$ = 3852 (m), 3742 (m), 3647 (m), 3628 (m), 1771 (w), 1733 (m), 1717 (w), 1699 (m), 1683 (m), 1669 (vs), 1652 (m), 1646 (w), 1634 (w), 1584 (m), 1558 (s), 1539 (s), 1506 (m), 1456 (s), 1435 (s), 1418 (m), 1321 (vs), 1278 (vs), 1190 (m), 1168 (s), 1103 (vs), 1090 (vs), 1049 (m), 1028 (vs), 921 (w), 863 (m), 851 (m), 829 (s), 819 (s), 786 (m), 755 (m), 744 (s), 736 (vs), 674 (m).

Melting point: 141 – 144 °C.

rac-C/D-1

¹H-NMR (800 MHz, CDCl₃) δ = 7.74 – 7.72 (m, 2H, H-C(6_C), H-C(6_D)), 7.50 – 7.47 (m, 2H, H-C(2_C), H-C(2_D)), 7.39 (t, J = 8.2 Hz, 1H, H-C(13_C)), 7.37 (t, J = 8.2 Hz, 1H, H-C(13_D)), 7.35 – 7.31 (m, 2H, H-C(3_C), H-C(3_D)), 7.29 (dd, J = 8.1, 1.1 Hz, 1H, H-C(14_C)), 7.27 – 7.26 (m, 1H, H-C(14_D)), 7.21 – 7.17 (m, 2H, H-C(1_C), H-C(1_D)), 7.07 (d, J = 7.7 Hz, 1H, H-C(12_D)), 6.99 (d, J = 8.2 Hz, 1H, H-C(12_C)), 6.75 (s, 1H, H-C(18_D)), 6.72 (s, 1H, H-C(18_C)), 6.50 (s, 1H, H-C(20_C)), 6.44 (s, 1H, H-C(20_D)), 3.72 (s, 3H, H-C(22_D)), 3.61 (s, 3H, H-C(22_C)), 3.57 (s, 3H, H-C(26_C)), 3.36 (s, 3H, H-C(26_D)), 2.45 (s, 3H, H-C(24_C)), 2.43 (s, 3H, H-C(24_D)), 2.32 (s, 3H, H-C(25_C)), 2.30 (s, 3H, H-C(25_D)) ppm.

^{13}C -NMR (200 MHz, CDCl_3) δ = 186.7 (C(7_c)), 186.5 (C(7_D)), 158.5 (C(11_D)), 158.1 (C(21_D)), 157.6 (C(21_c)), 157.1 (C(11_c)), 145.9 (C(6_D)), 145.8 (C(4_c)), 140.0 (C(19_D)), 139.8 (C(19_c)), 139.6 (C(8/9_c)), 139.4 (C(17_c)), 139.2 (C(17_D)), 137.3 (C(8/9_D)), 136.6 (C(8/9_c)), 136.4 (C(8/9_D)), 134.8 (C(2_c)), 134.7 (C(2_D)), 132.3 (C(5_c)), 132.1 (C(5_D)), 131.5 (q, J = 31.0 Hz, (C(15_D))), 128.8 (C(13_c)), 128.7 – 128.4 (m, (C(10_D), (C(13_D), (C(15_D))), 126.9 (C(6_c)), 126.8 (C(16_D)), 126.7 (C(6_D)), 126.3 (C(10_c)), 125.1 (C(16_c)), 124.8 (C(1_c)), 124.8 (C(1_D)), 124.8 (C(18_D)), 124.0 (C(18_c)), 123.4 (C(3_c)), 123.3 (C(3_D)), 119.8 (C(14_c)), 118.3 (C(14_D)), 114.0 (C(12_c)), 113.5 (C(12_D)), 110.2 (C(20_D)), 109.6 (C(20_c)), 56.4 (C(22_D)), 55.8 (C(22_c)), 55.7 (C(26_D)), 55.0 (C(26_c)), 21.7 (C(25_c)), 21.6 (C(25_D)), 21.1 (C(24_D)), 20.5 (C(24_c)).

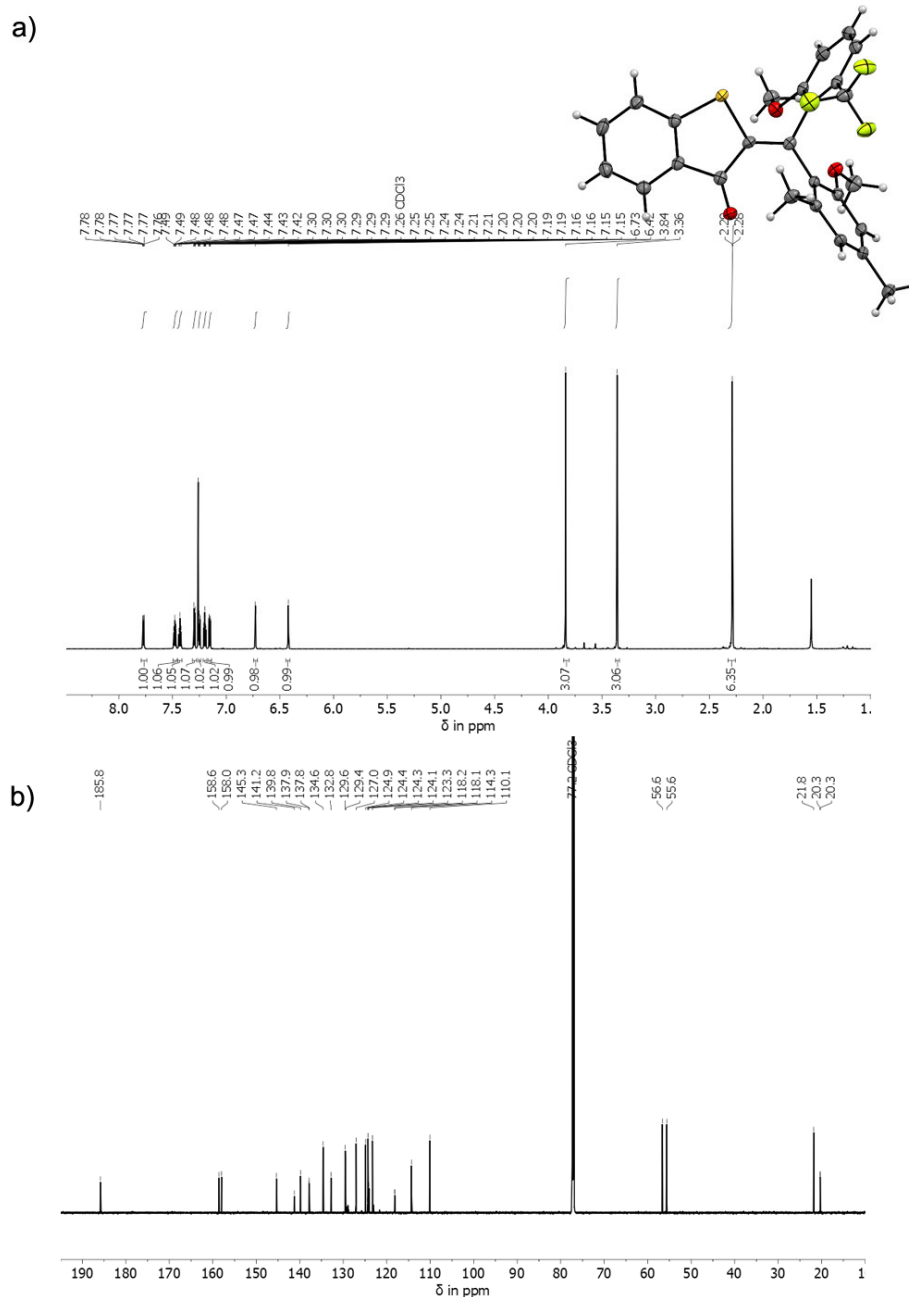
IR (ATR for pure crystalline isomers *rac*-C): $\tilde{\nu}/\text{cm}^{-1}$ = 1671 (m), 1589 (m), 1450 (m), 1322 (s), 1267 (s), 1163 (s), 1092 (vs), 1035 (vs), 865 (m), 830 (m), 807 (m), 783 (w), 749 (s), 732 (vs).

Decomposition point: 180 – 182 °C.

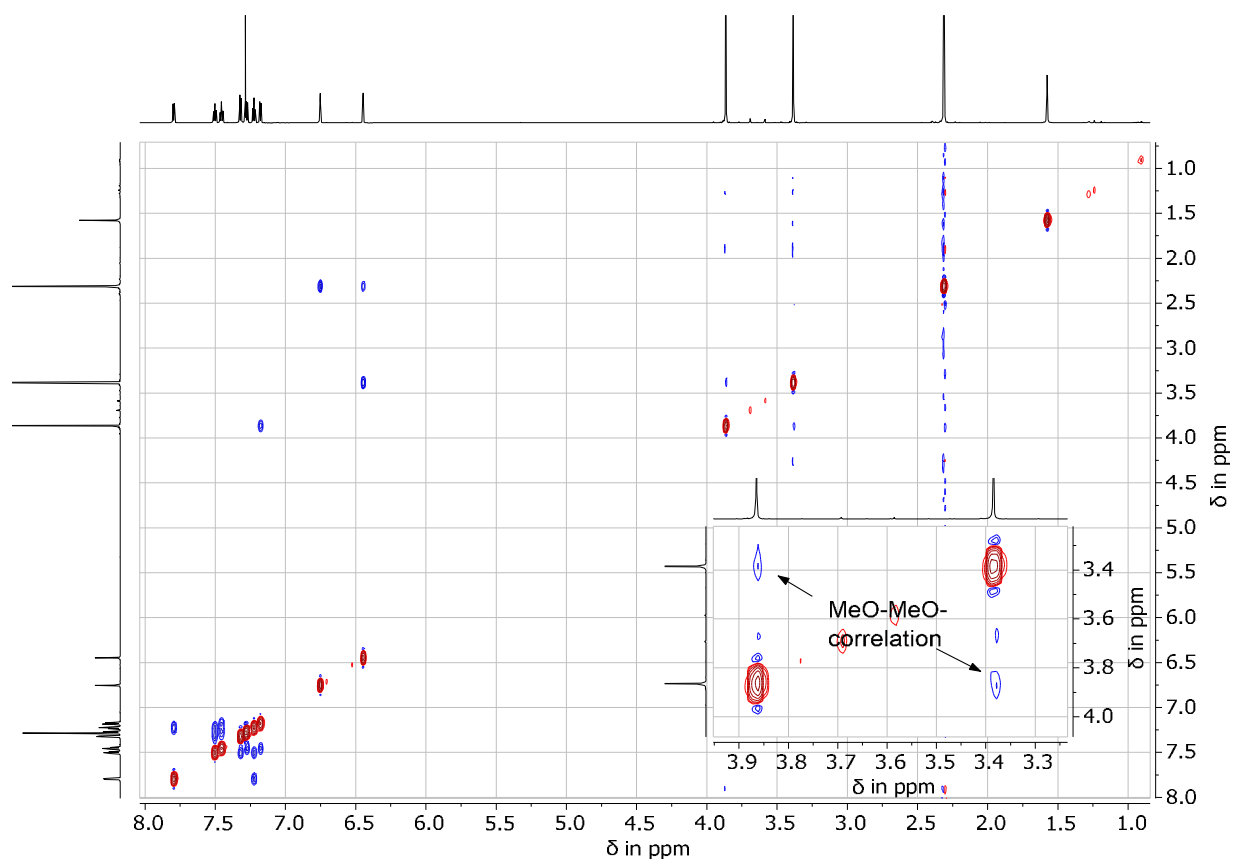
For all isomers (measured from a mixture of *rac*-A, *rac*-B, *rac*-C and *rac*-D):

HRMS (EI^+), $[\text{M}^+]$: m/z calcd: 470.1158 for $[\text{C}_{21}\text{H}_{22}\text{O}_4\text{S}]^+$, found: 470.1158.

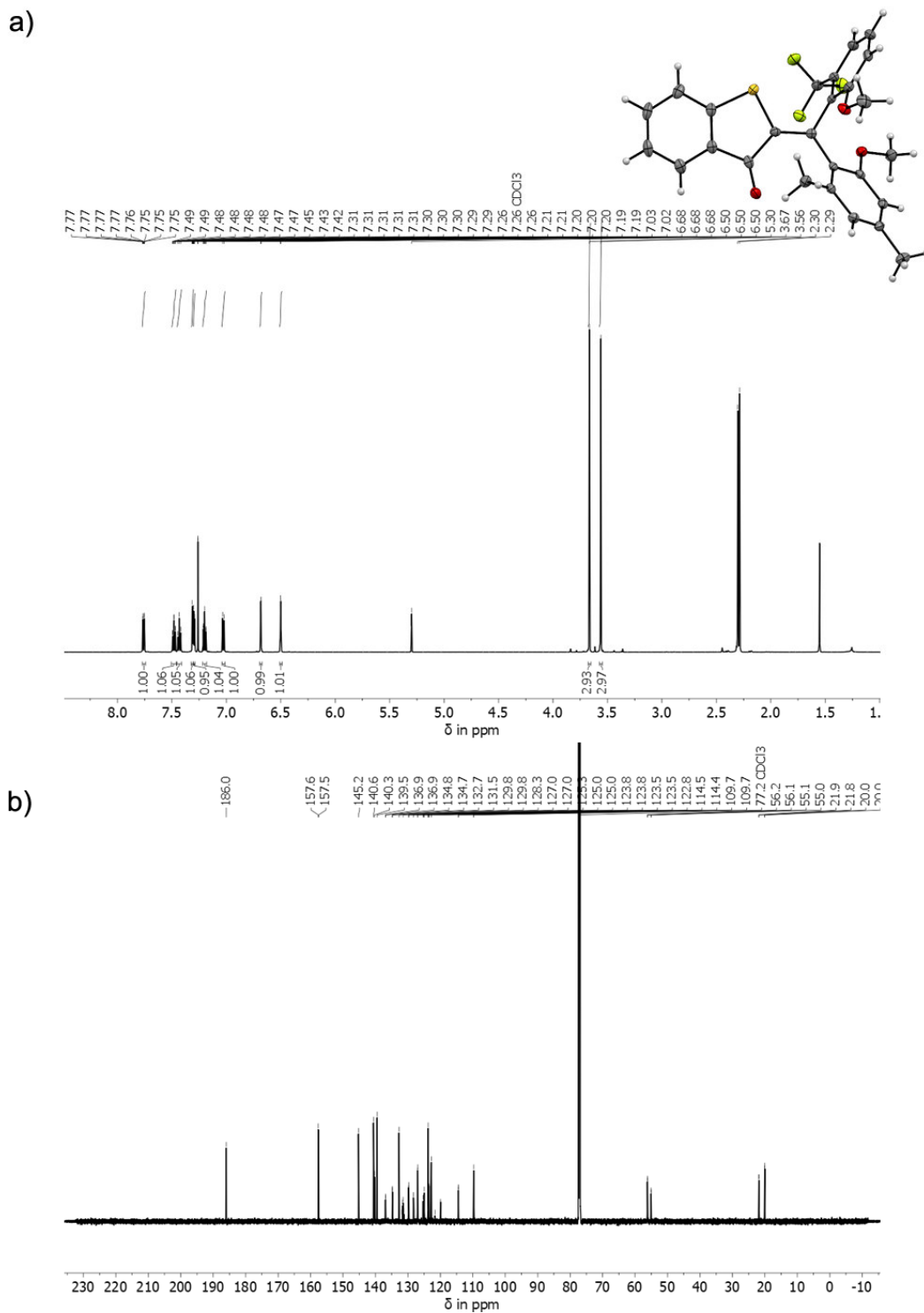
Determination of constitution and conformation in the crystalline state and in solution



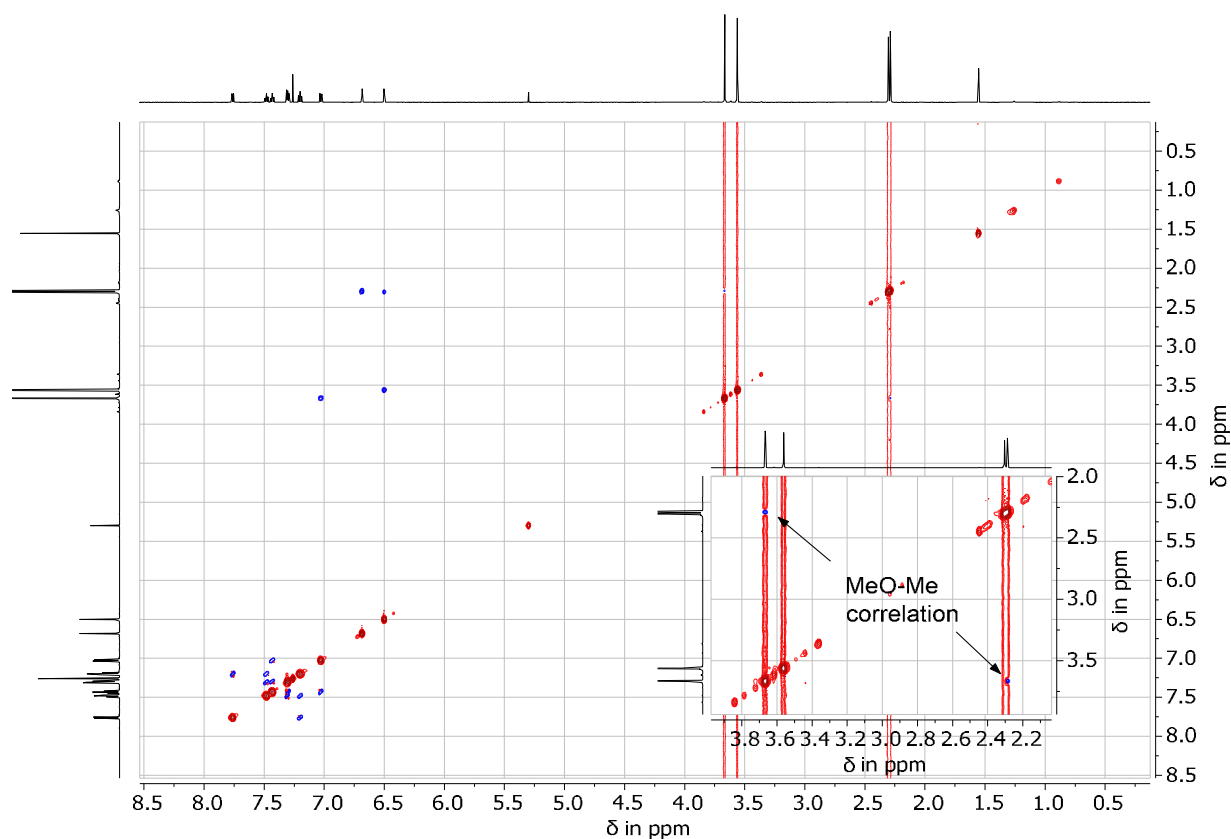
Supplementary Figure 1. a) Structure of A-1 in the crystalline state and the corresponding ^1H NMR spectrum (CDCl₃, 800 MHz, 27 °C) of the same crystal batch. The signals of only one single species are observed in the ^1H NMR spectrum, which could thus be directly assigned to A-1. b) Corresponding ^{13}C NMR spectrum (CDCl₃, 200 MHz, 27 °C).



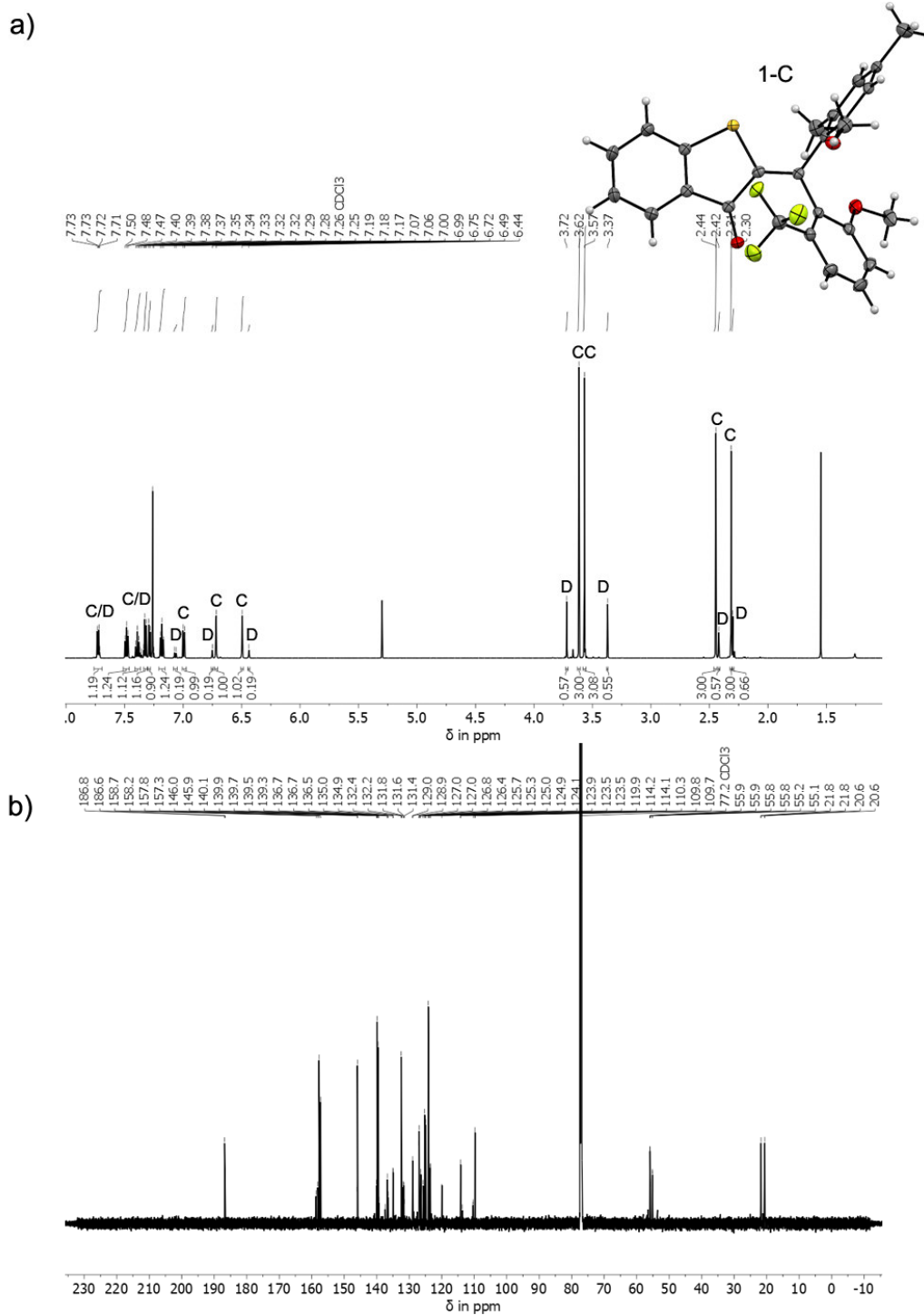
Supplementary Figure 2. NOESY NMR spectrum (CDCl_3 , 800 MHz, 27 °C) of **A-1**. The inset shows the methoxy part of the spectrum enlarged. A correlation between both methoxy groups can be observed. This is indicative for the **A-1** structure with *syn*-relation of the methoxy groups and is also in agreement with the molecular structure in the crystalline state.



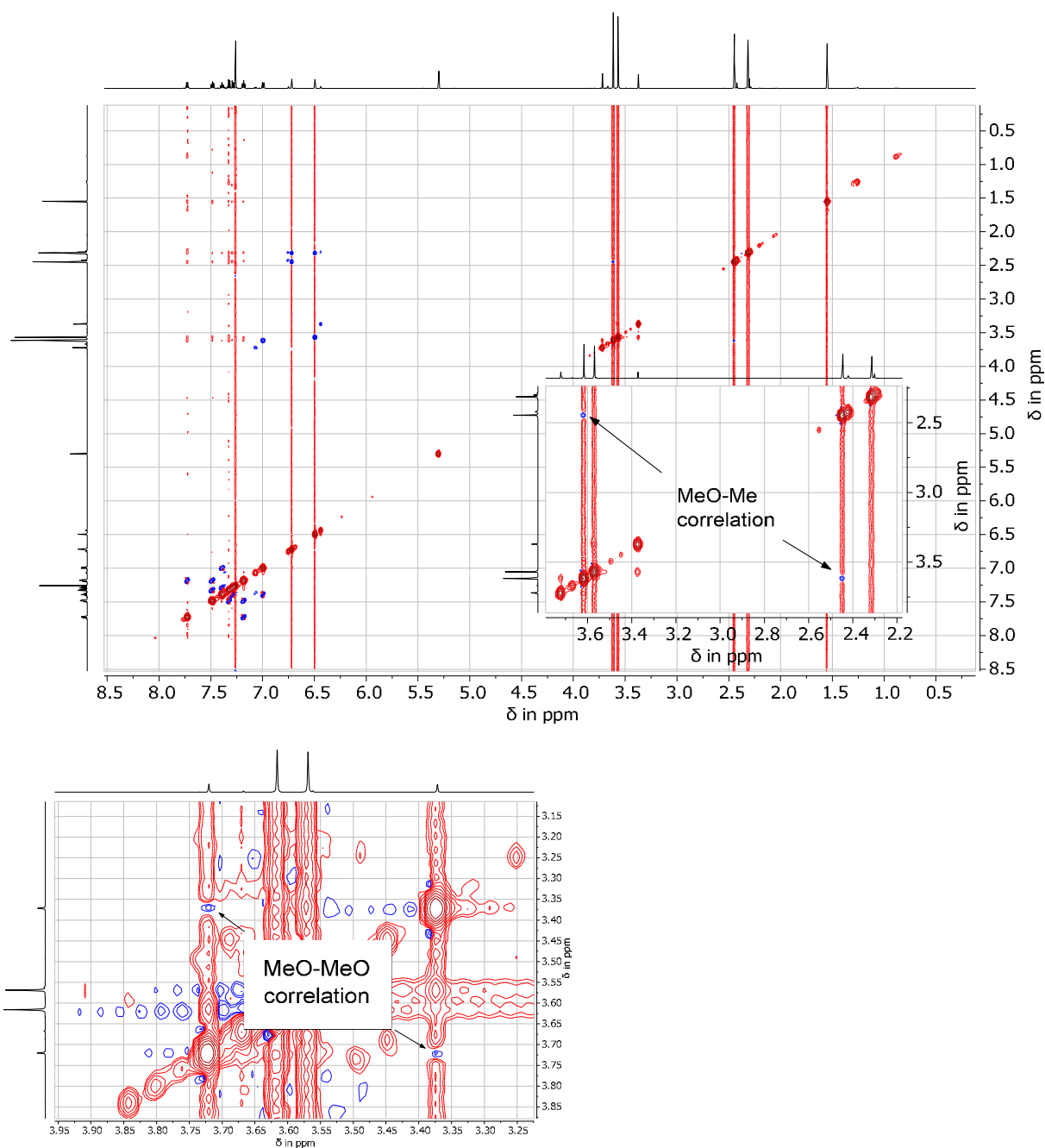
Supplementary Figure 3. a) Structure of **B-1** in the crystalline state and the corresponding ^1H NMR spectrum (CDCl₃, 600 MHz, 27 °C) of the same crystal batch. The signals of only one single species are observed in the ^1H NMR spectrum, which could thus be directly assigned to **B-1**. b) Corresponding ^{13}C NMR spectrum (CDCl₃, 150 MHz, 27 °C).



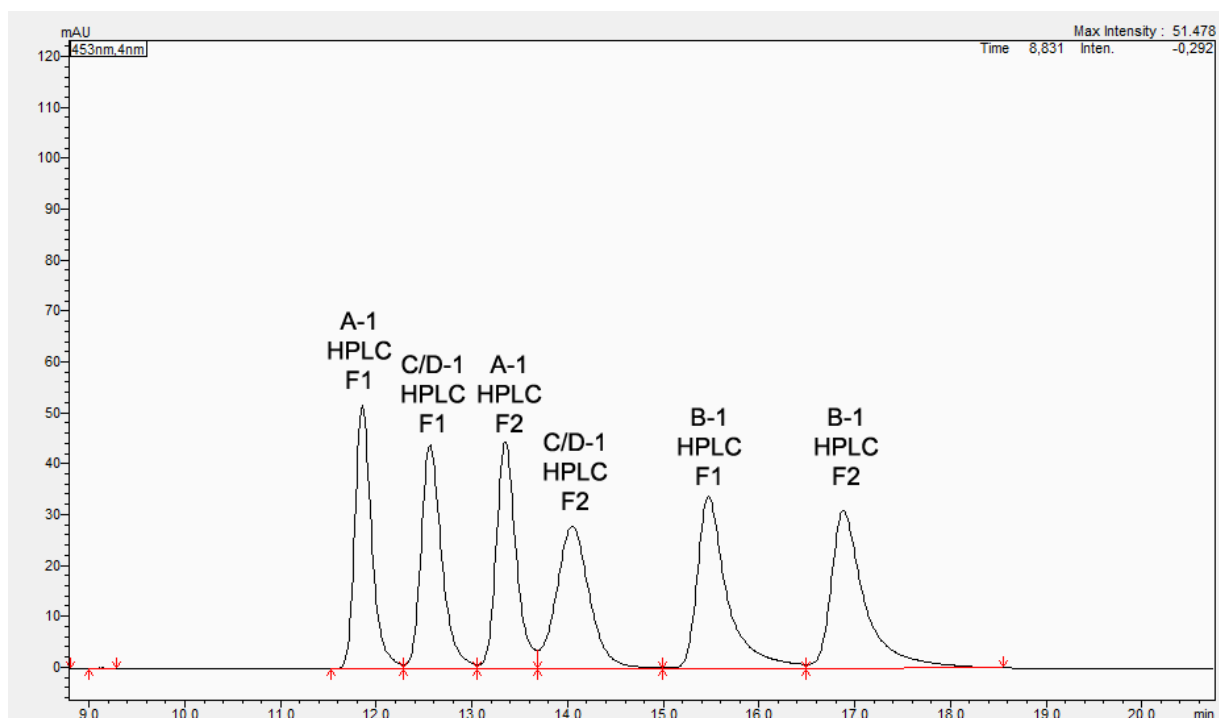
Supplementary Figure 4. NOESY NMR spectrum (CDCl_3 , 600 MHz, 27 °C) of **B-1**. The aliphatic part of the spectrum is enlarged. A small correlation between a methoxy and a methyl group can be observed. This is indicative for the **B-1** structure with *anti*-relation of the methoxy groups and is also in agreement with the molecular structure in the crystalline state.



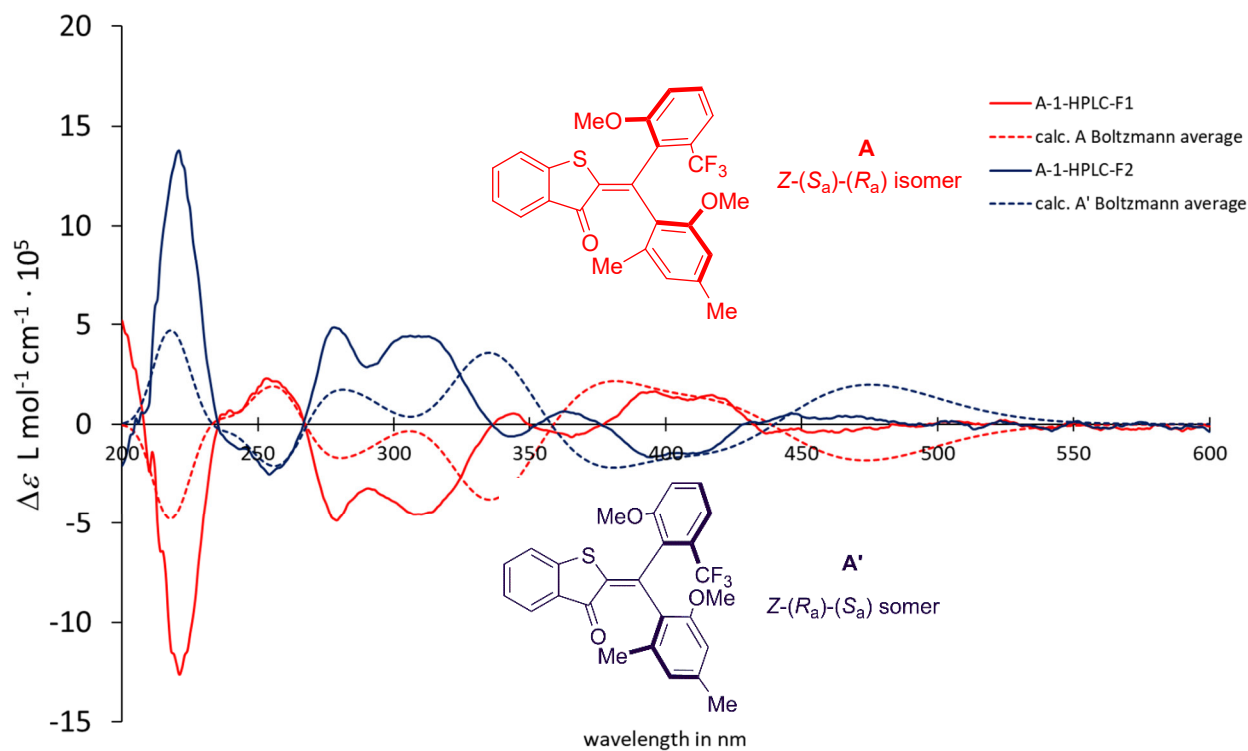
Supplementary Figure 5. a) Structure of **C-1** in the crystalline state and the corresponding ^1H NMR spectrum (CDCl₃, 600 MHz, 27 °C) of the same crystal batch. **C-1** is not stable at ambient temperatures and atropisomerizes to **D-1**. Therefore, a mixture of both isomers is present. The signals are thus labeled with the corresponding isomer designation. The assignment of signals to a specific isomer is based on the NOESY NMR spectrum as shown below. b) Corresponding ^{13}C NMR spectrum (CDCl₃, 150 MHz, 27 °C).



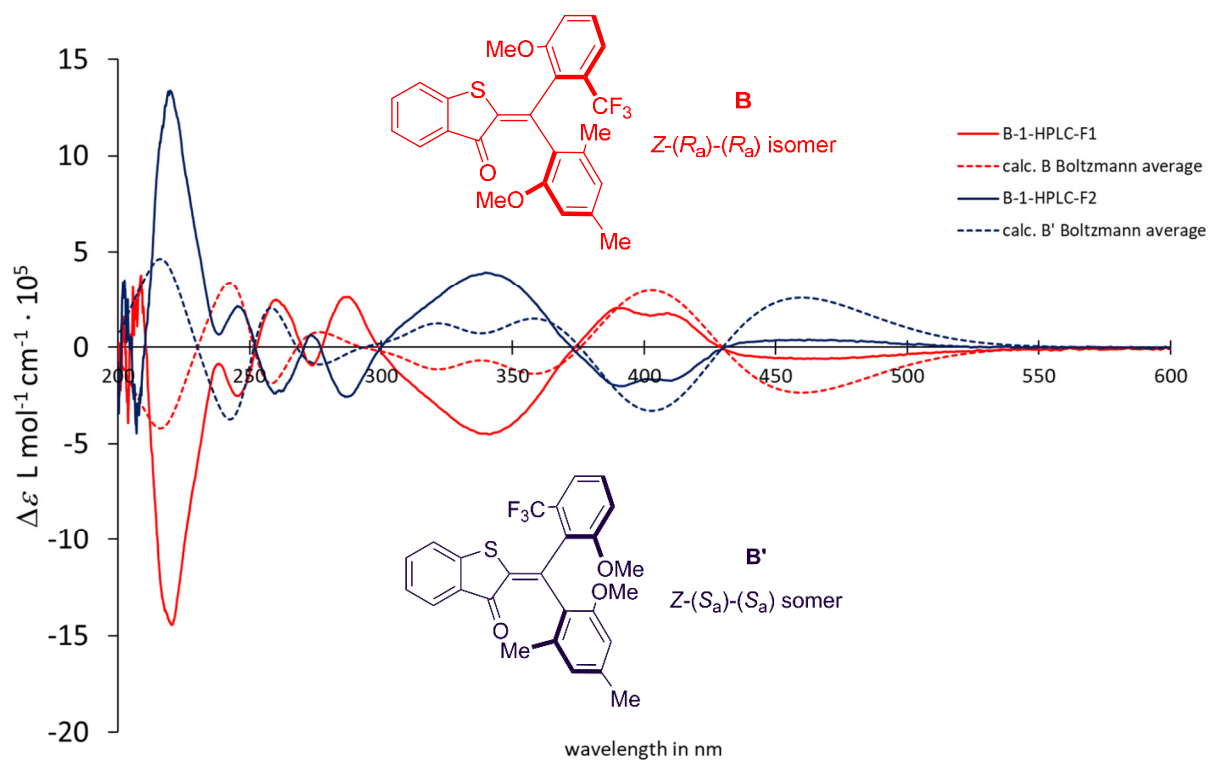
Supplementary Figure 6. NOESY NMR spectrum (CDCl_3 , 600 MHz, 27 °C) of an isomeric mixture of **C-1** and **D-1** in thermal equilibrium. The aliphatic part of the spectrum is enlarged. A correlation between a methoxy and methyl group can be observed for the more intense set of signals. This correlation is indicative for *anti*-relation of the methoxy groups and therefore the respective set of most intense signals is assigned to the **C-1** isomer. A very small correlation between both methoxy groups is observed for the set of signals with lower intensity. This is indicative for a *syn*-relation of the methoxy groups and therefore the set of less intense signals is assigned to the **D-1** isomer. The NMR-spectra show that **C-1** is thermally more stable than **D-1**. This finding is in agreement with the theoretical description.



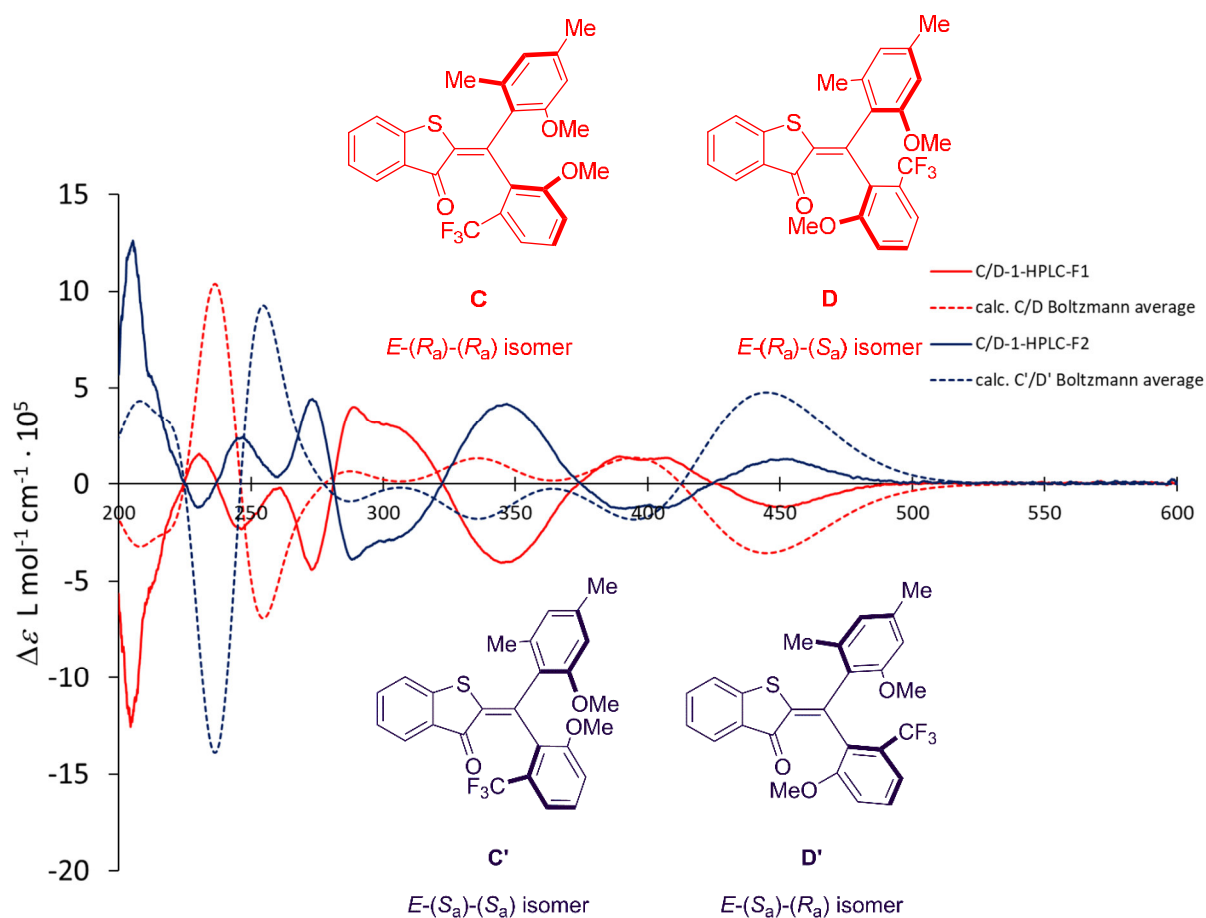
Supplementary Figure 7. HPLC chromatogram trace of all isomers of **1** at 453 nm. Separation was performed on a DAICEL CHIRALPAK ID column (20 mm \varnothing x 20 mmL) with an eluent of 11% EtoAc in *n*-heptane at 60 °C and a flow of 3 mL. All isomers are separated except C and D, which are in rapid equilibrium with each other at 22 °C or more elevated temperatures. However, two different fractions for the C and D isomers are separated in the HPLC run, which evidences that only one single bond (connecting to the dimethyl-methoxy-substituted aryl residue) is rotating in the thermal equilibrium converting either C in D or C' in D'. The other single bond (connecting to the trifluoromethyl-methoxy-substituted aryl residue) does not rotate, which would otherwise result in a conversion of all four isomers C, C', D, and D' into each other (e.g. C in C', D and D'). Therefore, the mixture of C/D isomers after HPLC separation is expected to give an ECD signal and assignment to an absolute configuration should thus be possible.



Supplementary Figure 8. Experimental and calculated (see chapter “Calculated Ground State Energy Profile of Compound 1” for details of the calculations) ECD spectra of both enantiomers of **A-1** in MeCN at 20 °C. The fraction termed “A-HPLC-F1” was assigned to the **A-1** isomer and “A-1-HPLC-F2” was assigned to the **A'-1** isomer.



Supplementary Figure 9. Experimental and calculated (see chapter “Calculated Ground State Energy Profile of Compound **1**” for details of the calculations) ECD spectra of both enantiomers of **B-1** in MeCN at 20 °C. The fraction termed “B-HPLC-F1” was assigned to the **B-1** isomer and “B-1-HPLC-F2” was assigned to the **B'-1** isomer.



Supplementary Figure 10. Experimental and calculated (see chapter “Calculated Ground State Energy Profile of Compound 1” for details of the calculations) ECD spectra of both enantiomers of **C/D-1** in Me CN at 20 °C. The fraction termed “C/D-HPLC-F1” was assigned to the **C/D-1** isomers and “C/D-1-HPLC-F2” was assigned to the **C/D'-1** isomer.

Physical and photophysical properties

Thermal atropisomerizations *rac-A* to *rac-B* and *rac-D* to *rac-C*

An amberized NMR tube was charged with 0.5 mg of isomer *rac-A* in 0.7 mL of deuterated solvent. Subsequent heating at 62 °C was carried out in an oil bath and kinetics were followed by ¹H NMR measurements at defined time intervals. The equilibrium concentrations of isomers after prolonged heating were obtained from integration of the corresponding signals in the ¹H NMR spectrum.

The kinetics of thermal atropisomerization of *rac-D* to *rac-C* were measured starting from an irradiated sample of 0.5 mg *rac-B* with 450 nm at -30 °C. An Isomer composition of *rac-A*:*rac-B*:*rac-C*:*rac-D* of 16:67:5:12 was achieved after 1 h of irradiation in the NMR-instrument. The irradiation was stopped and after heating to -20 °C the thermal kinetics from *rac-D* to *rac-C* isomerization were measured over a time of 100 min.

The thermal atropisomerizations are unimolecular first order reactions and proceed towards an equilibrium composition with both atropisomers present according to eq. 1 and eq. 2, respectively.

$$\ln\left(\frac{[\mathbf{A}]_{t_0}-[\mathbf{A}]_{eq}}{[\mathbf{A}]_t-[\mathbf{A}]_{eq}}\right) = (k_{\mathbf{A}/\mathbf{B}} + k_{\mathbf{B}/\mathbf{A}})t \quad (\text{eq. 1})$$

$$\ln\left(\frac{[\mathbf{D}]_{t_0}-[\mathbf{D}]_{eq}}{[\mathbf{D}]_t-[\mathbf{D}]_{eq}}\right) = (k_{\mathbf{D}/\mathbf{C}} + k_{\mathbf{C}/\mathbf{D}})t \quad (\text{eq. 2})$$

with $[\mathbf{A}, \mathbf{D}]_0$ being the initial concentration of the isomers **A** or **D** at the time $t = 0$, $[\mathbf{A}, \mathbf{D}]_{eq}$ being the concentration of the isomers **A** or **D** at equilibrium, $[\mathbf{A} \text{ or } \mathbf{D}]_t$ representing the concentration of the isomers **A** or **D** at specific times in the measurement t , $k_{\mathbf{A}/\mathbf{B}}$ being the rate constant k of the **A** to **B** conversion, $k_{\mathbf{B}/\mathbf{A}}$ being the rate constant k of the **B** to **A** conversion, $k_{\mathbf{C}/\mathbf{D}}$ being the rate constant k of the **C** to **D** conversion, $k_{\mathbf{D}/\mathbf{C}}$ being the rate constant k of the **D** to **C** conversion and t being the elapsed time. When plotting the logarithmic left part of eq. 1 or eq. 2 versus time t the obtained slope m contains rate constants for the isomerization reactions taking place. The rate constants $k_{\mathbf{A}/\mathbf{B}}$ and $k_{\mathbf{D}/\mathbf{C}}$ can then be calculated according to eq. 3 and eq. 4:

$$k_{\mathbf{A}/\mathbf{B}} = \frac{m}{1 + \frac{[\mathbf{A}]_{eq}}{[\mathbf{B}]_{eq}}} \quad (\text{eq. 3})$$

$$k_{\mathbf{D}/\mathbf{C}} = \frac{m}{1 + \frac{[\mathbf{D}]_{eq}}{[\mathbf{C}]_{eq}}} \quad (\text{eq. 4})$$

when taking into account the corresponding laws of mass action (eq. 5 and eq. 6):

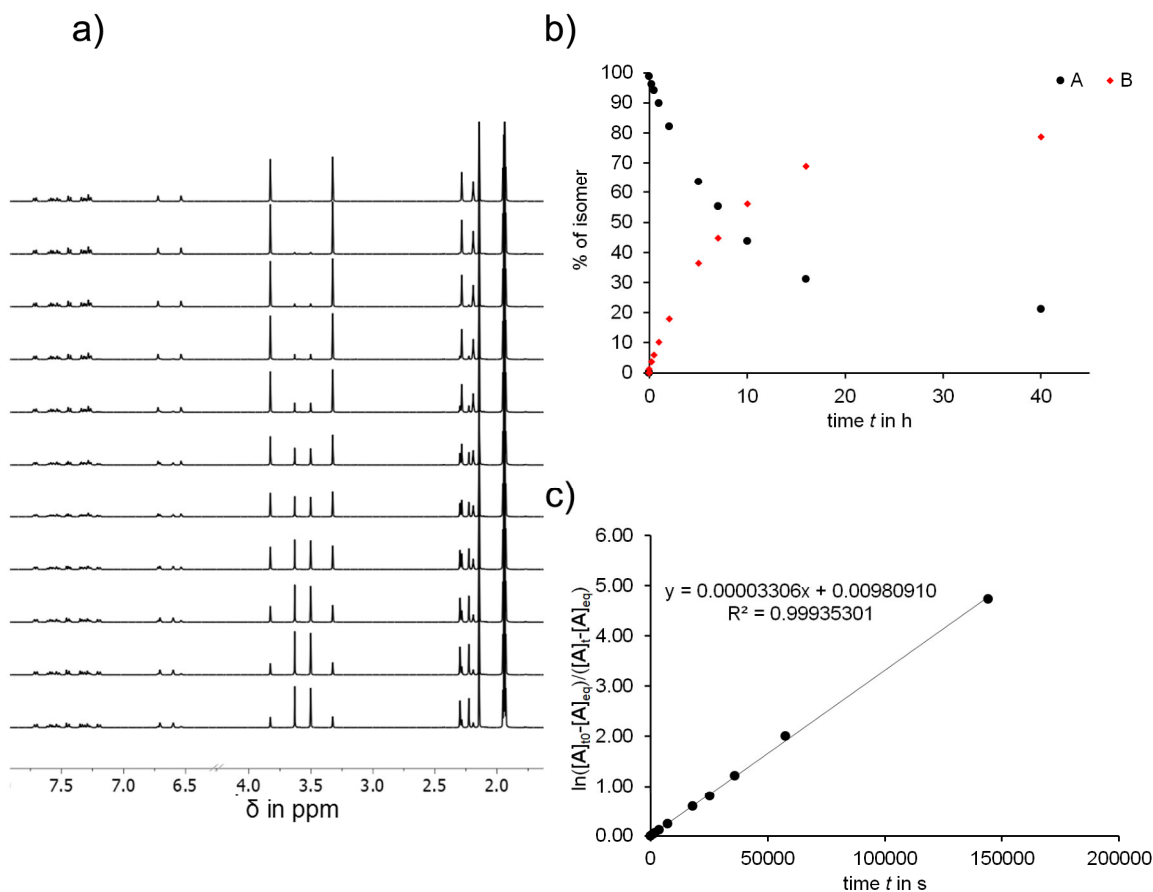
$$\frac{[\mathbf{A}]_{eq}}{[\mathbf{B}]_{eq}} = \frac{k_{\mathbf{B}/\mathbf{A}}}{k_{\mathbf{A}/\mathbf{B}}} \quad (\text{eq. 5})$$

$$\frac{[\mathbf{D}]_{eq}}{[\mathbf{C}]_{eq}} = \frac{k_{\mathbf{C}/\mathbf{D}}}{k_{\mathbf{D}/\mathbf{C}}} \quad (\text{eq. 6})$$

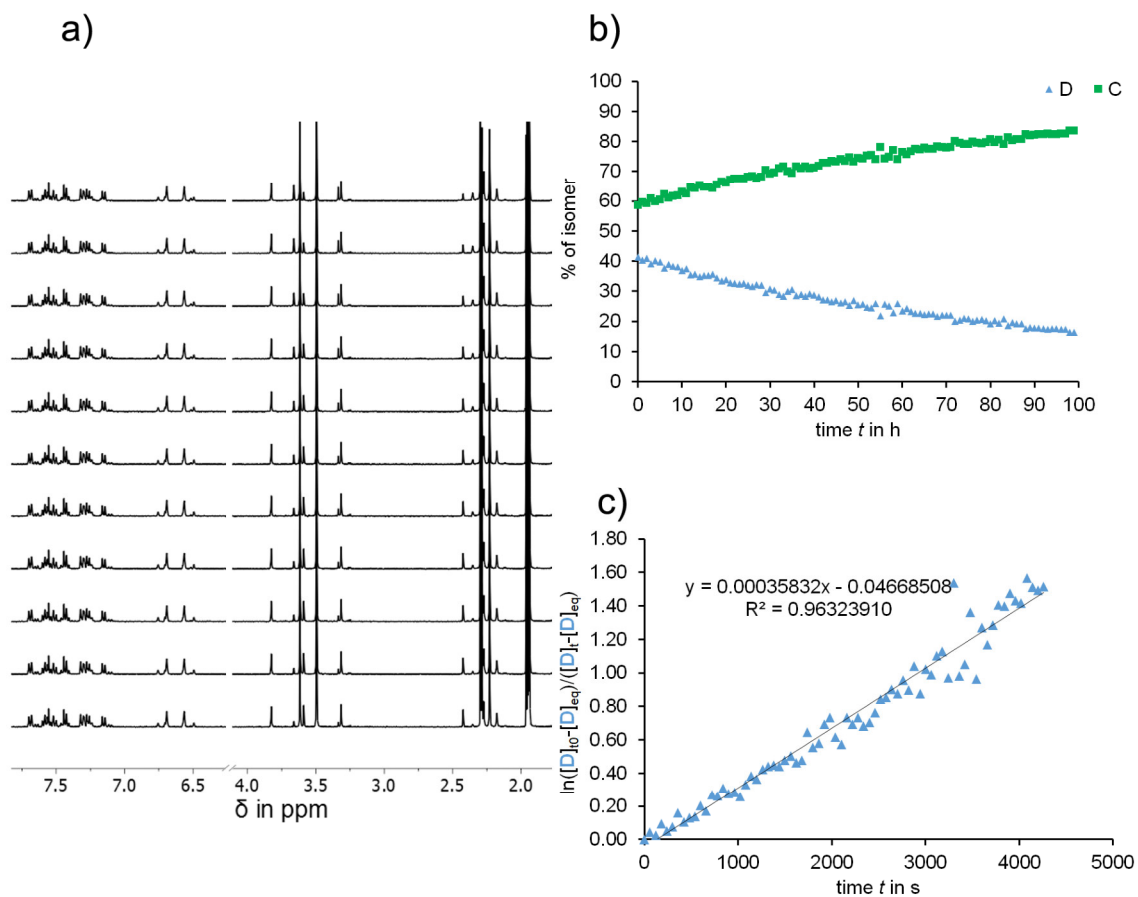
By using the *Eyring* equation (eq. 7) the ΔG^\ddagger can be calculated from the rate constants of the corresponding reaction. The obtained Gibbs energies of activation ΔG^\ddagger for the thermal isomerizations between **A** to **B** and **C** to **D** and *vice versa* in MeCN-*d*₃ and the corresponding half-lives at 25 °C are given in Supplementary Table 1 together with the equilibrium compositions obtained at elevated temperatures.

$$\Delta G^\ddagger = \ln\left(\frac{k \cdot h}{k_B \cdot T}\right) * R * T \quad (\text{eq. 7})$$

From these measurements we could quantify the ground state energy profile of HTI **1**. The equilibrium compositions at high temperatures deliver the thermodynamic energy differences between the corresponding states (red Δ values in Supplementary Figure 13) according to the relation of the change of *Gibbs* free energy and the equilibrium constant $-\Delta G = R \cdot T \cdot \ln K$ (see also Supplementary Table 1). The theoretical values are in good agreement with the experimentally determined ones.



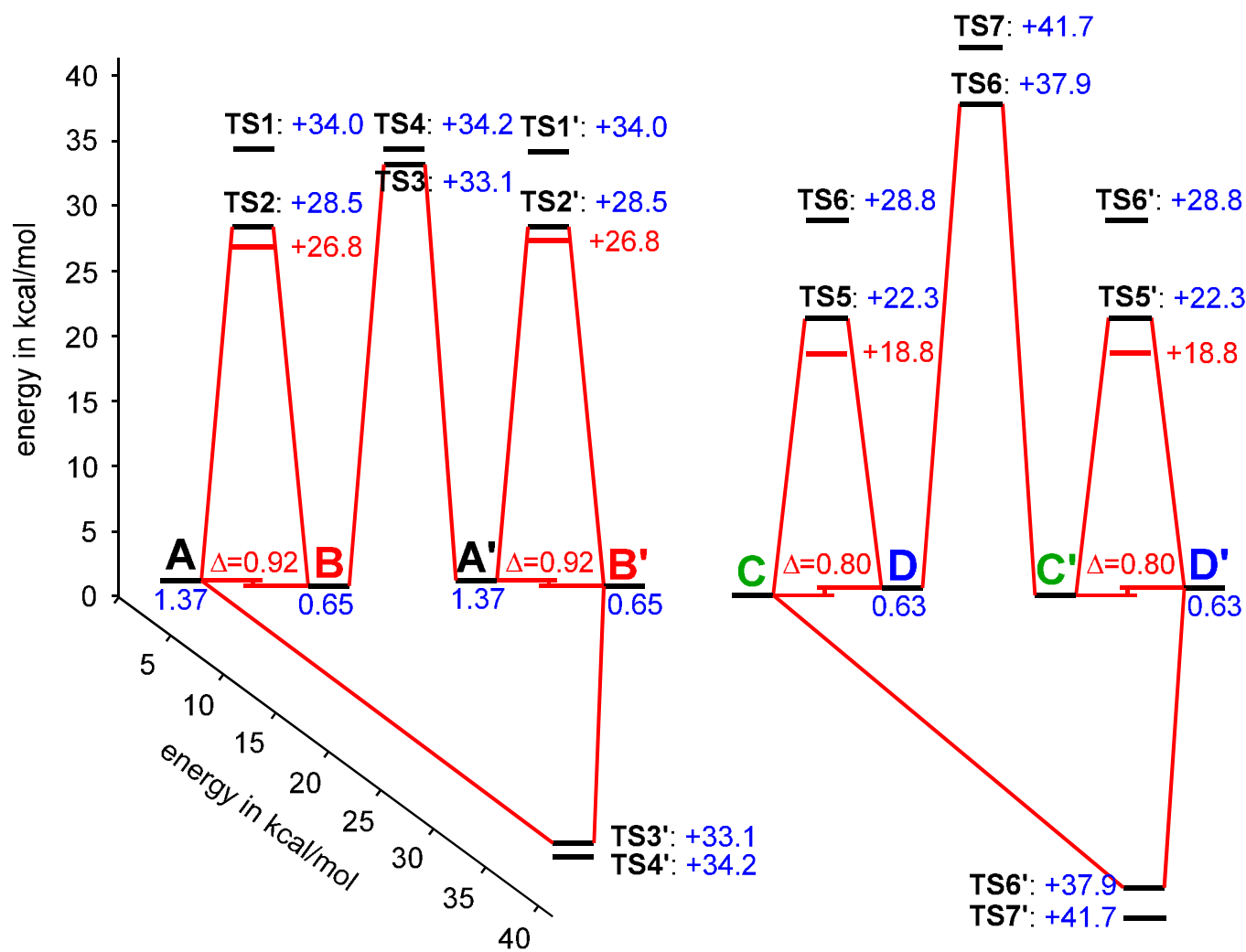
Supplementary Figure 11. a) Thermal atropisomerization of **A** to **B** in $\text{MeCN-}d_3$ at $62\text{ }^\circ\text{C}$ followed by ^1H NMR spectroscopy (400 MHz, $20\text{ }^\circ\text{C}$) in regular time intervals. b) Atropisomer conversion over time. c) First order kinetic analysis of the thermal atropisomerization of **A** to **B**. Taking into account the dynamic equilibrium by plotting according to eq. 1 gives a linear relationship. The slope m can be translated into the rate constants $k_{(A/B)}$ according to eq. 3. The corresponding Gibbs energy of activation for the thermal **A** to **B** isomerization is given in Supplementary Table 1.



Supplementary Figure 12. a) Thermal atropisomerization of **D** to **C** in $\text{MeCN-}d_3$ at $-20\text{ }^\circ\text{C}$ followed by ^1H NMR spectroscopy (400 MHz, $-20\text{ }^\circ\text{C}$) in regular time intervals (only every tenth spectrum is shown). b) Atropisomer conversion over time. c) First order kinetic analysis of the thermal atropisomerization of **D** to **C**. Taking into account the dynamic equilibrium by plotting according to eq. 2 gives a linear relationship. The slope m can be translated into the rate constants $k_{(D/C)}$ according to eq. 4. The corresponding Gibbs energy of activation for the thermal **D** to **C** isomerization are given in Supplementary Table 1.

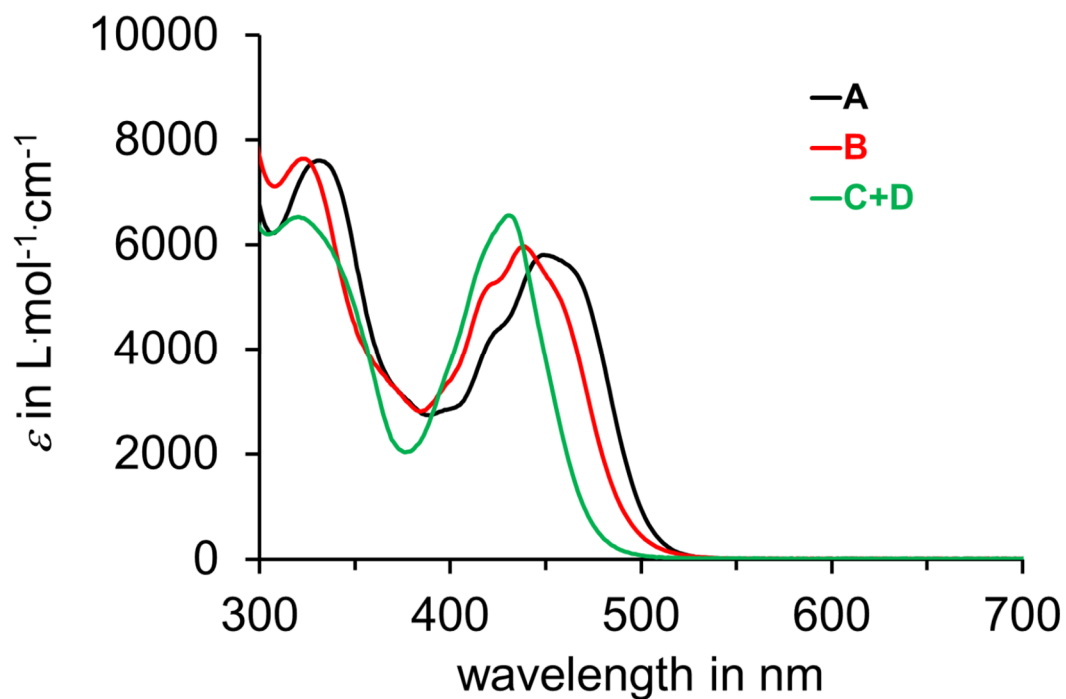
Supplementary Table 1. Thermal isomerization behavior of HTI **1** in MeCN-*d*₃ at different temperatures.

Isomer	$k_{(\text{isom. 1/isom. 2})} / \text{s}^{-1}$ (at $T / ^\circ\text{C}$)	ΔG^\ddagger (therm. isomer equilibration) /kcal mol ⁻¹	Equilibration half- life of pure isomer at 25 °C	Thermodynamic isomer 1/isomer 2 equilibrium in the dark (at $T / ^\circ\text{C}$)	$\Delta G(\text{isomer 1} /$ $\text{isomer 2}) /$ kcal mol ⁻¹	Slope $m /$ s ⁻¹ (at $T / ^\circ\text{C}$)
<i>rac</i> - A	$k_{(\text{A/B})} = 2.513 \times 10^{-5}$ (62 °C)	$\Delta G^\ddagger (\text{A/B}) =$ 26.75	54 d	A/B = 20/80 (62 °C)	$\Delta G(\text{A/B}) =$ 0.92	3.16×10^{-5} (62 °C)
<i>rac</i> - D	$k_{(\text{D/C})} = 2.992 \times 10^{-4}$ (-20 °C)	$\Delta G^\ddagger (\text{D/C}) =$ 18.8	6.9 s	D/C = 14/86 (20 °C)	$\Delta G(\text{D/C}) =$ 0.80	3.58×10^{-4} (-20 °C)

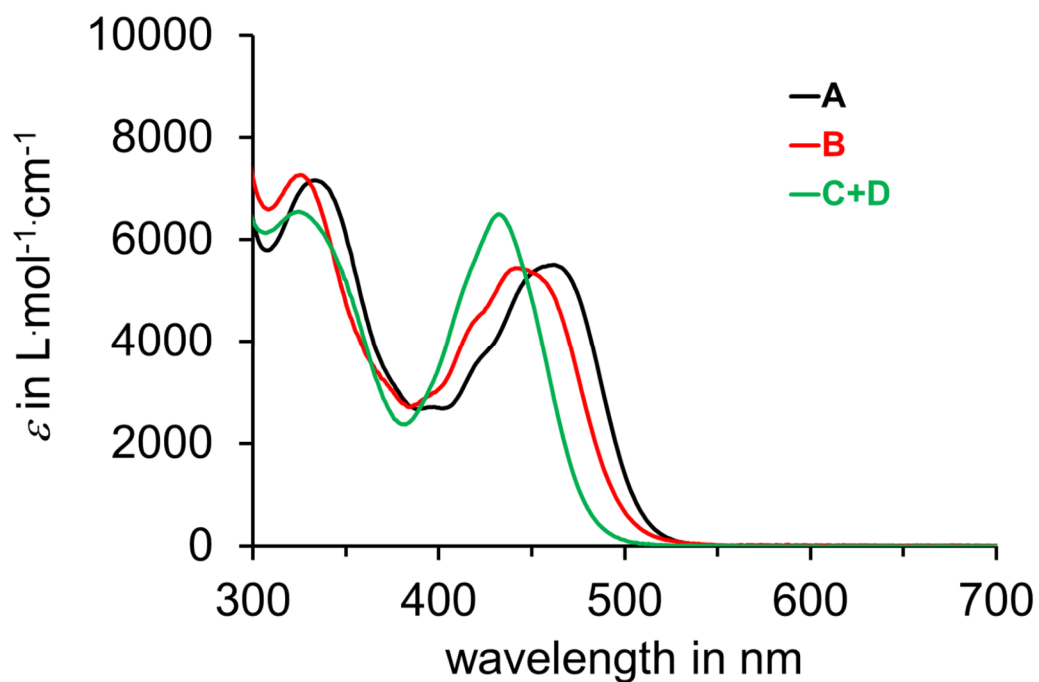


Supplementary Figure 13. Ground state energy profile for **1**. Possible thermal interconversions between the different isomers **A** to **D** by rotating one single bond are shown with red connections. Black values are derived from quantum chemical calculations (B3LYP/6-311G(d,p)), red values were determined experimentally in MeCN-*d*₃. The Δ values correspond to the experimentally determined ΔG values.

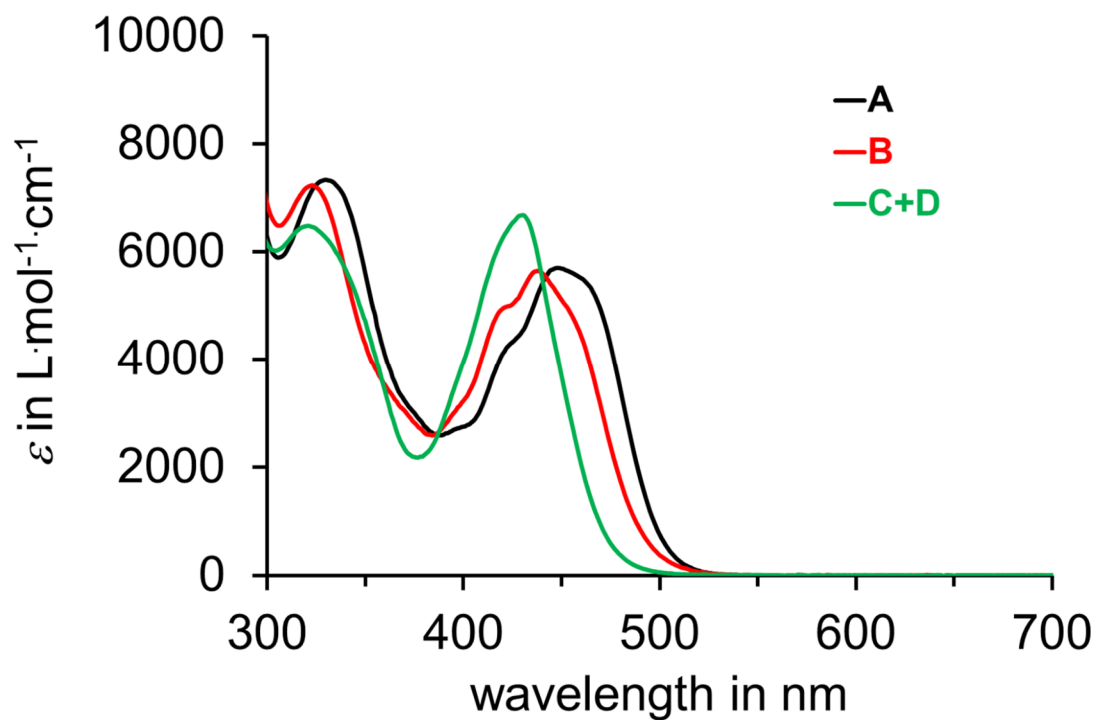
Molar extinction coefficients



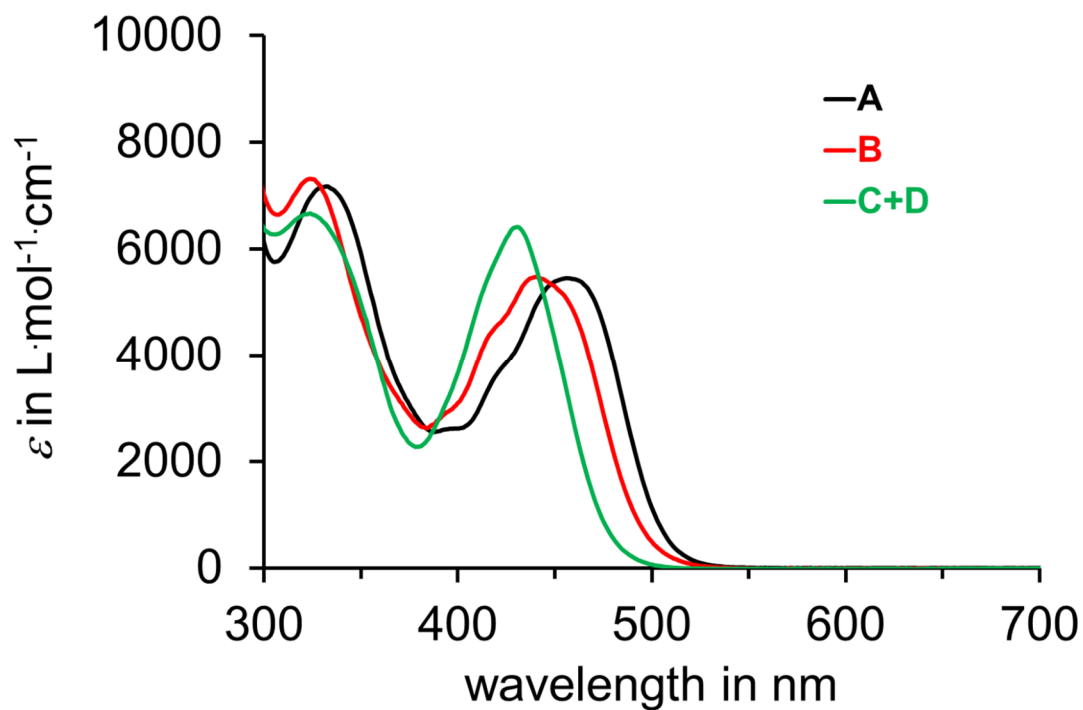
Supplementary Figure 14. Molar extinction coefficients of A (black), B (red), and C + D in thermal equilibrium (green) at 20 °C in toluene solution.



Supplementary Figure 15. Molar extinction coefficients of A (black), B (red), and C + D in thermal equilibrium (green) at 20 °C in CH_2Cl_2 solution.

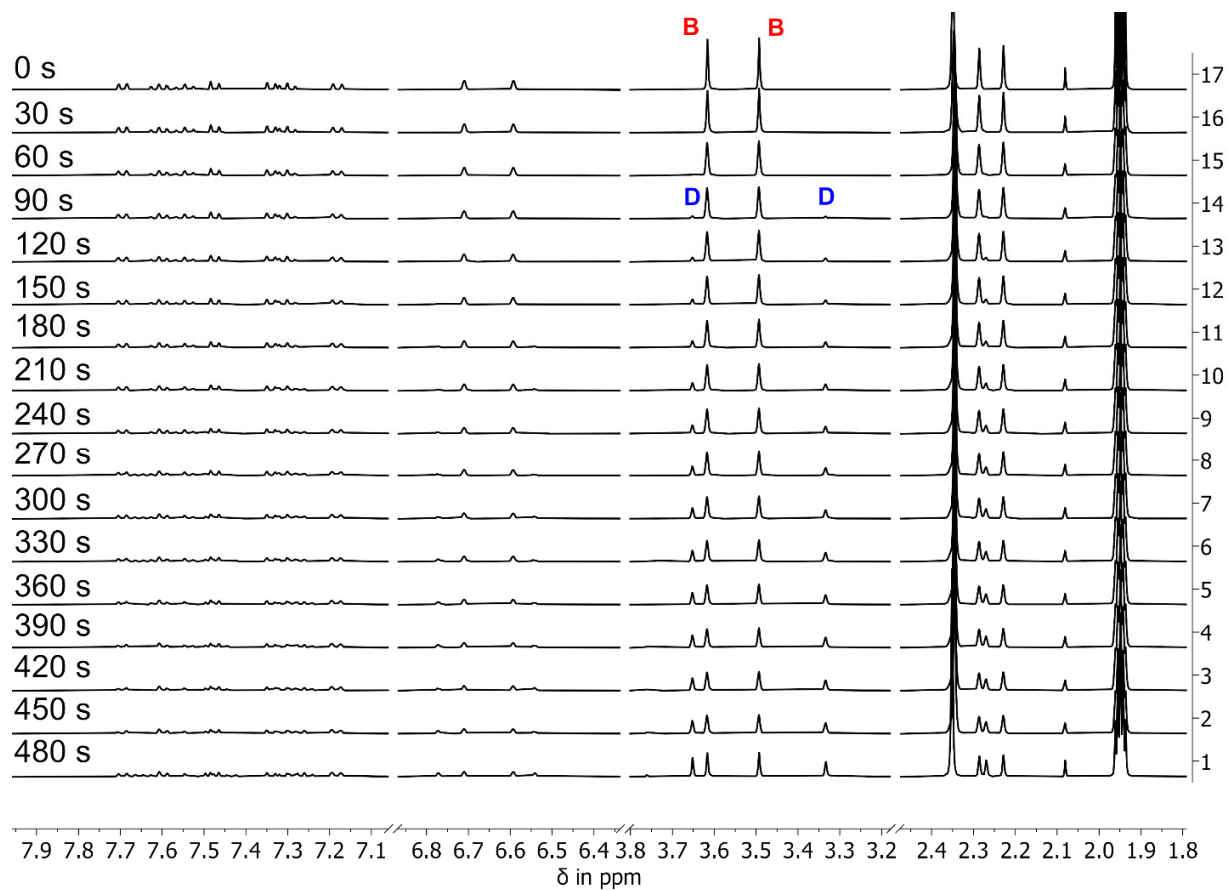


Supplementary Figure 16. Molar extinction coefficients of **A** (black), **B** (red), and **C + D** in thermal equilibrium (green) at 20 °C in THF solution.

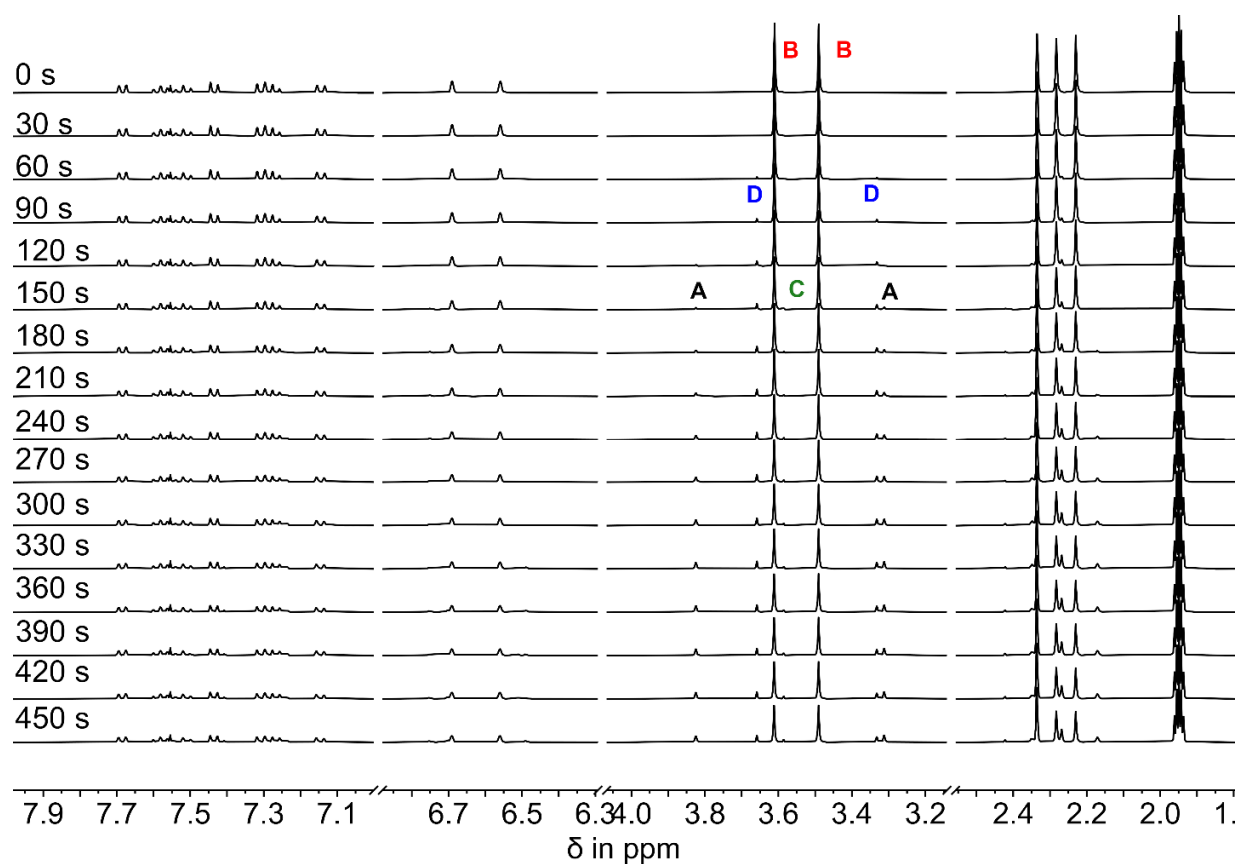


Supplementary Figure 17. Molar extinction coefficients of **A** (black), **B** (red), and **C + D** in thermal equilibrium (green) at 20 °C in MeCN solution.

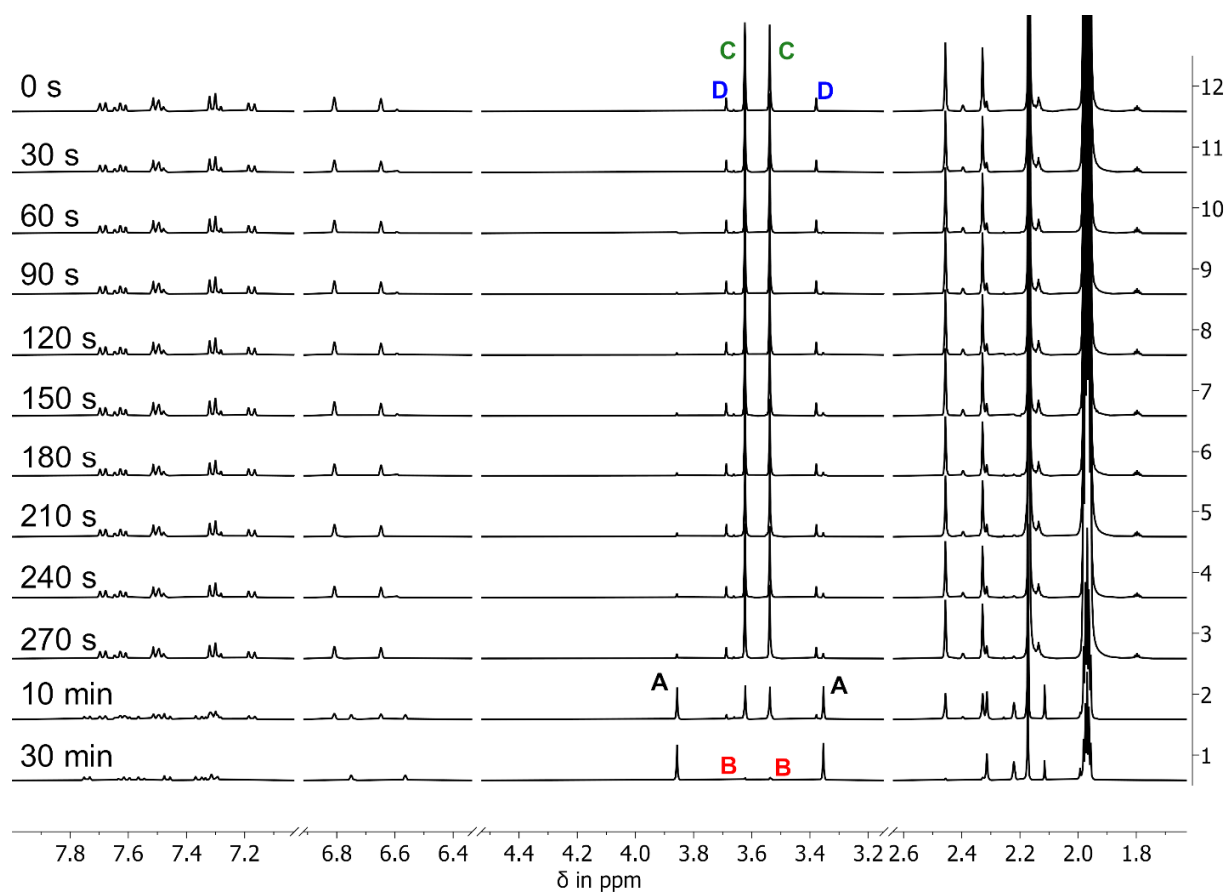
Photoconversion of *rac-A*, *rac-B*, *rac-C*, and *rac-D* followed by NMR-spectroscopy



Supplementary Figure 18: Photoconversion of isomer *rac-B* to isomer *rac-D* followed by ¹H NMR spectroscopy in MeCN-*d*₃ at -40 °C under illumination with 450 nm.



Supplementary Figure 19: Photoconversion of isomer *rac-B* to isomer *rac-D* followed by NMR spectroscopy in $\text{MeCN-}d_3$ at $-30\text{ }^\circ\text{C}$ under illumination with 450 nm. At $-30\text{ }^\circ\text{C}$ a thermal reaction from isomer **D** to isomer **C** can occur. The kinetic for this reaction without illumination is shown in Supplementary Figure 12. Under continued illumination isomer **C** is converted photochemically into isomer **A**.



Supplementary Figure 20: Photoconversion of an isomeric mixture of *rac*-C/D to isomer *rac*-A followed by NMR spectroscopy in MeCN-*d*₃ at 20 °C under illumination with 405 nm. A is nearly exclusively formed in the PSS in up to 95%.

Photoconversion of *rac-B*, *rac-C*, and *rac-D* determined by quantum yield measurements

The photochemical quantum yield of the different photconversion reactions ϕ were calculated as the ratio between the numbers of isomerized molecules $n(\text{molecules isomerized})$ and the number of absorbed photons $n(h\nu)$ according to eq. 8:

$$\phi = \frac{n(\text{molecules isomerized})}{n(h\nu)} \quad (\text{eq. 8})$$

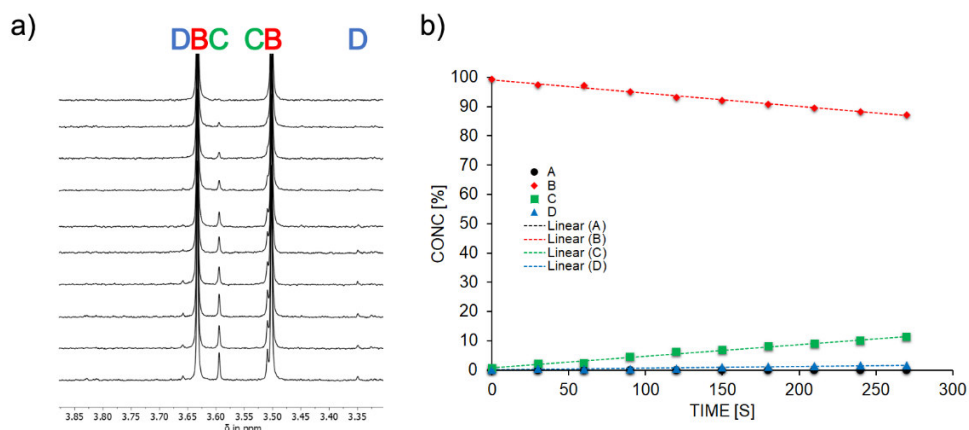
To determine the quantum yields ϕ a sample with known concentration of each pure isomer *rac-A*, *rac-B*, *rac-C*, or *rac-D* in MeCN- d_3 was irradiated with a 450 nm LED within the published instrumental setup from the group of *E. Riedle*⁴ extended with an *Oxford DN 1704* optical cryostat controlled by an *Oxford ITC 4* device to set the temperature during the measurement. The number of absorbed photons over time $n(h\nu)$ was measured directly at the thermal photometer of the instrument according to eq. 9:

$$n(h\nu) = \frac{\Delta P \cdot \lambda_{\text{ex}} \cdot t}{c \cdot h} \quad (\text{eq. 9})$$

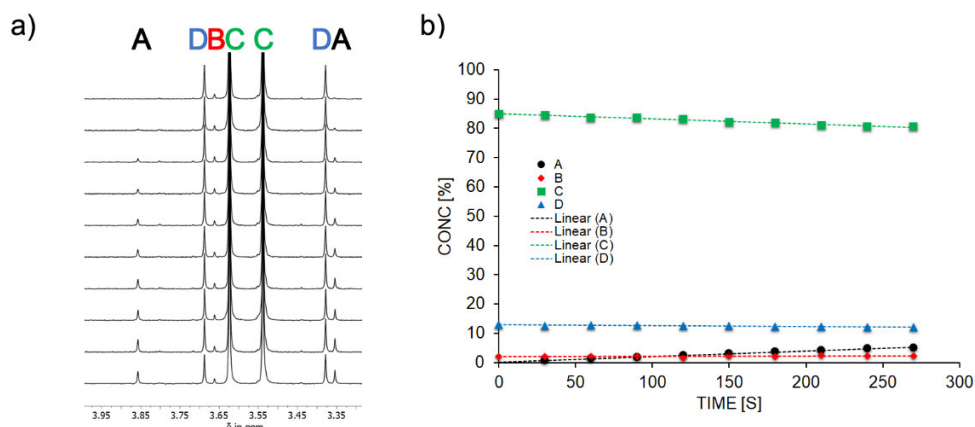
Where c is the speed of light ($2.99792 \cdot 10^8 \text{ m}\cdot\text{s}^{-1}$), h is Planck's constant ($6.62607 \cdot 10^{-34} \text{ J}\cdot\text{s}$), λ_{ex} is the excitation wavelength in m, t is the elapsed time during irradiation in s, and ΔP is the difference in power read-outs at the thermal photometer between a solvent filled cuvette (P_0) and a cuvette containing the sample solution (P_t) during the irradiation period in Watt (eq. 10). The power read out during irradiation did not change substantially (<5%) over the irradiation periods.

$$\Delta P = P_t - P_0 \quad (\text{eq.10})$$

If more than one photoproduct is formed during irradiation the number of each type of photoconverted molecules $n(\text{molecules isomerized})$ was determined by ^1H NMR spectroscopy directly after the irradiation step. Multiple measurements with increasing time of irradiation were conducted and the obtained ϕ values were averaged. The amount of isomerized molecules was also plotted against irradiation time showing linear behavior over measurement periods up to 30 min in case of *rac-B* and *rac-C* (Supplementary Figure 21 and 22). Therefore, the quantum yield measurements conform to initial-slope behavior, where only the initial isomer is photoconverted but not the photoproducts.



Supplementary Figure 21. Quantum yield ϕ measurement for the photoconversion of *rac*-**B-1** at -40 °C in MeCN-*d*₃ solution (0.91 mM) using a 450 nm LED for irradiation. a) ¹H NMR spectra (400 MHz, 20 °C) recorded after different irradiation durations. Signals of individual isomers are indicated. b) The relative changes of the isomer composition are plotted against different duration times of irradiation. After irradiation the sample was allowed to warm up to 20 °C. Therefore, the initial photoproduct is converted into *rac*-**C-1** and the thermodynamic equilibrium of *rac*-**C-1** and *rac*-**D-1** is formed and observed by NMR spectroscopy at 20 °C. From low temperature measurements it is known that *rac*-**B-1** only converts into *rac*-**D-1**, hence the quantum yield for the reaction *rac*-**B-1** to *rac*-**D-1** is calculated from the sum of the rising isomers *rac*-**C-1** and *rac*-**D-1**. Each point represents an individual measurement, the relative isomer ratios were determined by ¹H NMR spectroscopy. Linear behavior is observed showing that only *rac*-**B-1** undergoes significant photoreactions. Quantum yields were determined by averaging over all experiments (see Supplementary Table 2).



Supplementary Figure 22. Quantum yield ϕ measurement for the photoconversion of *rac-C-1* and *rac-D-1* at -40 °C in MeCN- d_3 solution (1.12 mM) using a 450 nm LED for irradiation. a) ¹H NMR spectra (400 MHz, 20 °C) recorded after different irradiation durations. Signals of individual isomers are indicated. b) The relative changes of the isomer composition are plotted against different duration times of irradiation. Relative isomer ratios were determined by ¹H NMR spectroscopy. At 20 °C isomers *rac-C-1* and *rac-D-1* are in rapid exchange with each other and a thermodynamic equilibrium of 87:13 for the *rac-C-1*:*rac-D-1* ratio is observed in solution. This ratio is maintained when the samples are cooled quickly to -40 °C for the quantum yield measurement. Therefore, both isomers can undergo photoreactions in this experiment, but the previous low temperature NMR studies show that isomer *rac-C-1* is photoreacting only to isomer *rac-A-1* and isomer *rac-D-1* is only in photoexchange with isomer *rac-B-1*. In the quantum yield measurement and in the continuous irradiation inside the NMR device at 20 °C only a photoreaction to *rac-A-1* is observable. The formation of *rac-A-1* must occur exclusively from *rac-C-1* and a photoreaction from *rac-C-1* to *rac-B-1* is not observed. The photoreaction of *rac-D-1* to *rac-B-1* is therefore much slower than the photoreaction from *rac-C-1* to *rac-A-1* and cannot be measured. This may be caused by lower quantum yield or by a lower extinction coefficient of *rac-D-1* in relation to isomer *rac-C-1* and by the lower concentration of *rac-D-1*. The molar extinction coefficients of pure *rac-C-1* or *rac-D-1* are not measurable individually at 20 °C. A determination of the quantum yield of the isomer *rac-D-1* is therefore also not possible as it is not known how much light isomer *rac-D-1* is absorbing, overshadowing the photoreaction of *rac-C-1*. However, as in practice both isomers cannot be separated and the small overshadowing of the quantum yield of *rac-C-1* by *rac-D-1* cannot be circumvented, the quantum yield of the formation of *rac-A-1* is given from the thermodynamic mixture *rac-C-1* and *rac-D-1*. Quantum yields were determined by averaging over all experiments (see Supplementary Table 2).

Supplementary Table 2. Quantum yields ϕ in % for different photoconversions of **1** under irradiation with a 450 nm LED in MeCN-*d*₃ at different temperatures. SBR = single bond rotation, DBI = double bond isomerization, HT = hula twist. ^a values determined at -40 °C, ^b values determined at -40 °C from the thermodynamic equilibrium of *rac*-**C-1** and *rac*-**D-1** at 20 °C, ^c The dual single bond rotation (DSBR) reaction **B** to **B'** is not observable in the NMR experiment and was determined by multiplication of the quantum yield of **B** to **D** (HT reaction) with the ratio of **B** to **D** (HT reaction) to **B** to **B'** (DSBR reaction) as determined by the Markov matrix studies using chiral HPLC analysis (see the next section for details). All values marked with – were too small to enable a quantitative determination (at least a factor of 10 less than the more productive photoreactions), this was the general case for isomers *rac*-**A-1** and *rac*-**D-1**.

Photoreaction (all racemic)	ϕ
A to B SBR	-
A to C HT	-
A to D DBI	-
B to A SBR	- ^a
B to C DBI	- ^a
B to D HT	1.4% ^a
C to A HT	5.2% ^b
C to B DBI	- ^b
C to D SBR	- ^b
D to A DBI	- ^b
D to B HT	- ^b
D to C SBR	- ^b
B to B' DSBR	0.9% ^c

Photo and thermal conversions of the enantiomers determined by chiral HPLC and Markov matrix analysis

To determine, which enantiomer converts into which enantiomer upon irradiation or thermally we used a Markov matrix simulation model, which was used previously e.g. by the group of *B. Feringa*⁵ or our own⁶⁻⁸ to elucidate the interconversion of multiple species. The kinetic data for the photoisomerization steps were obtained by preparing a stock solution (10 ml) of every enantiomer of HTI **1** in the respective solvent, transferring an aliquot of 1 ml from this stock solution into an UV-Vis cuvette, which was cooled down to the desired temperature with an *Oxford DN 1704* optical cryostat controlled by an *Oxford ITC 4* device if needed. The cuvette was placed into the published instrumental setup for quantum yield determination from the group of *E. Riedle*⁴ to ensure constant illumination conditions and was irradiated for the given time under continuous stirring. Afterwards the solution was allowed to warm up to 20 °C (if cooled down) and transferred into an amberized sample vial and the solvent was evaporated. The sample was dissolved in the HPLC-solvent and separation of the photoproducts was performed on a DAICEL CHIRALPAK ID column (20 mm Ø x 20 mmL) with an eluent of 11 % EtoAc in *n*-heptane at 60 °C and a flow of 3 mL. All isomers could be separated except for **C** and **D**, which are in rapid equilibrium with each other at 20 °C or above that temperature. This procedure was repeated for different irradiation times until the stock solution was consumed.

Kinetic data for the corresponding thermal steps were obtained by a similar method but as the exact number of molecules does not matter for analysis of thermal kinetics the whole stock solution was heated and aliquots were withdrawn after different heating times for HPLC analysis. The resulting HPLC chromatograms are shown in Supplementary Figure 23 exemplarily for the irradiation of isomer **B-1**. Kinetic data were quantified by integration of individual chromatogram peaks and dividing through the molar extinction coefficient of the isomers at the recording wavelength of 450 nm. The kinetics were then fitted by a Markov matrix as described earlier,⁵⁻⁸ but now the simulation was extended to 8 states and included also the rates of the thermal reactions. The derivation is therefore comprehensively explained below.

For HTI **1** the rate of an individual phototransition e.g. **A** to **B**, depends on all other absorbing species present at the same time and is described by the corresponding rate matrix element $r_{P(A/B)}$ (eq. 11):

$$r_{P(A/B)} = \phi_{A/B} \cdot I_0 \cdot \epsilon_A \cdot d \cdot [A] \cdot \left(\frac{1 - e^{-d \sum_i \epsilon_i [i]}}{d \sum_i \epsilon_i [i]} \right) \quad (\text{eq. 11})$$

Likewise every phototransition from isomer **i** to isomer **j** can be written as:

$$r_{P(ij)} = \phi_{ij} \cdot I_0 \cdot \varepsilon_i \cdot d \cdot [i] \cdot \left(\frac{1 - e^{-d \sum_i \varepsilon_i [i]}}{d \sum_i \varepsilon_i [i]} \right) \quad (\text{eq. 12})$$

with ϕ_{ij} = photoisomerization quantum yield for the phototransition of **i** to **j**, I_0 the photon flux (Einstein L⁻¹ s⁻¹) of the light, ε_i the molar extinction coefficient of **i** at the wavelength of irradiation, d the pathlength of the light through the sample, $[i]$ the concentration of **i**, ε_i the molar extinction coefficient of species **i**.

In addition every reaction can occur thermally in which case the Eyring equation expresses the rate of the reaction:

$$r_{T(ij)} = \frac{k_B}{h} e^{\frac{-E_a}{RT}} \quad (\text{eq. 13})$$

with k_B = Boltzmann constant, h = Planck's constant, E_a activation energy for the reaction **i** to **j**, R = gas constant, T = temperature. The total rate of one reaction is the sum of the rates of the thermal- and photoreaction:

$$r_{(ij)} = r_{T(ij)} + r_{P(ij)} \quad (\text{eq. 14})$$

The corresponding rate matrix containing all possible rates r_{ij} for the transitions of isomers **i** into isomers **j** for HTI **1** is therefore written as:

$$M_1 = \begin{pmatrix} r_{A/A} & r_{A/A'} & r_{A/B} & r_{A/B'} & r_{A/C} & r_{A/C'} & r_{A/D} & r_{A/D'} & \mathbf{A} \\ r_{A'/A} & r_{A'/A'} & r_{A'/B} & r_{A'/B'} & r_{A'/C} & r_{A'/C'} & r_{A'/D} & r_{A'/D'} & \mathbf{A'} \\ r_{B/A} & r_{B/A'} & r_{B/B} & r_{B/B'} & r_{B/C} & r_{B/C'} & r_{B/D} & r_{B/D'} & \mathbf{B} \\ r_{B'/A} & r_{B'/A'} & r_{B'/B} & r_{B'/B'} & r_{B'/C} & r_{B'/C'} & r_{B'/D} & r_{B'/D'} & \mathbf{B'} \\ r_{C/A} & r_{C/A'} & r_{C/B} & r_{C/B'} & r_{C/C} & r_{C/C'} & r_{C/D} & r_{C/D'} & \mathbf{C} \\ r_{C'/A} & r_{C'/A'} & r_{C'/B} & r_{C'/B'} & r_{C'/C} & r_{C'/C'} & r_{C'/D} & r_{C'/D'} & \mathbf{C'} \\ r_{D/A} & r_{D/A'} & r_{D/B} & r_{D/B'} & r_{D/C} & r_{D/C'} & r_{D/D} & r_{D/D'} & \mathbf{D} \\ r_{D'/A} & r_{D'/A'} & r_{D'/B} & r_{D'/B'} & r_{D'/C} & r_{D'/C'} & r_{D'/D} & r_{D'/D'} & \mathbf{D'} \end{pmatrix} \quad (\text{eq. 15})$$

Matrix M_1 (eq. 15) describes all possible photo and thermal conversions quantitatively, but each element for the photoreactions is a nonlinear differential equation dependent on the other elements at a given time, which makes an analytical solution impossible.

We have used the different rate elements r_{ij} in the rate matrix M_1 to simulate our kinetic measurements. For every incremental irradiation step (Δt) we have used the following expressions (eq. 16 - 19) to describe the corresponding next concentration of the respective isomer:

$$[\mathbf{i}]_{t+1} = [\mathbf{i}]_t - [\mathbf{i}]_{t+1} = -[\mathbf{i}]_t - \sum r_{i/j} \Delta t + \sum r_{j/i} \Delta t \quad (\text{eq. 16})$$

While the thermal step elements in the matrix are already known from previous experiments the photo-step elements are not known and not all variables in eq. 12 are determinable in the experiment. However, the relative ratios of the quantum yields of the different photoreactions can still be identified as explained below. In general, a Markov matrix describes the probabilities for different transitions of different states $\mathbf{p}(\mathbf{ij})$ within a given time increment. For a photoreaction the probabilities are directly proportional to the rate r_{ij} of the transition if all molar extinction coefficients are the same (this is to a good approximation the case for HTI **1** at the irradiation wavelength of 450 nm as seen by the molar absorption coefficients):

$$\mathbf{p}(\mathbf{ij}) = k_{\mathbf{p}(\mathbf{ij})} \cdot \Delta t = \frac{r_{ij}}{[\mathbf{i}]} \cdot \Delta t = \frac{\phi_{ij} \cdot I_0 \cdot \varepsilon_i \cdot d \cdot [\mathbf{i}] \cdot \left(\frac{1 - e^{-d \sum_i \varepsilon_i [\mathbf{i}]}}{d \sum_i \varepsilon_i [\mathbf{i}]} \right)}{[\mathbf{i}]} \cdot \Delta t \quad (\text{eq. 17})$$

Additionally we have to include the diagonal elements $\mathbf{p}(\mathbf{ii})$ describing the probability that no conversion occurs:

$$\mathbf{p}(\mathbf{ij}) = 1 - \sum_j \mathbf{p}_{P(\mathbf{ij})} \quad (\text{eq. 18})$$

We conducted independent irradiation experiments for each solvent starting from enantiomerically pure samples. If it is possible to keep I_0 , d , and the initial concentration of the pure isomer $[\mathbf{i}]$ constant and the same in every experiment and if also the molar extinction coefficients of all different isomers are the same at the irradiation wavelength, the same Markov matrix can be used to describe all experiments. In this case eq. 18 transforms into:

$$\mathbf{p}(\mathbf{ij}) = \frac{\phi_{ij} \cdot I_0 \cdot \varepsilon_i \cdot d \cdot [\mathbf{i}] \cdot \left(\frac{1 - e^{-d \sum_i \varepsilon_i [\mathbf{i}]}}{d \sum_i \varepsilon_i [\mathbf{i}]} \right)}{[\mathbf{i}]} \cdot \Delta t = \phi_{ij} \cdot I_0 \cdot \varepsilon_i \cdot d \cdot \left(\frac{1 - e^{-d \sum_i \varepsilon_i [\mathbf{i}]}}{d \sum_i \varepsilon_i [\mathbf{i}]} \right) \cdot \Delta t = \phi_{ij} \cdot \text{const} \cdot \Delta t \quad (\text{eq. 19})$$

and only depends on the individual quantum yields ϕ_{ij} .

Even if the mentioned variables are not constant the relative ratios of off-diagonal elements in each row of the Markov matrix reproduce the relative ratios of the corresponding quantum yields ϕ according to eq. 20 (exemplarily for the photoconversions of **A** to **B** and **C**):

$$\frac{p(\mathbf{AB})}{p(\mathbf{AC})} = \frac{\phi_{\mathbf{AB}} \cdot I_0 \cdot \varepsilon_{\mathbf{A}} \cdot d \cdot \left(\frac{1 - e^{-d \sum_i \varepsilon_i [\mathbf{i}]}}{d \sum_i \varepsilon_i [\mathbf{i}]} \right) \cdot \Delta t}{\phi_{\mathbf{AC}} \cdot I_0 \cdot \varepsilon_{\mathbf{A}} \cdot d \cdot \left(\frac{1 - e^{-d \sum_i \varepsilon_i [\mathbf{i}]}}{d \sum_i \varepsilon_i [\mathbf{i}]} \right) \cdot \Delta t} = \frac{\phi_{\mathbf{AB}}}{\phi_{\mathbf{AC}}} \quad (\text{eq. 20})$$

As can be seen from eq. 20 the relative ratios of off-diagonal elements in each row of a Markov matrix directly correspond to the respective quantum yield ratios even if the molar extinction coefficients of different present isomers are different to each other (the sum expressions cancel each other out). As the matrix elements of one row correspond to one and the same experiment I_0 , d , and the initial concentration of the pure isomer $[\mathbf{i}]$ are constant per se. Therefore, the relative ratios within one row of each Markov matrix have to be the same for all matrices.

Likewise, the ratio of one off-diagonal probability to the sum of all off-diagonal probabilities within one row of the Markov matrix is related to the corresponding ratio of the quantum yields giving the relative percentage of each process:

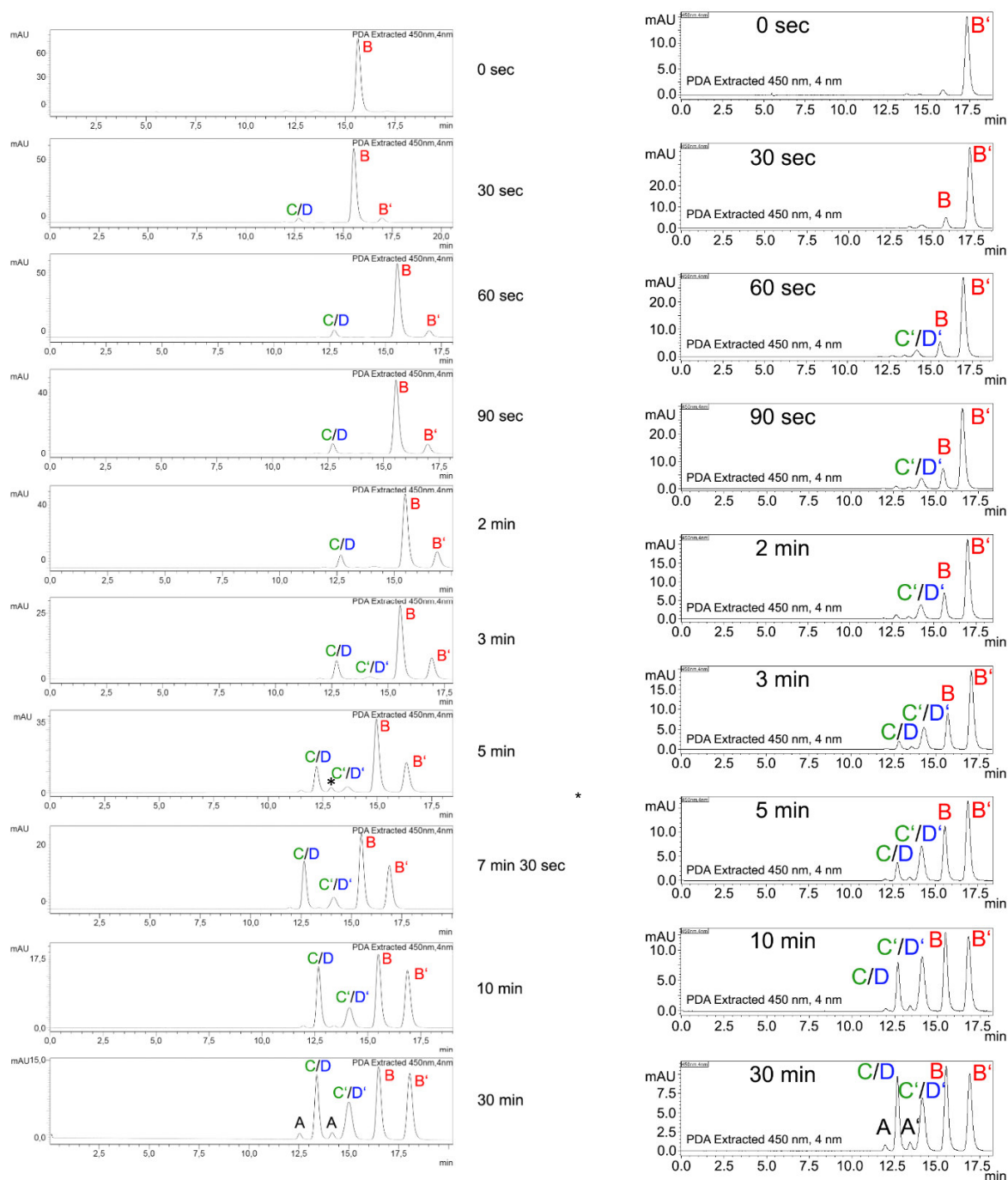
$$\text{rel. \%} = \frac{p(\mathbf{ij})}{\sum p(\mathbf{ij})} = \frac{\phi(\mathbf{ij})}{\sum \phi(\mathbf{ij})} \quad (\text{eq. 21})$$

Additionally, the diagonal elements in the same Markov matrix can be compared at least qualitatively if the different molar extinction coefficients ε_i are similar enough. This gives a quantitative assessment of the relative efficiencies of the overall photoconversions for each starting isomer.

By plotting the relative isomer percentage against the elapsed time during irradiation, different kinetic plots (starting from the eight pure isomers) were obtained from the experiments. These plots show the changes in isomer composition over time during the irradiation. This experimental kinetics were then simulated via an iterative process in which a Markov matrix M_1 (eq. 15) is multiplied with the corresponding isomer percentage vector for each time point (eq. 22). The product vector is then multiplied by the same Markov matrix to give the corresponding vector of the next time point:

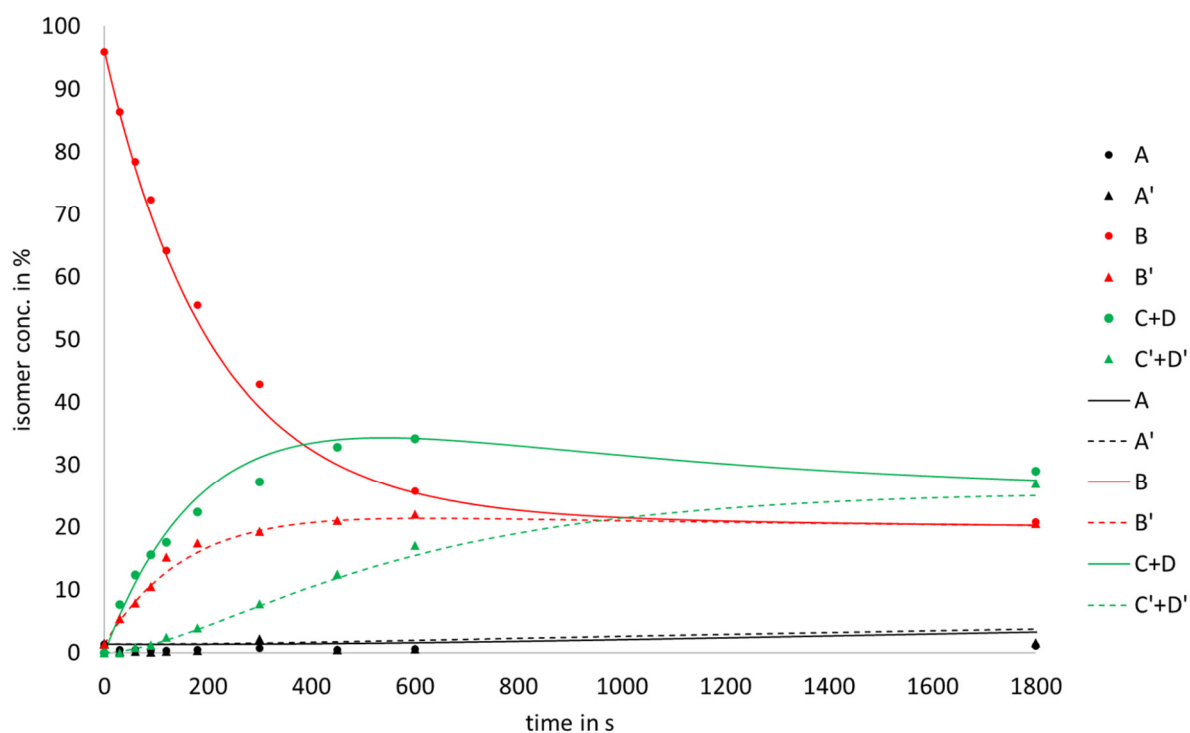
$$\begin{pmatrix} \%A \\ \%A' \\ \%B \\ \%B' \\ \%C \\ \%C' \\ \%D \\ \%D' \end{pmatrix}_{t_{x+1}} = \begin{pmatrix} r_{A/A} & r_{A/A'} & r_{A/B} & r_{A/B'} & r_{A/C} & r_{A/C'} & r_{A/D} & r_{A/D'} \\ r_{A'/A} & r_{A'/A'} & r_{A'/B} & r_{A'/B'} & r_{A'/C} & r_{A'/C'} & r_{A'/D} & r_{A'/D'} \\ r_{B/A} & r_{B/A'} & r_{B/B} & r_{B/B'} & r_{B/C} & r_{B/C'} & r_{B/D} & r_{B/D'} \\ r_{B'/A} & r_{B'/A'} & r_{B'/B} & r_{B'/B'} & r_{B'/C} & r_{B'/C'} & r_{B'/D} & r_{B'/D'} \\ r_{C/A} & r_{C/A'} & r_{C/B} & r_{C/B'} & r_{C/C} & r_{C/C'} & r_{C/D} & r_{C/D'} \\ r_{C'/A} & r_{C'/A'} & r_{C'/B} & r_{C'/B'} & r_{C'/C} & r_{C'/C'} & r_{C'/D} & r_{C'/D'} \\ r_{D/A} & r_{D/A'} & r_{D/B} & r_{D/B'} & r_{D/C} & r_{D/C'} & r_{D/D} & r_{D/D'} \\ r_{D'/A} & r_{D'/A'} & r_{D'/B} & r_{D'/B'} & r_{D'/C} & r_{D'/C'} & r_{D'/D} & r_{D'/D'} \end{pmatrix} \cdot \begin{pmatrix} \%A \\ \%A' \\ \%B \\ \%B' \\ \%C \\ \%C' \\ \%D \\ \%D' \end{pmatrix}_{t_x} \quad (\text{eq. 22})$$

The elements of the Markov matrix in eq. 22 were adjusted manually until the best match with the experimental data was obtained. All ratios determined from the irradiation experiments in different solvents are summarized in Supplementary Table 2 and shown in Supplementary Figures 24-39. Note that column values signify the starting point isomer and the row elements signify the product formed, i.e. the individual elements, e.g. $r_{A/A'}$ in the matrix read as starting point **A** and product **A'** of the transformation.



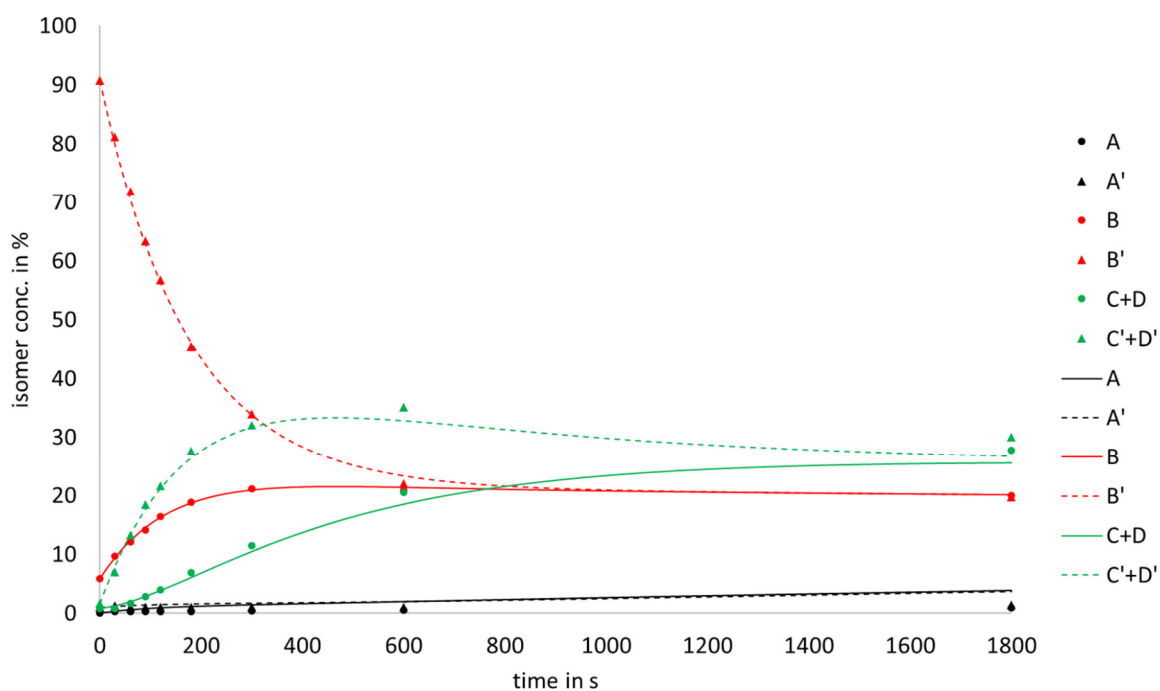
Supplementary Figure 23. Photoconversion of **B-1** (HPLC traces shown at the left) and of **B'-1** (HPLC traces shown at the right) at $-40\text{ }^{\circ}\text{C}$ in MeCN solution using a 450 nm LED for irradiation. HPLC chromatograms (measured at 450 nm absorption, DAICEL CHIRALPAK ID column (20 mm \varnothing x 20 mL) with an eluent of 11 % EtoAc in *n*Heptane at $60\text{ }^{\circ}\text{C}$ and a flow of 3 mL) were recorded after different irradiation durations. Signals of individual isomers are indicated. The corresponding integration values and resulting kinetics are shown in Supplementary Figure 24 and 25.
* Impurity.

B irradiation 450 nm



Supplementary Figure 24. Photoconversion of **B-1** at $-40\text{ }^{\circ}\text{C}$ in MeCN solution using a 450 nm LED for irradiation. The isomer composition (dots) was determined by integration of the respective HPLC chromatogram peaks (DAICEL CHIRALPAK ID column (20 mm \varnothing x 20 mL) with an eluent of 11 % EtoAc in *n*Heptane at $60\text{ }^{\circ}\text{C}$ and a flow of 3 mL). HPLC chromatograms were recorded after different irradiation durations. Kinetics are modeled by the Markov matrix shown in Supplementary Figure 26 (lines).

B' irradiation 450 nm

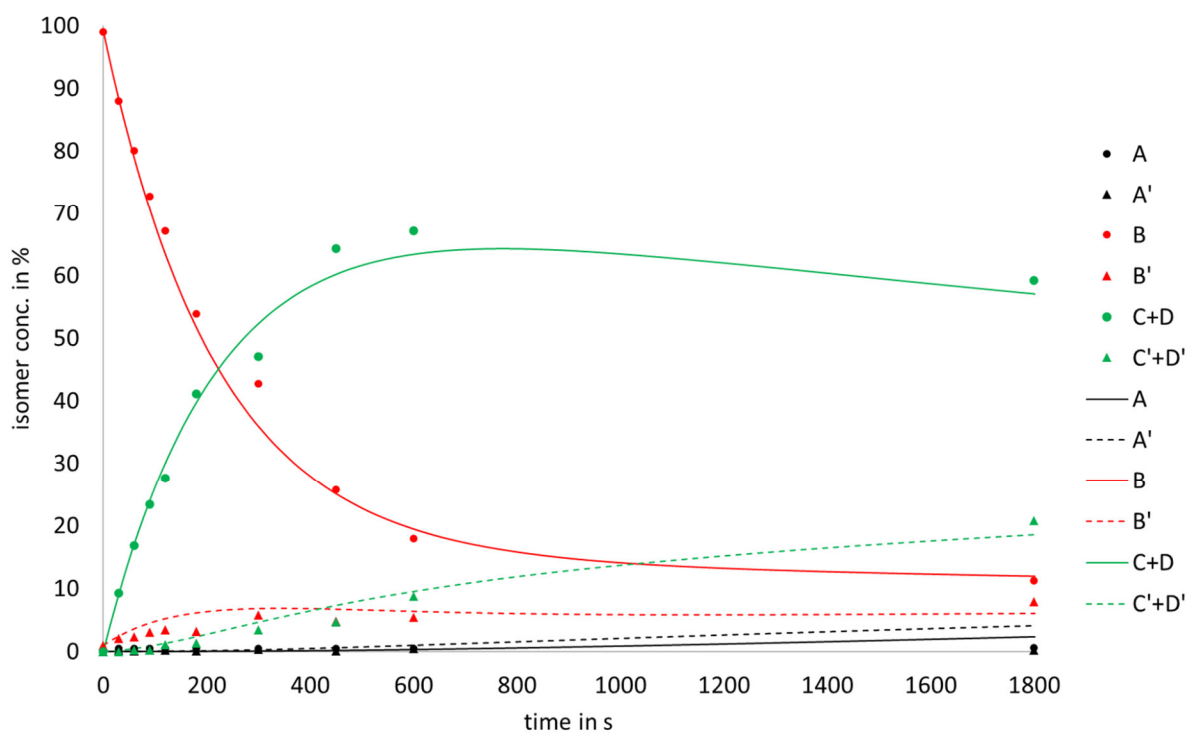


Supplementary Figure 25. Photoconversion of **B'-1** at $-40\text{ }^{\circ}\text{C}$ in MeCN solution using a 450 nm LED for irradiation. The isomer composition (dots) was determined by integration of HPLC chromatogram peaks (DAICEL CHIRALPAK ID column (20 mm \varnothing x 20 mmL) with an eluent of 11 % EtoAc in *n*Heptane at $60\text{ }^{\circ}\text{C}$ and a flow of 3 mL). HPLC chromatograms were recorded after different irradiation durations. Kinetics are modeled by the Markov matrix shown in Supplementary Figure 26 (lines).

A	A'	B	B'	C	C'	D	D'	
-	$1.88 \cdot 10^{-4}$	28.7	27.1	$1.25 \cdot 10^{-4}$	$6.25 \cdot 10^{-5}$	-	-	A
$2.25 \cdot 10^{-4}$	-	27.1	28.7	$6.25 \cdot 10^{-5}$	$1.25 \cdot 10^{-4}$	-	-	A'
29.6	28.0	-	$1.47 \cdot 10^{-3}$	-	-	$2.28 \cdot 10^{-3}$	-	B
28.0	29.6	$1.47 \cdot 10^{-3}$	-	-	-	-	$2.28 \cdot 10^{-3}$	B'
$7.29 \cdot 10^{-4}$	$7.29 \cdot 10^{-3}$	-	-	-	$7.29 \cdot 10^{-4}$	18.85	-	C
$7.29 \cdot 10^{-3}$	$7.29 \cdot 10^{-4}$	-	-	$7.29 \cdot 10^{-4}$	-	-	18.85	C'
-	-	$8.75 \cdot 10^{-4}$	$8.75 \cdot 10^{-5}$	18.1	-	-	-	D
-	-	$8.75 \cdot 10^{-5}$	$8.75 \cdot 10^{-4}$	-	18.1	-	-	D'

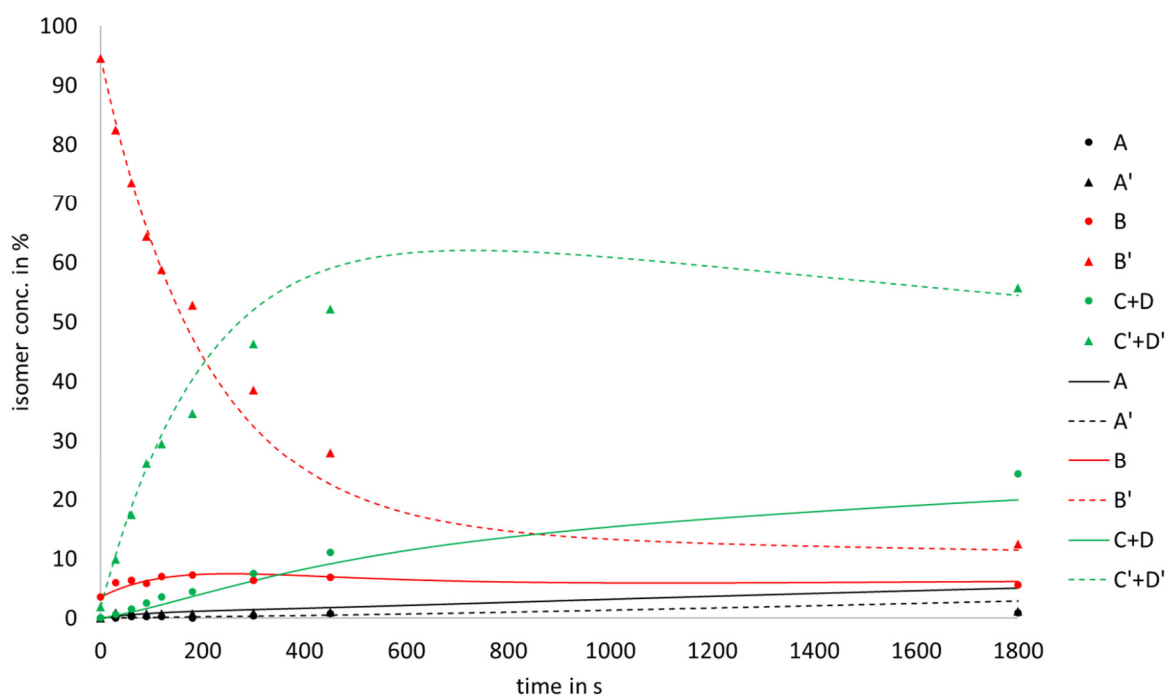
Supplementary Figure 26. Markov matrix used for modeling the kinetics of the photoconversion of **1** at -40 °C in MeCN solution using a 450 nm LED for irradiation. Black and blue values indicate photoreactions, which must be multiplied with the relative light intensity. Blue values signify the most dominant photoreaction pathways, which are preferred strongly over the other possibilities giving rise to high photochemical selectivity. Red values indicate thermal reactions and are given in $\text{kcal} \cdot \text{mol}^{-1}$, which must be converted into reaction rates using the Eyring equation for the appropriate temperature. Note that the values for the reactions of the **A-1**, **C-1**, and **D-1** enantiomers may not be highly accurate as their reactions were not measured with the pure isomers and are only fitted with the data obtained by the irradiation of the **B-1** enantiomers. These values are therefore not used in further discussions.

B irradiation 450 nm



Supplementary Figure 27. Photoconversion of **B-1** at $-80\text{ }^{\circ}\text{C}$ in MeOH solution using a 450 nm LED for irradiation. The isomer composition (dots) was determined by integration of HPLC chromatogram peaks (DAICEL CHIRALPAK ID column (20 mm \varnothing x 20 mL) with an eluent of 11 % EtoAc in *n*Heptane at $60\text{ }^{\circ}\text{C}$ and a flow of 3 mL). HPLC chromatograms were recorded after different irradiation durations. Kinetics are modeled by the Markov matrix shown in Supplementary Figure 29 (lines).

B' irradiation 450 nm

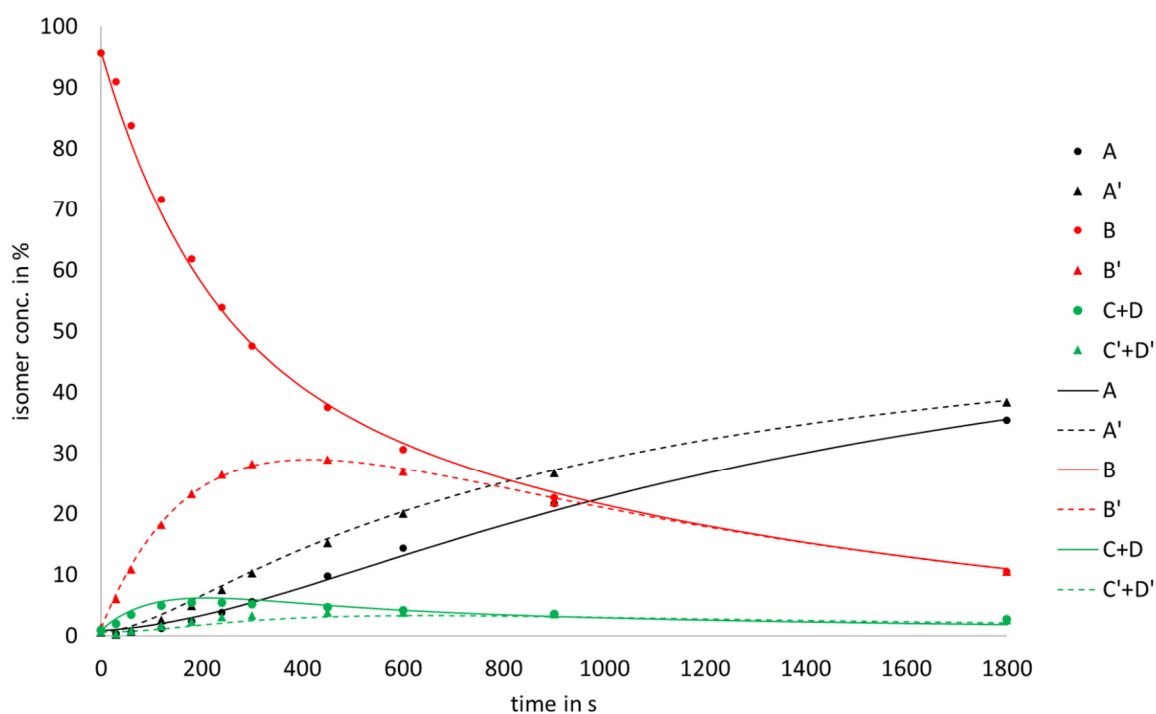


Supplementary Figure 28. Photoconversion of **B'-1** at $-80\text{ }^{\circ}\text{C}$ in MeOH solution using a 450 nm LED for irradiation. The isomer composition (dots) was determined by integration of HPLC chromatogram peaks (DAICEL CHIRALPAK ID column (20 mm \varnothing x 20 mmL) with an eluent of 11 % EtoAc in *n*Heptane at $60\text{ }^{\circ}\text{C}$ and a flow of 3 mL). HPLC chromatograms were recorded after different irradiation durations. Kinetics are modeled by the Markov matrix shown in Supplementary Figure 29 (lines).

A	A'	B	B'	C	C'	D	D'	
-	$1.95 \cdot 10^{-4}$	28.7	27.1	$1.30 \cdot 10^{-4}$	$6.50 \cdot 10^{-5}$	-	-	A
$2.25 \cdot 10^{-4}$	-	27.1	28.7	$1.50 \cdot 10^{-5}$	$1.50 \cdot 10^{-4}$	-	-	A'
29.6	28.0	-	$5.91 \cdot 10^{-4}$	-	-	$3.31 \cdot 10^{-3}$	-	B
28.0	29.6	$5.91 \cdot 10^{-4}$	-	-	-	-	$3.31 \cdot 10^{-3}$	B'
$7.58 \cdot 10^{-4}$	$7.58 \cdot 10^{-3}$	-	-	-	$7.58 \cdot 10^{-4}$	18.85	-	C
$7.58 \cdot 10^{-3}$	$7.58 \cdot 10^{-4}$	-	-	$7.58 \cdot 10^{-4}$	-	-	18.85	C'
-	-	$7.09 \cdot 10^{-4}$	$7.09 \cdot 10^{-5}$	18.1	-	-	-	D
-	-	$7.09 \cdot 10^{-5}$	$7.09 \cdot 10^{-4}$	-	18.1	-	-	D'

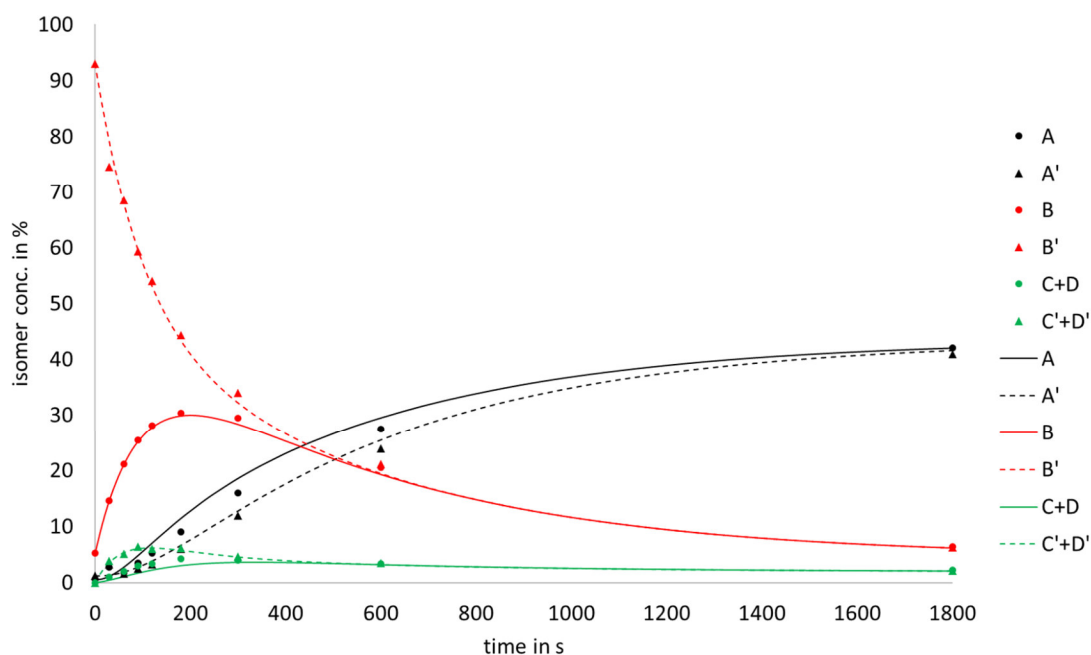
Supplementary Figure 29. Markov matrix used for modeling the kinetics of the photoconversion of **1** at -80 °C in MeOH solution using a 450 nm LED for irradiation. Black and blue values indicate photoreactions, which must be multiplied with the relative light intensity. Blue values signify the most dominant photoreaction pathways, which are preferred strongly over the other possibilities giving rise to high photochemical selectivity. Red values indicate thermal reactions and are given in $\text{kcal} \cdot \text{mol}^{-1}$, which must be converted into reaction rates using the Eyring equation for the appropriate temperature. Note that the values for the reactions of the **A-1**, **C-1**, and **D-1** enantiomers are not perfectly accurate as their reactions were not measured starting from the respective pure isomers and are only fitted with the data obtained by irradiation of the **B-1** enantiomers. These values are therefore not used in further discussions.

B irradiation 450 nm



Supplementary Figure 30. Photoconversion of **B-1** at 20 °C in toluene solution using a 450 nm LED for irradiation. The isomer composition (dots) was determined by integration of HPLC chromatogram peaks (DAICEL CHIRALPAK ID column (20 mm \varnothing x 20 mmL) with an eluent of 11 % EtoAc in *n*Heptane at 60 °C and a flow of 3 mL). HPLC chromatograms were recorded after different irradiation durations. Kinetics are modeled by the Markov matrix shown in Supplementary Figure 32 (lines).

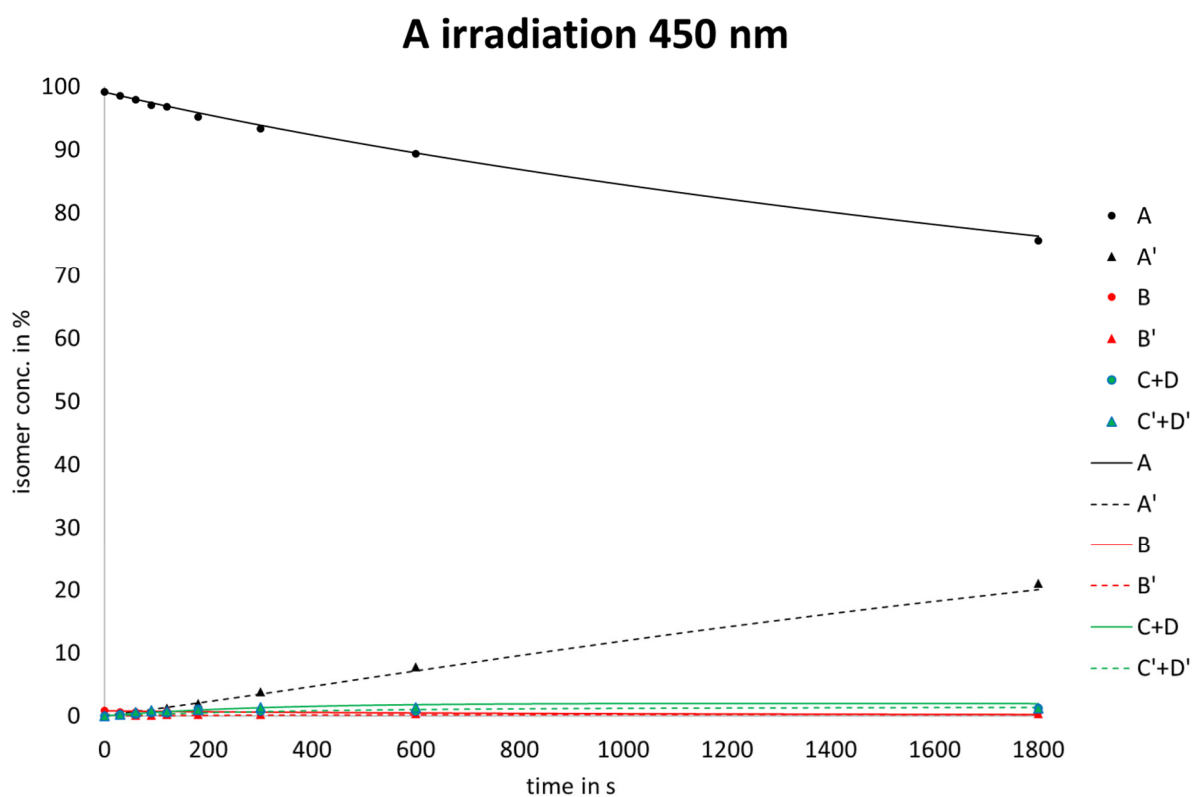
B' irradiation 450 nm



Supplementary Figure 31. Photoconversion of **B'-1** at 20 °C in toluene solution using a 450 nm LED for irradiation. The isomer composition (dots) was determined by integration of HPLC chromatogram peaks (DAICEL CHIRALPAK ID column (20 mm \varnothing x 20 mmL) with an eluent of 11 % EtoAc in *n*Heptane at 60 °C and a flow of 3 mL). HPLC chromatograms were recorded after different irradiation durations. Kinetics are modeled by the Markov matrix shown in Supplementary Figure 32 (lines).

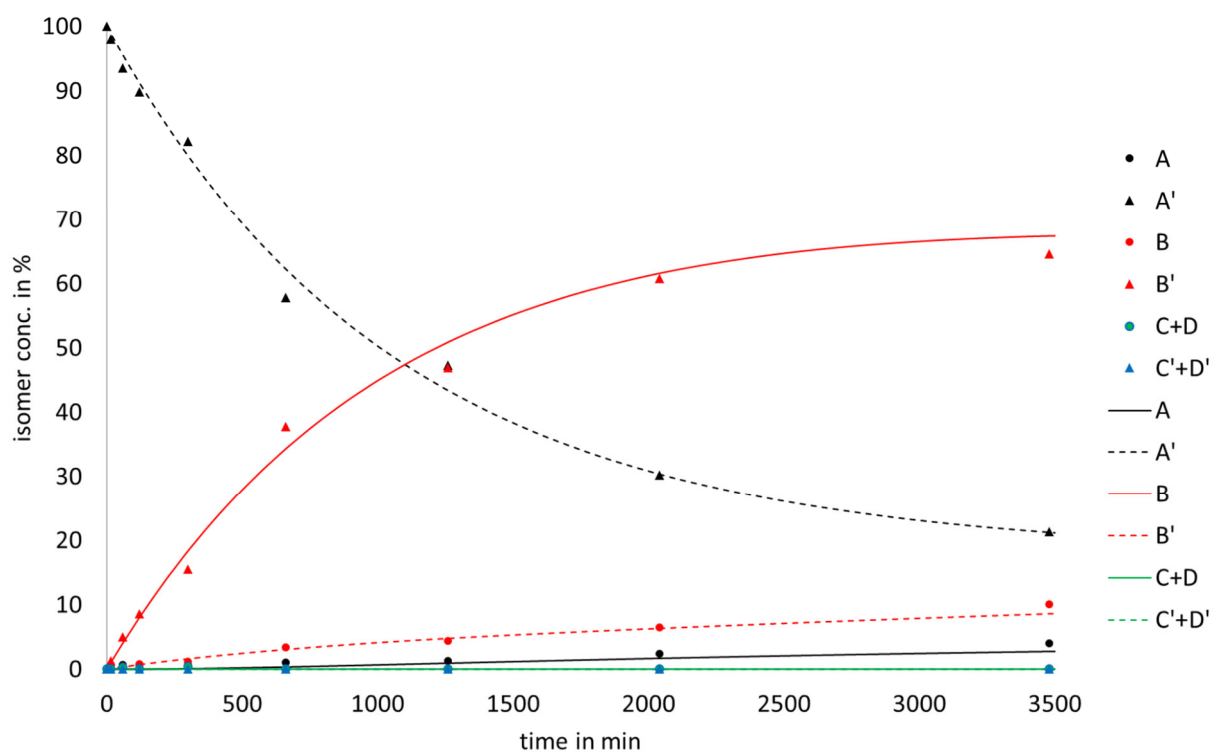
A	A'	B	B'	C	C'	D	D'	
-	$1.54 \cdot 10^{-4}$	28.7 $+2.57 \cdot 10^{-5}$	27.1 $+2.57 \cdot 10^{-5}$	$1.03 \cdot 10^{-4}$	$5.14 \cdot 10^{-5}$	-	-	A
$1.54 \cdot 10^{-4}$	-	27.1 $+2.57 \cdot 10^{-5}$	28.7 $+2.57 \cdot 10^{-5}$	$5.14 \cdot 10^{-5}$	$1.03 \cdot 10^{-4}$	-	-	A'
29.6	28.0	-	$1.30 \cdot 10^{-3}$	-	-	$4.96 \cdot 10^{-4}$	-	B
28.0	29.6	$1.30 \cdot 10^{-3}$	-	-	-	-	$4.96 \cdot 10^{-4}$	B'
$1.00 \cdot 10^{-3}$	$5.00 \cdot 10^{-3}$	-	-	-	-	18.85	-	C
$5.00 \cdot 10^{-3}$	$1.00 \cdot 10^{-3}$	-	-	-	-	-	18.85	C'
-	-	-	-	18.1	-	-	-	D
-	-	-	-	-	18.1	-	-	D'

Supplementary Figure 32. Markov matrix used for modeling the kinetics of the photoconversion of **1** at 20 °C in toluene solution using a 450 nm LED for irradiation. Black and blue values indicate photoreactions, which must be multiplied with the relative light intensity. Blue values signify the most dominant photoreaction pathways, which are preferred strongly over the other possibilities giving rise to high photochemical selectivity. Red values indicate thermal reactions and are given in $\text{kcal} \cdot \text{mol}^{-1}$, which must be converted into reaction rates using the Eyring equation for the appropriate temperature. Note that the values for the reactions of the **A-1** and **C-1** enantiomers may not be accurate as their reactions were not measured starting from pure isomers and are only fitted with the data obtained by the irradiation of the **B-1** enantiomers. These values are therefore not used in further discussions. The thermal reaction of the **D-1** enantiomers to the **C-1** enantiomers is fast at 20 °C and therefore overlaying the photochemistry of the **D-1** enantiomers.



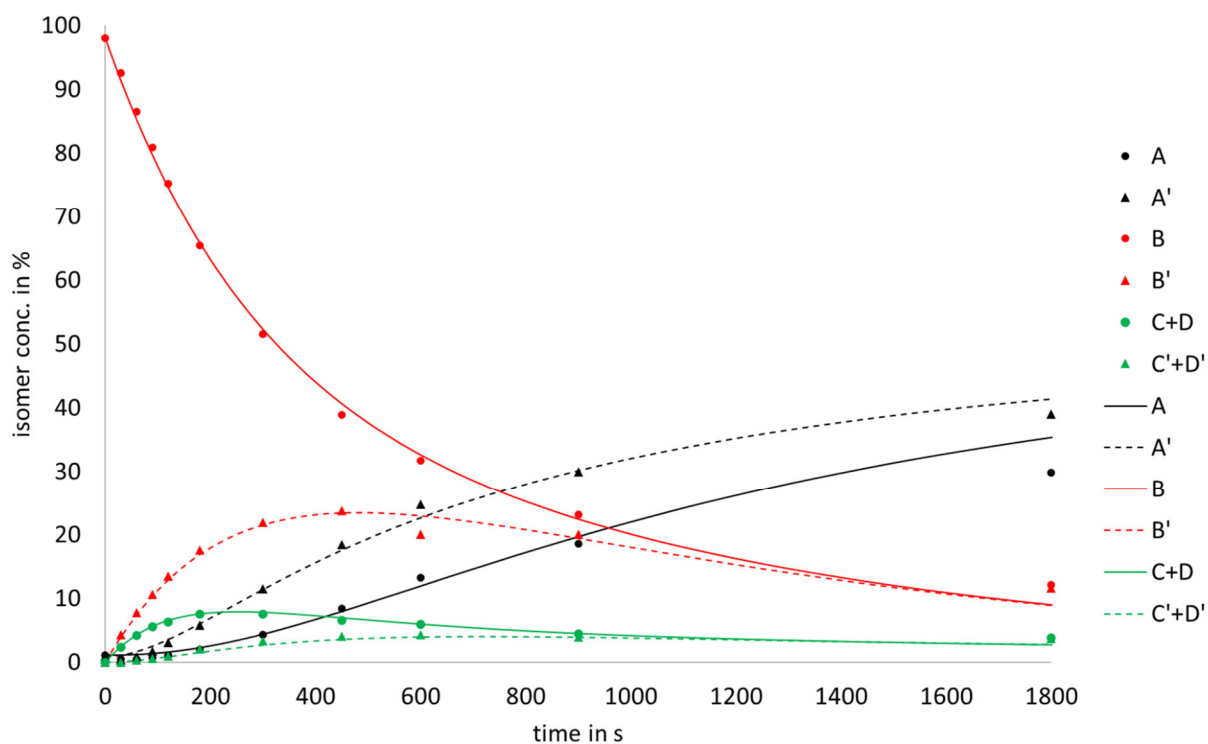
Supplementary Figure 33. Photoconversion of A-1 at 20 °C in MeCN solution using a 450 nm LED irradiation. The isomer composition (dots) was determined by integration of HPLC chromatogram peaks (DAICEL CHIRALPAK ID column (20 mm \varnothing x 20 mL) with an eluent of 11 % EtoAc in *n*Heptane at 60 °C and a flow of 3 mL). HPLC chromatograms were recorded after different irradiation durations. Kinetics are modeled by the Markov matrix shown in Supplementary Figure 39 (lines).

A' thermal reaction at 60 °C



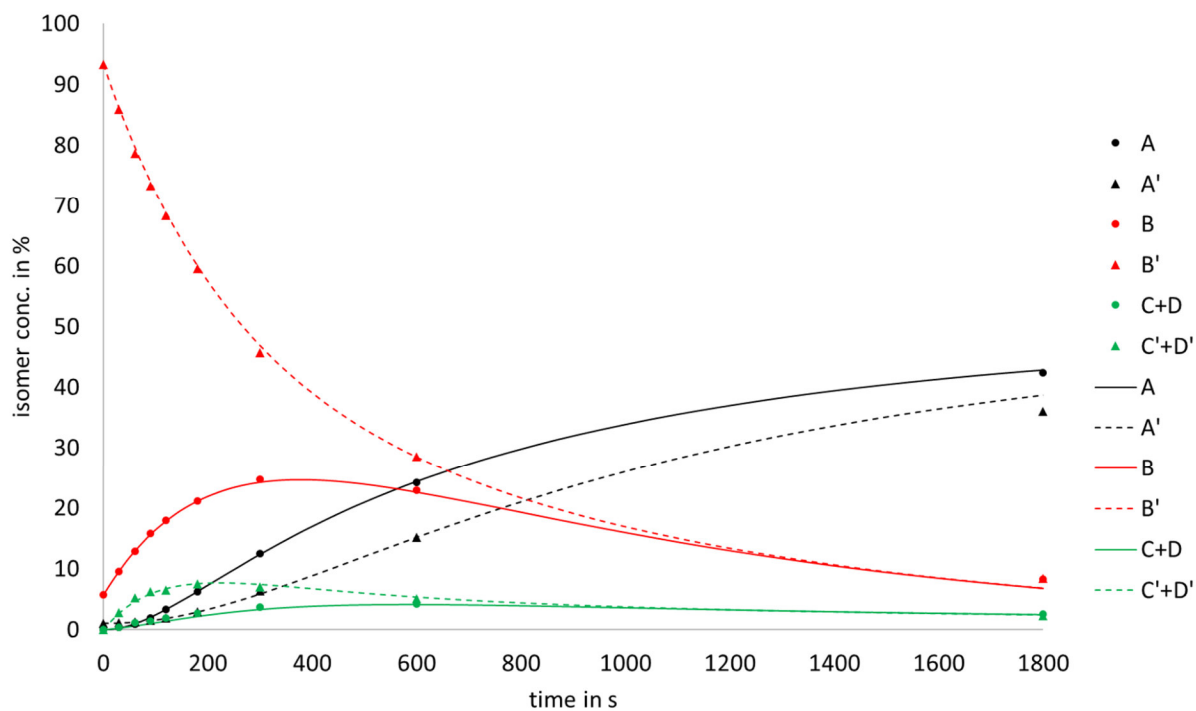
Supplementary Figure 34. Thermal conversion of A'-1 at 60 °C in MeCN solution. The isomer composition (dots) was determined by integration of HPLC chromatogram peaks (DAICEL CHIRALPAK ID column (20 mm \varnothing x 20 mmL) with an eluent of 11 % EtoAc in *n*Heptane at 60 °C and a flow of 3 mL). HPLC chromatograms were recorded after different heating durations. Kinetics are modeled by the Markov matrix shown in Supplementary Figure 39 (lines).

B irradiation 450 nm



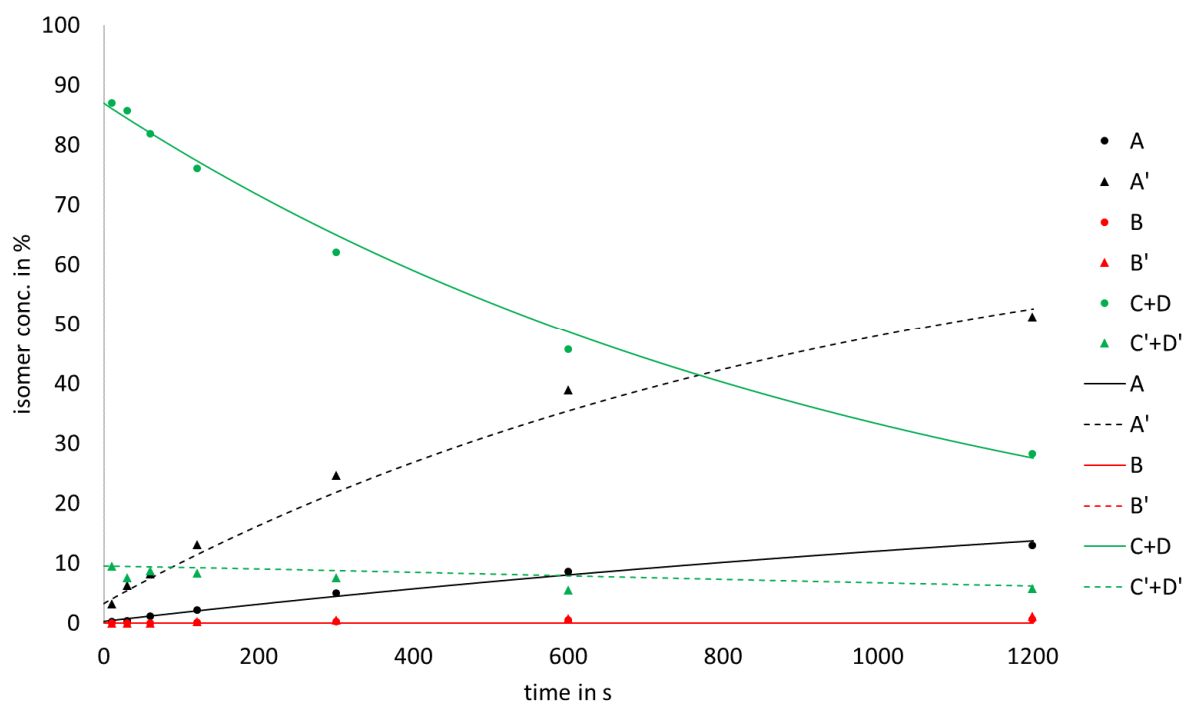
Supplementary Figure 35. Photoconversion of **B-1** at 20 °C in MeCN solution using a 450 nm LED for irradiation. The isomer composition (dots) was determined by integration of HPLC chromatogram peaks (DAICEL CHIRALPAK ID column (20 mm \varnothing x 20 mmL) with an eluent of 11 % EtoAc in *n*Heptane at 60 °C and a flow of 3 mL). HPLC chromatograms recorded after different irradiation durations. Kinetics are modeled by the Markov matrix shown in Supplementary Figure 39 (lines).

B' irradiation 450 nm

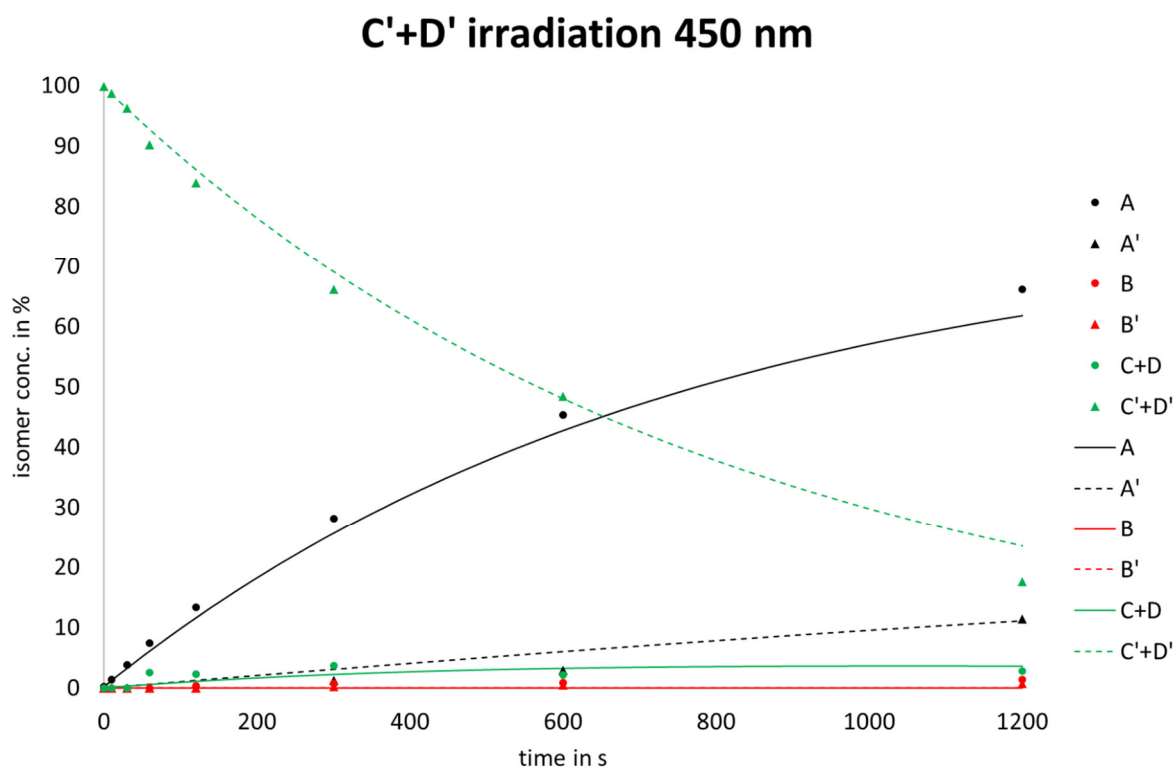


Supplementary Figure 36. Photoconversion of **B'-1** at 20 °C in MeCN solution using a 450 nm LED for irradiation. The isomer composition (dots) was determined by integration of HPLC chromatogram peaks (DAICEL CHIRALPAK ID column (20 mm \varnothing x 20 mmL) with an eluent of 11 % EtoAc in *n*Heptane at 60 °C and a flow of 3 mL). HPLC chromatograms were recorded after different irradiation durations. Kinetics are modeled by the Markov matrix shown in Supplementary Figure 39 (lines).

C+D irradiation 450 nm



Supplementary Figure 37. Photoconversion of C-1 and D-1 at 20 °C in MeCN solution using a 450 nm LED for irradiation. The isomer composition (dots) was determined by integration of HPLC chromatogram peaks (DAICEL CHIRALPAK ID column (20 mm \varnothing x 20 mL) with an eluent of 11 % EtoAc in *n*Heptane at 60 °C and a flow of 3 mL). HPLC chromatograms were recorded after different irradiation durations. Kinetics are modeled by the Markov matrix shown in Supplementary Figure 39 (lines).



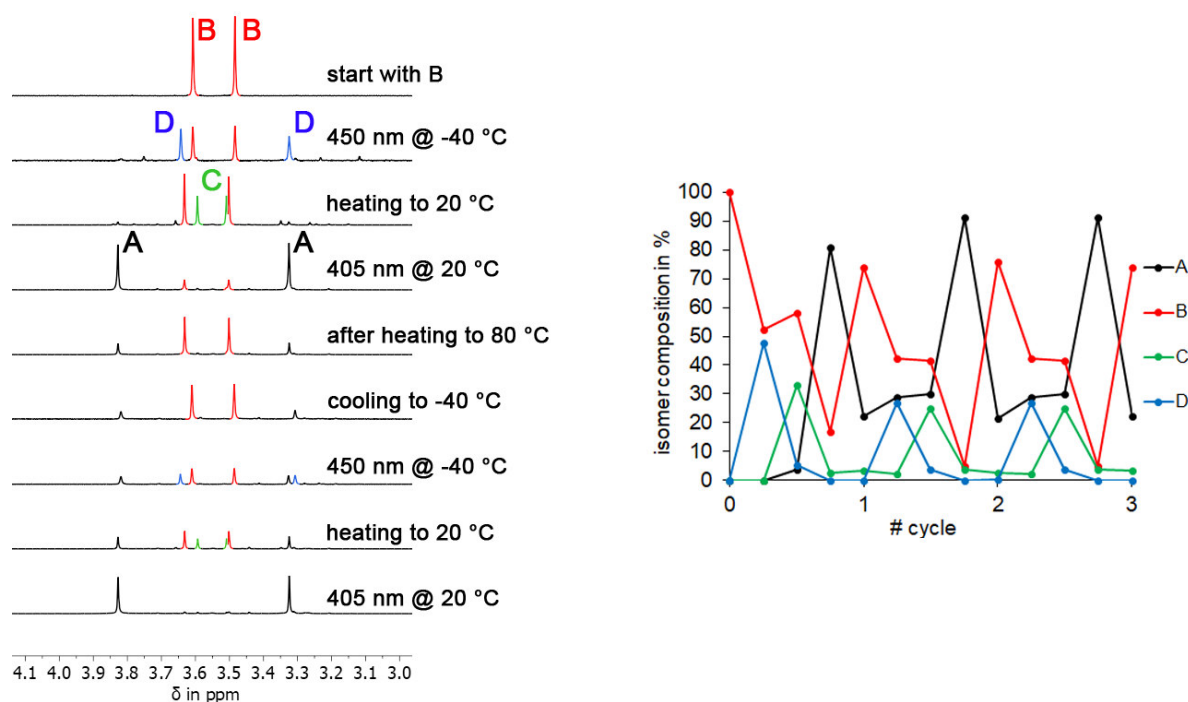
Supplementary Figure 38. Photoconversion of C'-1 and D'-1 at 20 °C in MeCN solution using a 450 nm LED for irradiation. The isomer composition (dots) was determined by integration of HPLC chromatogram peaks (DAICEL CHIRALPAK ID column (20 mm Ø x 20 mL) with an eluent of 11 % EtoAc in *n*Heptane at 60 °C and a flow of 3 mL). HPLC chromatograms were recorded after different irradiation durations. Kinetics are modeled by the Markov matrix shown in Supplementary Figure 39 (lines).

A	A'	B	B'	C	C'	D	D'	
-	$9.75 \cdot 10^{-5}$	28.7	27.1	$6.50 \cdot 10^{-5}$	$3.25 \cdot 10^{-5}$	-	-	A
$9.75 \cdot 10^{-5}$	-	27.1	28.7	$3.25 \cdot 10^{-5}$	$6.50 \cdot 10^{-5}$	-	-	A'
29.6	28.0	-	$6.30 \cdot 10^{-4}$	-	-	$4.10 \cdot 10^{-4}$	-	B
28.0	29.6	$6.30 \cdot 10^{-4}$	-	-	-	-	$4.10 \cdot 10^{-4}$	B'
$3.79 \cdot 10^{-4}$	$3.79 \cdot 10^{-3}$	-	-	-	$3.79 \cdot 10^{-4}$	18.85	-	C
$3.79 \cdot 10^{-3}$	$3.69 \cdot 10^{-4}$	-	-	$3.79 \cdot 10^{-4}$	-	-	18.85	C'
-	-	-	-	18.1	-	-	-	D
-	-	-	-	-	18.1	-	-	D'

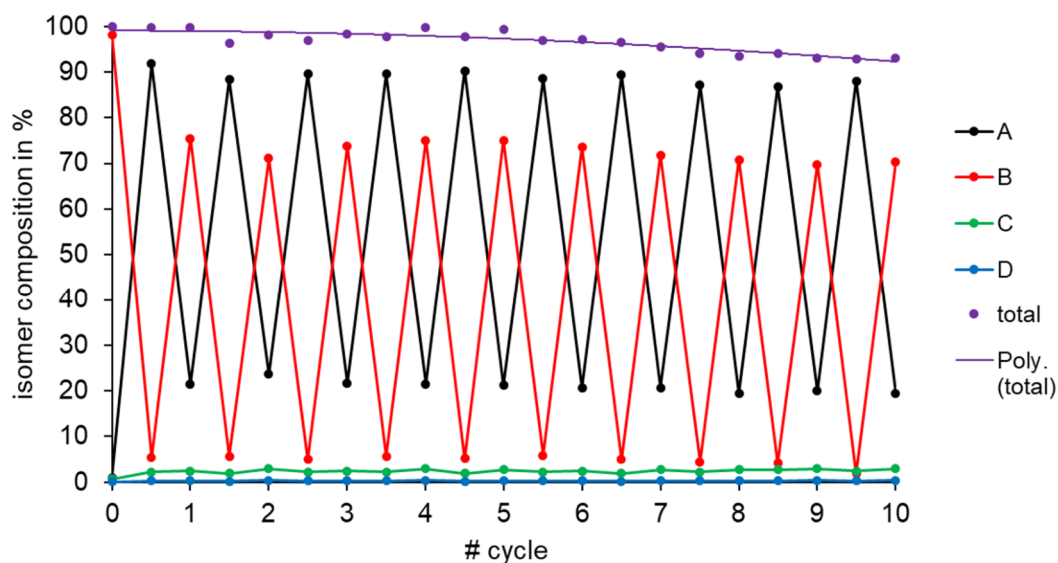
Supplementary Figure 39. Markov matrix used for modeling the kinetics of the photoconversion of **1** at 20 °C using a 450 nm LED for irradiation and thermal reactions at 60 °C in MeCN solution. Black and blue values indicate photoreactions, which must be multiplied with the relative light intensity. Blue values signify the most dominant photoreaction pathways, which are preferred strongly over the other possibilities giving rise to high photochemical selectivity. Red values indicate thermal reactions and are given in $\text{kcal} \cdot \text{mol}^{-1}$, which must be converted into reaction rates using the Eyring equation for the appropriate temperature. The thermal reaction of the **D-1** enantiomers to the **C-1** enantiomers is fast at the ambient irradiation temperature and therefore overlaying the photochemistry of the **D-1** enantiomers.

Cycle processes in the photoisomerization of HTI 1

HTI 1 isomerizes following the cycle $rac\text{-B} \rightarrow rac\text{-D} \rightarrow rac\text{-C} \rightarrow rac\text{-A} \rightarrow rac\text{-B}$ (ABDC), if racemates were used and observed. In this cycle one isomer can be populated after another in a sequential manner (Supplementary Figure 40). Starting with isomer $rac\text{-B}$ the $rac\text{-D}$ isomer can be obtained with 48% in the PSS. By thermal SBR $rac\text{-D}$ is converted into the $rac\text{-C}$ isomer with 33%, as the thermal equilibrium between $rac\text{-C}$ and $rac\text{-D}$ is 86:14. By further irradiation at 20 °C isomer $rac\text{-A}$ can be enriched up to 95% ($A:B:C:D = 95:3:2:0$). In the next thermal SBR isomer $rac\text{-B}$ is recovered with 78% ($A:B:C:D = 20:78:2:0$). Reproducibility of the cycle ABDC is given even when starting from an arbitrary mixture of isomers of HTI 1 because the A enriched solution can be obtained as “refocussing step” of the sequence. Full reversibility was demonstrated by executing the cycle experiment three times in a row (Supplementary Figure 40) or 10 times in a row with the same NMR-sample omitting the observation of isomer $rac\text{-C}$ and $rac\text{-D}$ at -40 °C to reduce the overall time needed in the experiment (Supplementary Figure 41).

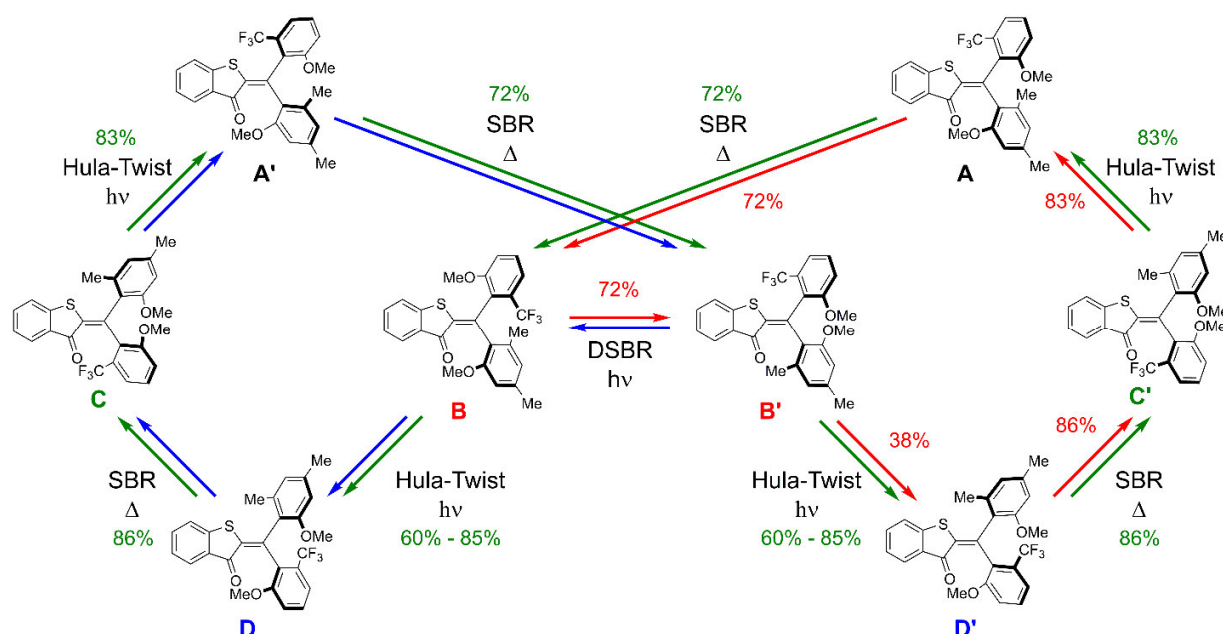


Supplementary Figure 40: Consecutive irradiation and heating steps showing the sequential isomerization cycle in HTI 1 in MeCN-*d*₃ solution. The ¹H NMR spectra of the first 1.75 cycles with assignment to the different isomers are shown on the left and the isomer composition during the cycles is shown on the right. After reaching cycle two the experiment starts always at the same isomer composition as enrichment of isomer A by irradiation with 450 nm light at 20 °C leads to the same ratio of $A:B:C:D = 95:3:2:0$.



Supplementary Figure 41: Stability of **1** during the sequential isomerization cycle process in MeCN- d_3 solution. The solution of **1** was irradiated with 450 nm until the PSS was reached (enrichment of isomer **A**). Afterwards the solution was heated to 80 °C until a thermal equilibrium was reached (enrichment of isomer **B**). These steps represent a complete *rac-B*→*rac-D*→*rac-C*→*rac-A* cycle but without monitoring the photoreaction from *rac-B* to *rac-D* followed by thermal reaction to *rac-C* individually. The cycle was repeated 10 times and the sum of integrals was compared with an internal standard. Only slight decomposition of about 5% after 10 cycles (20 photoisomerization steps and 20 heating steps) was observed.

Taking the enantiomers into account a cycle of $A \rightarrow B \rightarrow D \rightarrow C \rightarrow A' \rightarrow B' \rightarrow D' \rightarrow C' \rightarrow A$ is constituted from the main photoreactions and thermal reactions as elucidated by chiral HPLC kinetic analysis and shown in Supplementary Figure 40. In this cycle photochemical Hula-Twist reactions and thermal single bond rotations alternate and after in total eight steps the starting isomer is obtained again. This eight-step cycle can be bypassed by the dual single-bond rotation (DSBR) converting isomer **B** into **B'**. In this case HTI **1** pursues the two enantiomeric cycles $A \rightarrow B \rightarrow B' \rightarrow D' \rightarrow C' \rightarrow A$ and $A' \rightarrow B' \rightarrow B \rightarrow D \rightarrow C \rightarrow A'$. The two cycles with the corresponding reactions are shown in Supplementary Figure 42.



Supplementary Figure 42. Isomerization cycles of HTI **1** with depicted with the color code: five step cycle $A \rightarrow B \rightarrow B' \rightarrow D' \rightarrow C' \rightarrow A$ = red, the enantiomeric cycle $A' \rightarrow B' \rightarrow B \rightarrow D \rightarrow C \rightarrow A'$ = blue, and the eight step cycle $A \rightarrow B \rightarrow D \rightarrow C \rightarrow A' \rightarrow B' \rightarrow D' \rightarrow C' \rightarrow A$ = green. Interconversion percentages given (color-coded green for the eight step cycle and red for the five step cycle) describe the selectivities achieved for each individual isomer and individual step without taking into account bulk conversions that are determined i.a. by photo-equilibria and PSS compositions. Percentage values given are obtained from experimentally determined interconversions under different conditions.

To determine the preference for one cycle against the other possibilities the kinetic data obtained by the chiral HPLC Markov matrix analysis (Supplementary Figure 24-39) was used. It is found that every reaction (thermal or photochemical) yields exclusively the respective “next step” isomer in the error margin of the analysis except for the photoreaction of isomer **B** and **B'**. The photoreactions of *rac*-**B** are therefore the branching point for the two possible five-step and eight-step cycles. Which cycle is performed is therefore only dependent on the ratio of the Hula-Twist versus DSBR photoreactions. As this ratio is very dependent on the surrounding medium switching between the five- and eight-step cycle is possible by changing the irradiation conditions. If isomer **B** and **B'** perform a Hula-Twist photoreaction the eight-step cycle is

followed and if the DSBR occurs one of the five-step cycles is pursued. However, if exclusively the DSBR occurs, only photoswitching between **B** and **B'** is observed. The preference for one cycle is therefore given by the three equations:

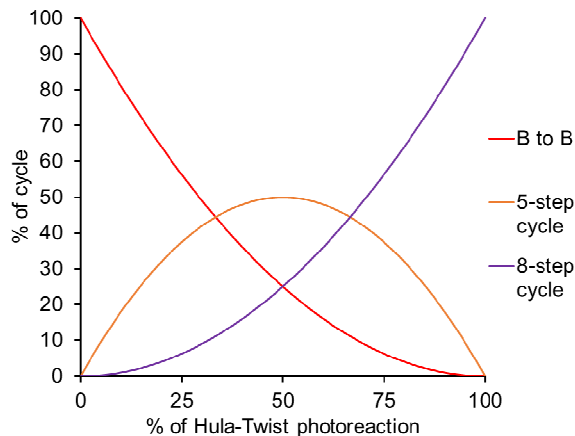
$$P_{(\mathbf{B} \leftrightarrow \mathbf{B}')} = P_{(\mathbf{B} \rightarrow \mathbf{B}')} \cdot P_{(\mathbf{B}' \rightarrow \mathbf{B})} \quad (\text{eq. 23})$$

$$P_{(\text{5-step})} = P_{(\mathbf{B} \rightarrow \mathbf{B}')} \cdot P_{(\mathbf{B} \rightarrow \mathbf{D})} + P_{(\mathbf{B}' \rightarrow \mathbf{B})} \cdot P_{(\mathbf{B}' \rightarrow \mathbf{D}')} \quad (\text{eq. 24})$$

$$P_{(\text{8-step})} = P_{(\mathbf{B} \rightarrow \mathbf{D})} \cdot P_{(\mathbf{B}' \rightarrow \mathbf{D}')} \quad (\text{eq. 25})$$

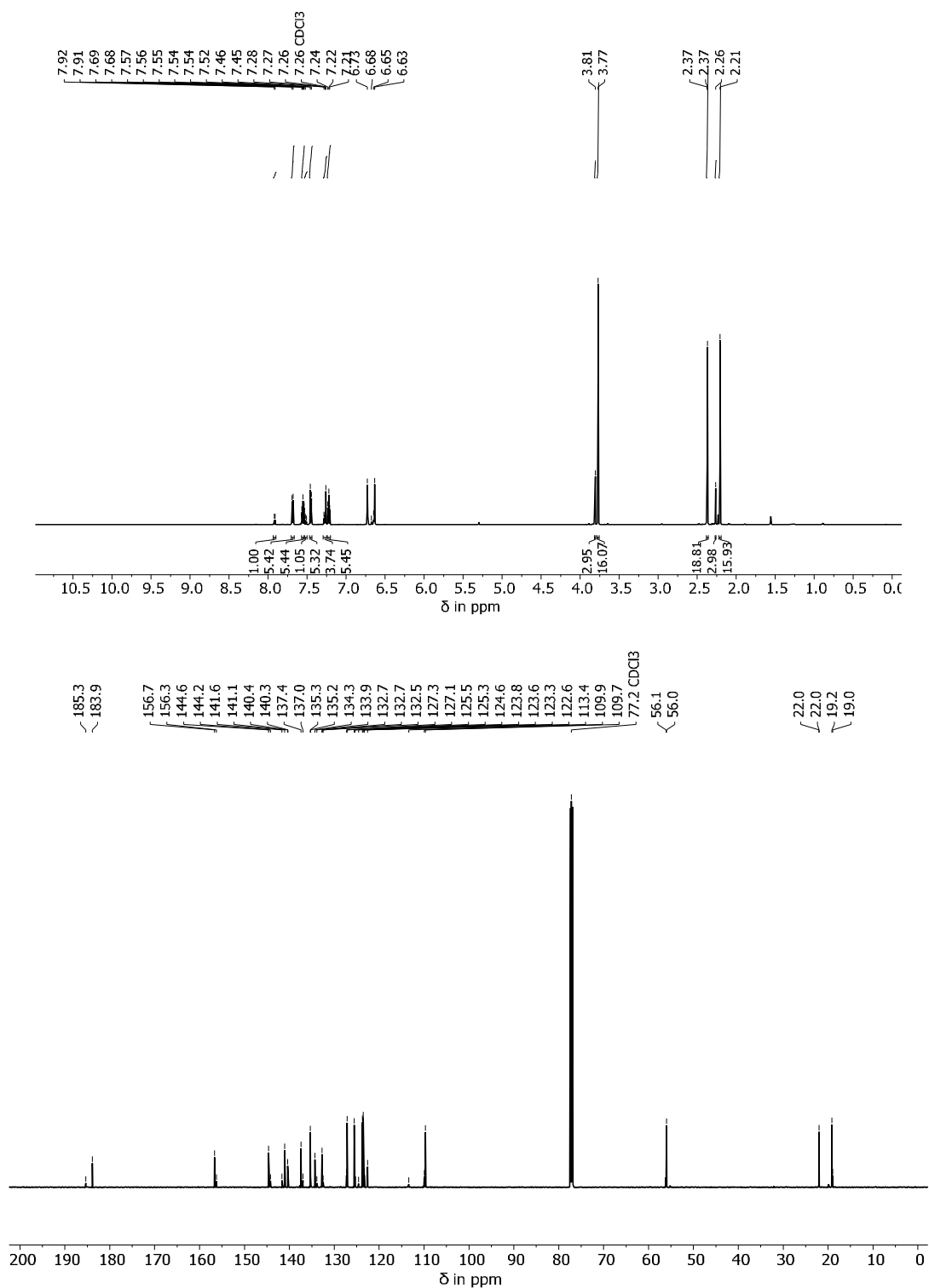
With $P_{(\mathbf{B} \leftrightarrow \mathbf{B}')} =$ probability of the switching between **B** and **B'**, $P_{(\text{5-step})} =$ probability of the five-step cycle, $P_{(\text{8-step})} =$ probability of the eight-step cycle and $P_{(i \rightarrow j)} =$ probability of the photoreaction from isomer *i* to *j* e.g. $P_{(\mathbf{B} \rightarrow \mathbf{B}')} =$ probability of the photoreaction from isomer **B** to **B'**.

Obviously, the probability of the eight-step cycle is 100% if the both **B** isomers perform exclusively the Hula-Twist reaction and the probability of the photoswitching between **B** and **B'** is 100% if exclusively DSBRs are observed. It is impossible to obtain exclusively the five-step cycle however, it can be favored significantly if conditions are suitable and the highest ratio of the five-step cycle is obtained if the Hula-Twist reaction and DSBR occur with the same probability. The preference of **1** for each cycle depending on the Hula-Twist reaction ratio is shown in Supplementary Figure 43.

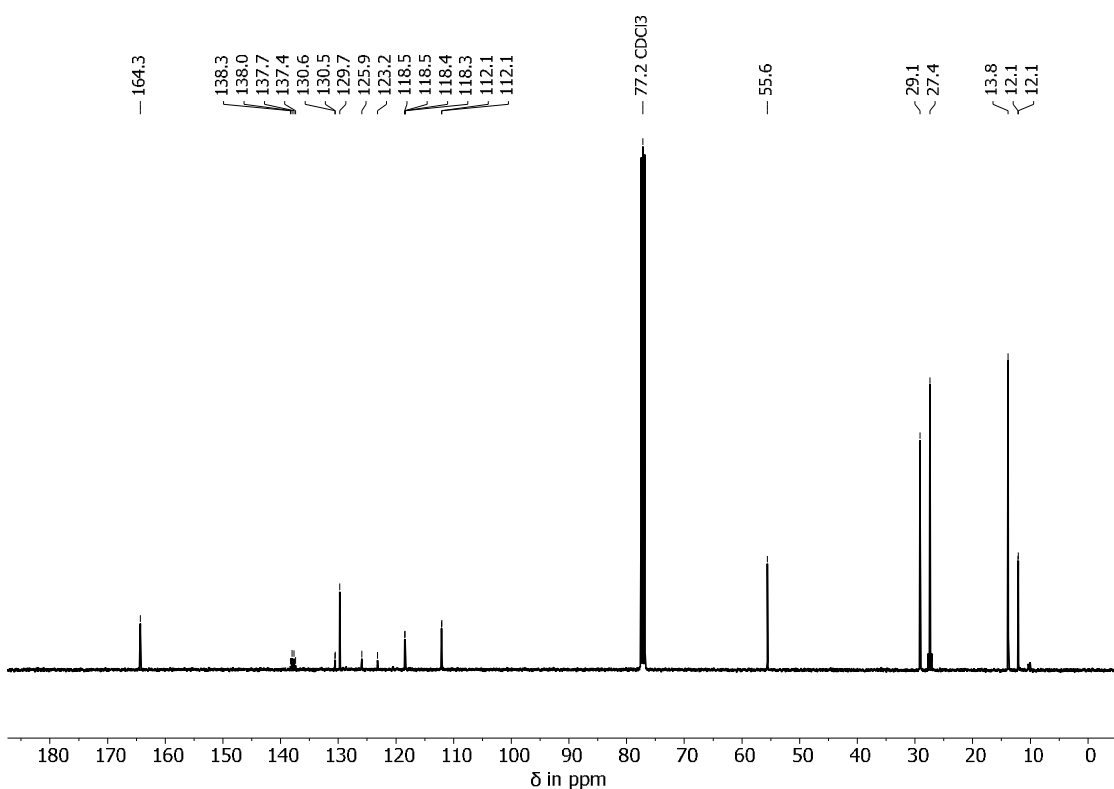
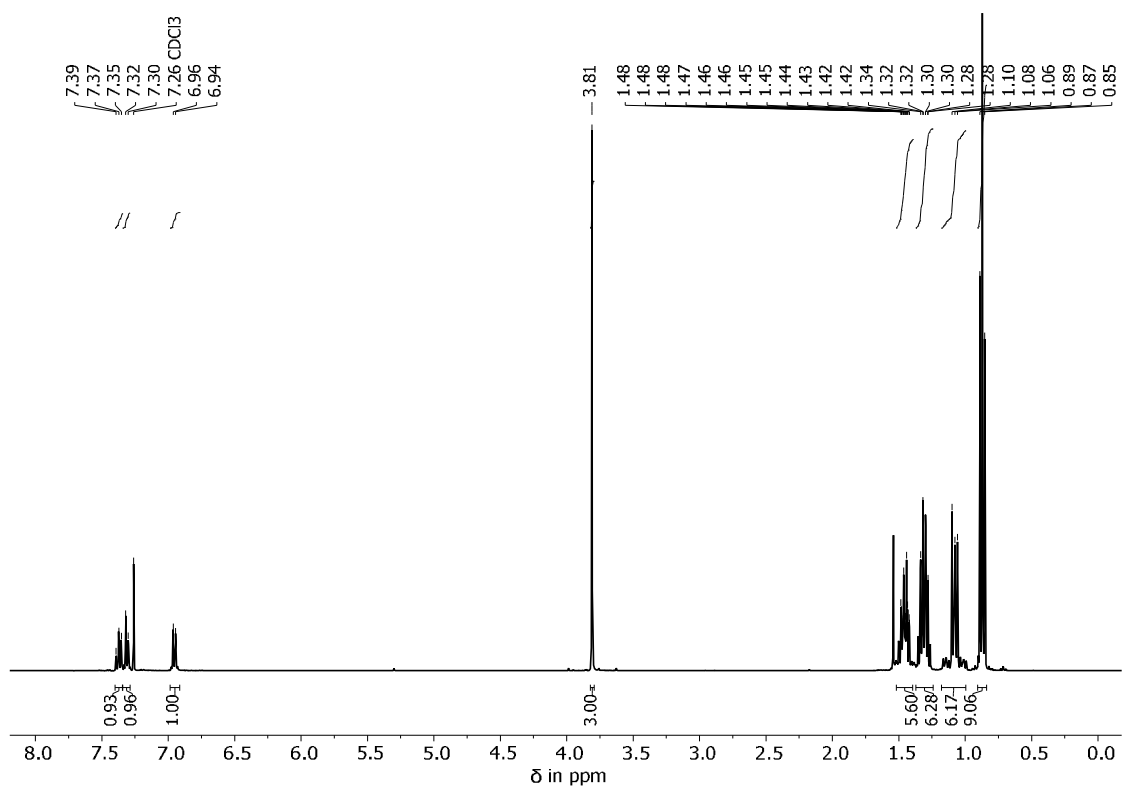


Supplementary Figure 43. Maximum achievable preference for each cycle depending on the amount of the Hula-Twist photoreaction.

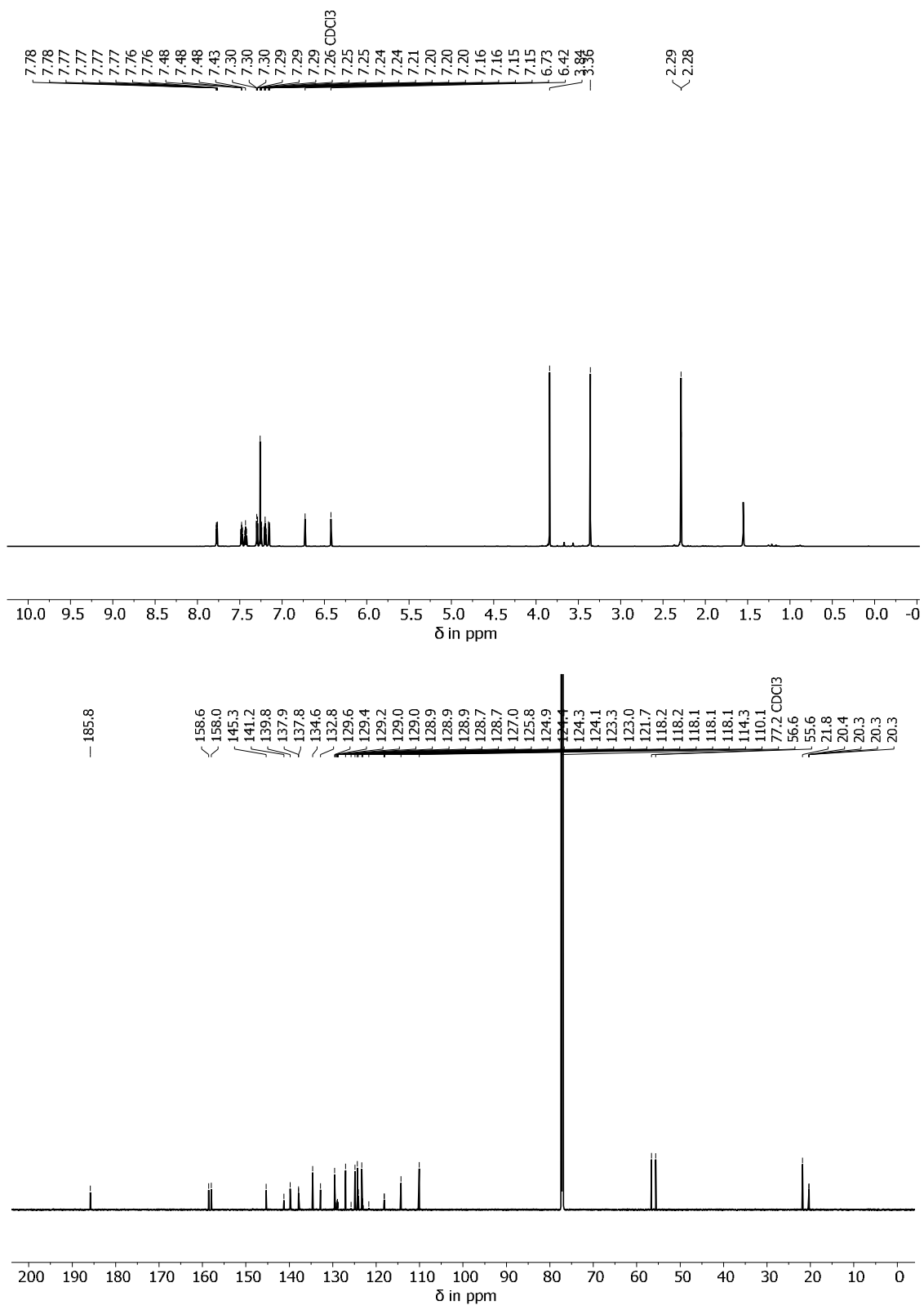
NMR-Spectra



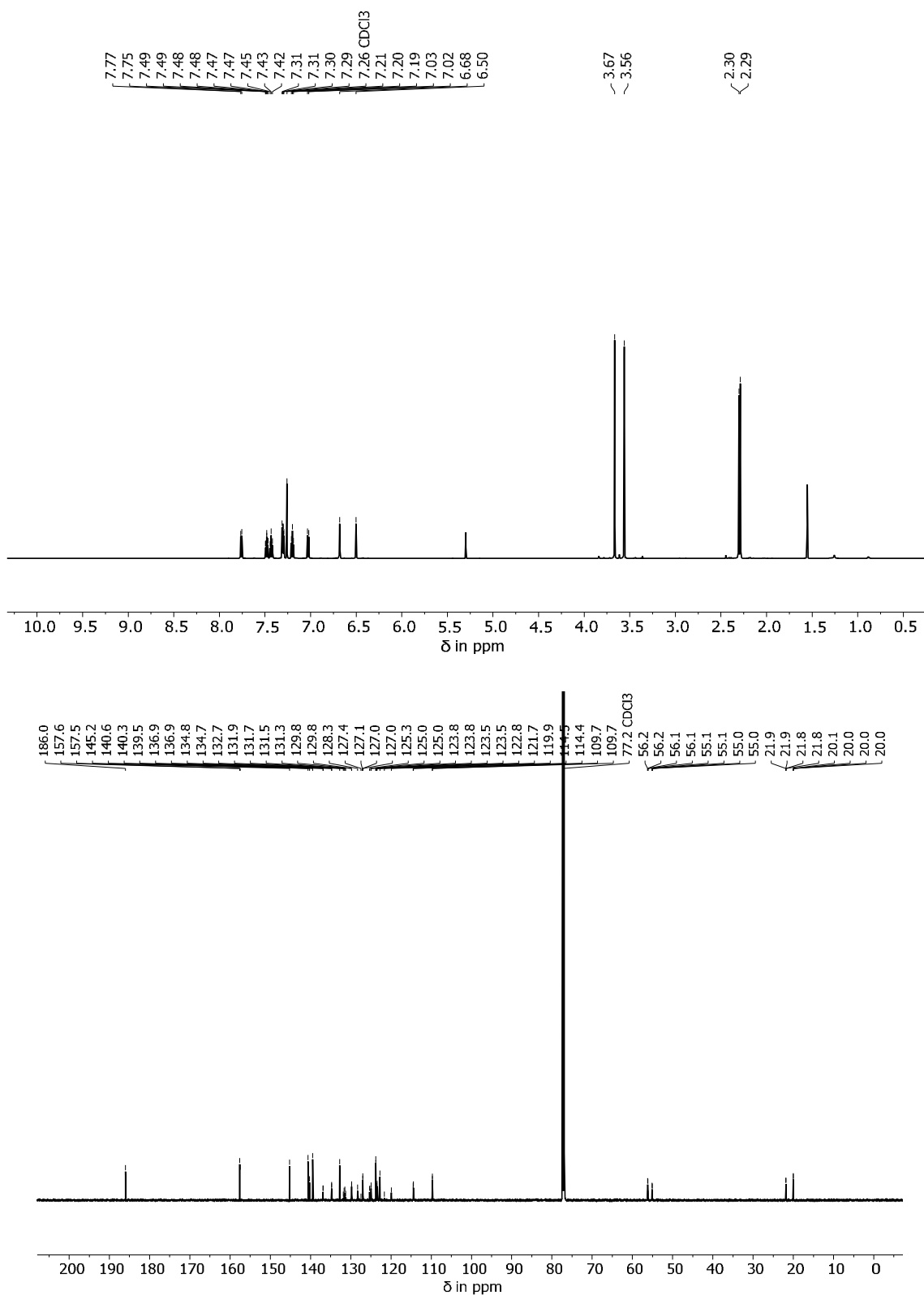
Supplementary Figure 44. 400 MHz ¹H-NMR spectrum (top) and 100 MHz ¹³C-NMR spectrum (bottom) of 2-(chloro(2-methoxy-4,6-dimethylphenyl)methylene)benzo[*b*]thiophen-3(2*H*)-one (**4**) (mix of *E/Z* isomers) in CDCl₃.



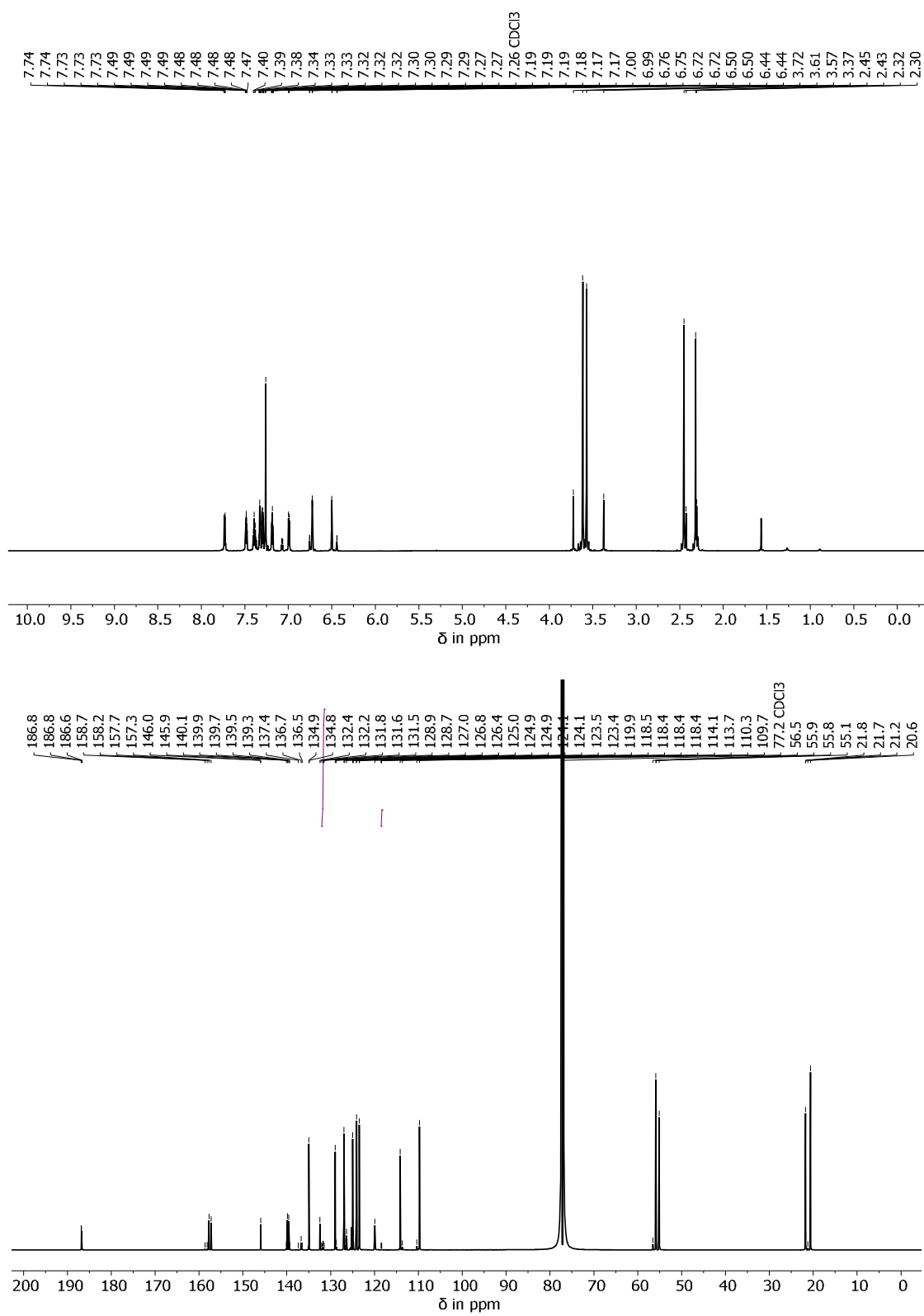
Supplementary Figure 45. 400 MHz ¹H-NMR spectrum (top) and 100 MHz ¹³C-NMR spectrum (bottom) of tributyl(2-methoxy-6-(trifluoromethyl)phenyl)stannane (**5**) in CDCl₃.



Supplementary Figure 46. 800 MHz ¹H-NMR spectrum (top) and 200 MHz ¹³C-NMR spectrum (bottom) of A-1 in CDCl₃.



Supplementary Figure 47. 600 MHz ^1H -NMR spectrum (top) and 150 MHz ^{13}C -NMR spectrum (bottom) of **B-1** in CDCl_3 .



Supplementary Figure 48. 800 MHz ^1H -NMR spectrum (top) and 200 MHz ^{13}C -NMR spectrum (bottom) of **-C/D-1** in CDCl_3 .

Crystal structure analysis

The X-ray intensity data were measured on a Bruker D8 Venture TXS system equipped with a multilayer mirror monochromator and a Mo K α rotating anode X-ray tube ($\lambda = 0.71073 \text{ \AA}$). The frames were integrated with the Bruker SAINT software package.⁹ Data were corrected for absorption effects using the Multi-Scan method (SADABS).¹⁰ The structure was solved and refined using the Bruker SHELXTL Software Package.¹¹ All C-bound hydrogen atoms have been calculated in ideal geometry riding on their parent atoms. The PLATON SQUEEZE program¹² has been applied in order to squeeze-out solvent contents which could not be modelled properly. All figures were drawn at the 50% ellipsoid probability level.¹³

Compound	<i>rac.</i> A-1/ A²-1 (wv225) CCDC 2100909	<i>rac.</i> B-1/ B²-1 (wv228) CCDC 2100907
net formula	C ₂₆ H ₂₁ F ₃ O ₃ S	C ₂₆ H ₂₁ F ₃ O ₃ S
<i>M_r</i> /g mol ⁻¹	470.49	470.49
crystal size/mm	0.100 × 0.060 × 0.040	0.090 × 0.050 × 0.020
<i>T</i> /K	100.(2)	100.(2)
radiation	MoK α	MoK α
diffractometer	'Bruker D8 Venture TXS'	'Bruker D8 Venture TXS'
crystal system	triclinic	monoclinic
space group	'P -1'	'P 1 21/c 1'
<i>a</i> /Å	9.7960(3)	7.8853(3)
<i>b</i> /Å	11.4686(4)	16.4888(6)
<i>c</i> /Å	11.8838(4)	17.2013(7)
α /°	94.3040(10)	90
β /°	105.6660(10)	101.400(2)
γ /°	93.8950(10)	90
<i>V</i> /Å ³	1276.46(7)	2192.37(15)
<i>Z</i>	2	4
calc. density/g cm ⁻³	1.224	1.425
μ /mm ⁻¹	0.172	0.200
absorption correction	Multi-Scan	Multi-Scan
transmission factor range	0.95–0.99	0.97–1.00
refls. measured	13332	21847
<i>R</i> _{int}	0.0269	0.0466
mean $\sigma(I)/I$	0.0355	0.0341
θ range	3.170–26.372	3.204–25.349
observed refls.	4338	3241
<i>x</i> , <i>y</i> (weighting scheme)	0.0375, 0.6276	0.0279, 1.7845
hydrogen refinement	constr	constr
Flack parameter	-	-
refls in refinement	5180	4009
parameters	302	302
restraints	0	0
<i>R</i> (<i>F</i> _{obs})	0.0377	0.0366
<i>R</i> _w (<i>F</i> ²)	0.0945	0.0859
<i>S</i>	1.042	1.036
shift/error _{max}	0.001	0.001
max electron density/e Å ⁻³	0.274	0.275
min electron density/e Å ⁻³	-0.256	-0.317

Compound	<i>rac.</i> C-1/ C'-1 (wv229) CCDC 2100908
net formula	C ₂₆ H ₂₁ F ₃ O ₃ S
<i>M_r</i> /g mol ⁻¹	470.49
crystal size/mm	0.090 × 0.050 × 0.040
<i>T</i> /K	100.(2)
radiation	MoKα
diffractometer	'Bruker D8 Venture TXS'
crystal system	triclinic
space group	'P -1'
<i>a</i> /Å	10.9833(3)
<i>b</i> /Å	11.7467(3)
<i>c</i> /Å	17.4631(5)
α/°	91.4340(10)
β/°	93.9910(10)
γ/°	103.9640(10)
<i>V</i> /Å ³	2179.12(10)
<i>Z</i>	4
calc. density/g cm ⁻³	1.434
μ/mm ⁻¹	0.201
absorption correction	Multi-Scan
transmission factor range	0.91–0.99
refls. measured	22166
<i>R</i> _{int}	0.0354
mean σ(<i>I</i>)/ <i>I</i>	0.0429
θ range	3.216–25.350
observed refls.	6223
<i>x</i> , <i>y</i> (weighting scheme)	0.0329, 1.4449
hydrogen refinement	constr
Flack parameter	-
refls in refinement	7910
parameters	603
restraints	0
<i>R</i> (<i>F</i> _{obs})	0.0386
<i>R</i> _w (<i>F</i> ²)	0.0927
<i>S</i>	1.027
shift/error _{max}	0.001
max electron density/e Å ⁻³	0.425
min electron density/e Å ⁻³	-0.399

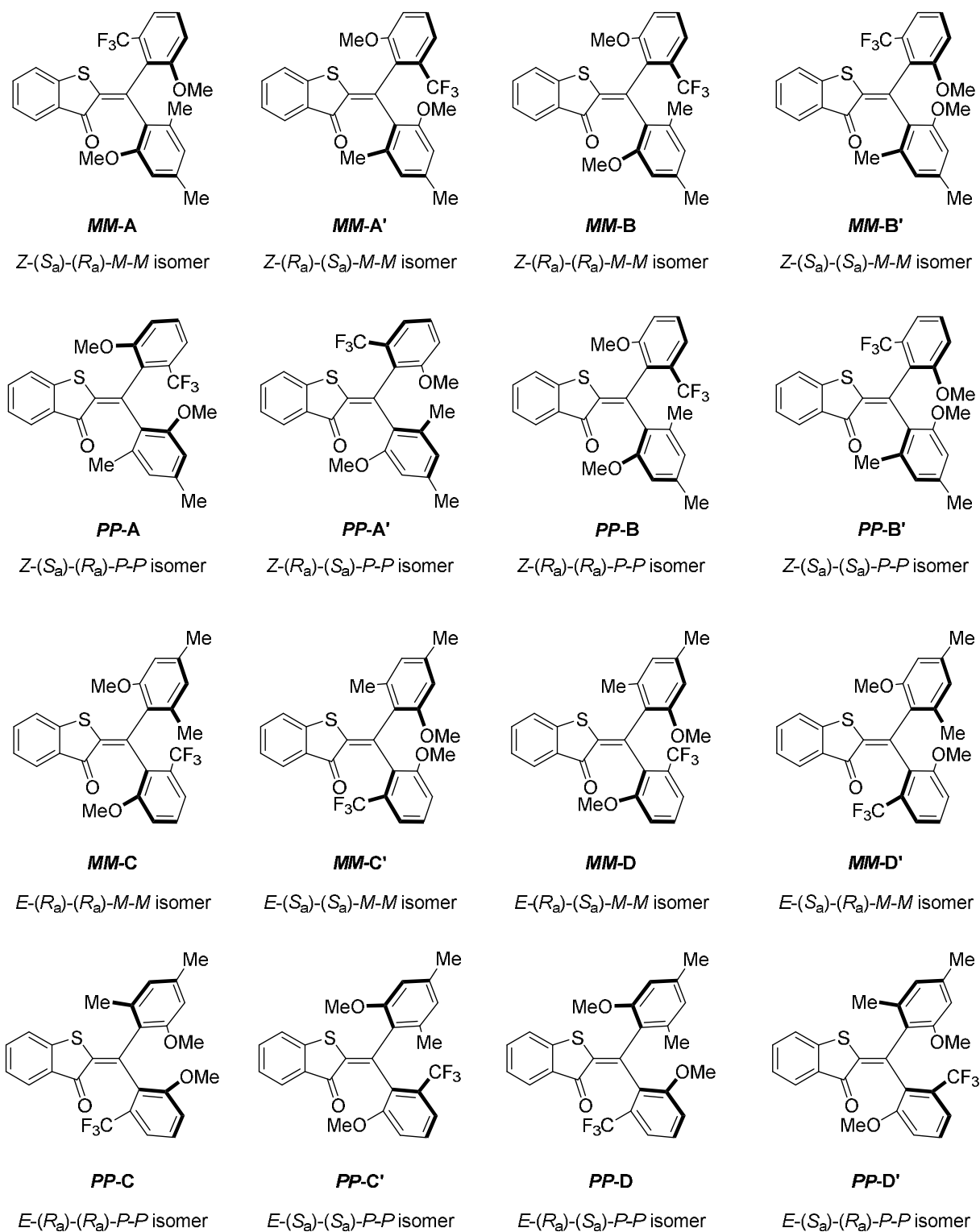
Compound	C-1 (yv157) CCDC 2100910	C'-1 (yv156) CCDC 2100911
net formula	C ₅₃ H ₄₄ Cl ₂ F ₆ O ₆ S ₂	C ₅₃ H ₄₄ Cl ₂ F ₆ O ₆ S ₂
<i>M_r</i> /g mol ⁻¹	1025.90	1025.90
crystal size/mm	0.100 × 0.060 × 0.060	0.100 × 0.030 × 0.030
<i>T</i> /K	102.(2)	102.(2)
radiation	MoKα	MoKα
diffractometer	'Bruker D8 Venture TXS'	'Bruker D8 Venture TXS'
crystal system	orthorhombic	orthorhombic
space group	'P 21 21 21'	'P 21 21 21'
<i>a</i> /Å	13.6458(10)	13.6343(5)
<i>b</i> /Å	18.6506(15)	18.6527(5)
<i>c</i> /Å	18.8599(16)	18.8361(6)
<i>α</i> /°	90	90
<i>β</i> /°	90	90
<i>γ</i> /°	90	90
<i>V</i> /Å ³	4799.9(7)	4790.3(3)
<i>Z</i>	4	4
calc. density/g cm ⁻³	1.420	1.422
<i>μ</i> /mm ⁻¹	0.297	0.297
absorption correction	Multi-Scan	Multi-Scan
transmission factor range	0.92–0.98	0.95–0.99
refls. measured	28148	28204
<i>R</i> _{int}	0.0536	0.0367
mean <i>σ</i> (<i>I</i>)/ <i>I</i>	0.0623	0.0439
<i>θ</i> range	2.844–26.371	2.846–26.371
observed refls.	8254	8460
<i>x</i> , <i>y</i> (weighting scheme)	0.0315, 1.3791	0.0322, 1.5945
hydrogen refinement	constr	constr
Flack parameter	0.12(3)	0.01(2)
refls in refinement	9729	9745
parameters	630	630
restraints	0	0
<i>R</i> (<i>F</i> _{obs})	0.0407	0.0383
<i>R</i> _w (<i>F</i> ²)	0.0975	0.0828
<i>S</i>	1.055	1.036
shift/error _{max}	0.001	0.001
max electron density/e Å ⁻³	0.343	0.342
min electron density/e Å ⁻³	-0.462	-0.436

Calculated Ground State Energy Profile of Compound 1

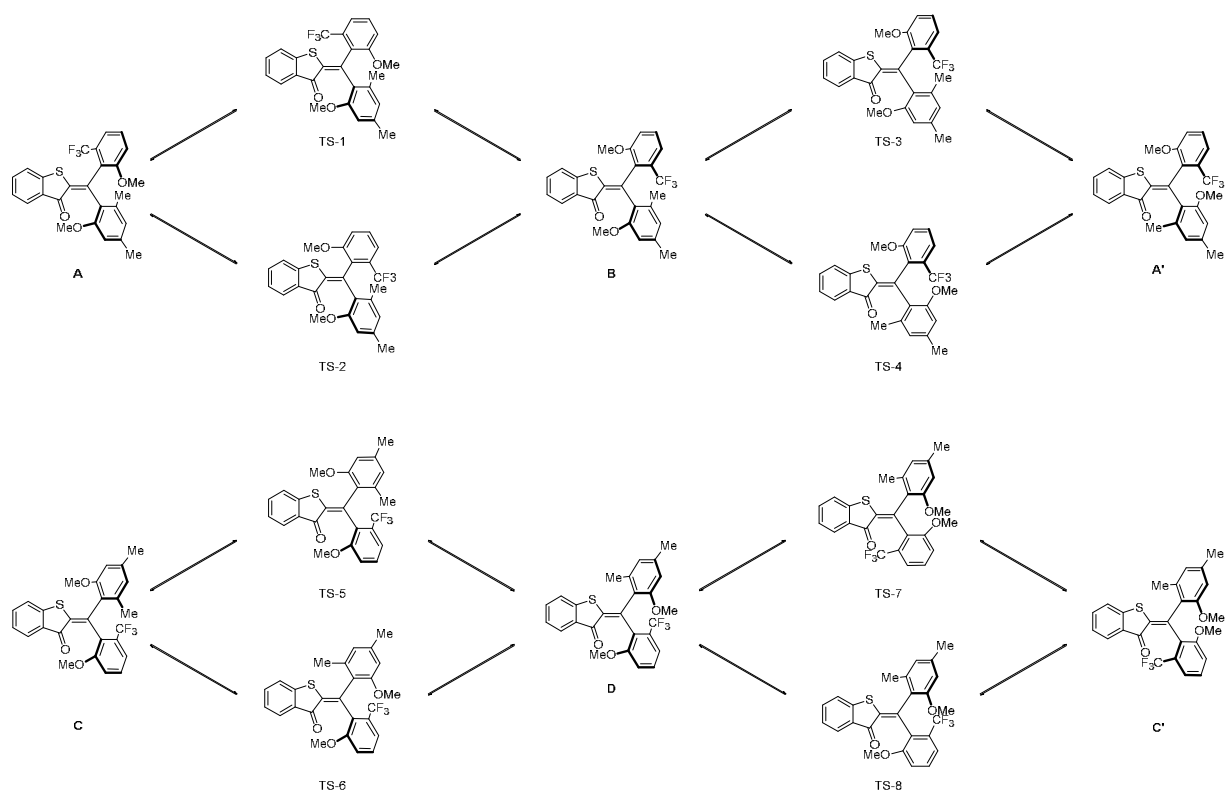
A relaxed optimization of the isomeric states and transition state structures of compound **1** has been conducted at the B3LYP level of theory with the 6-311G(d,p) basis set using the Gaussian09 Revision A.02 program package.¹⁴ To account for solvent effects, the calculations have been carried out using the Polarizable Continuum Model (PCM) with acetonitrile parameters. The convergence criteria have been set tight and an ultrafine integration grid has been used. A following frequency analysis confirmed 16 structures to be minimum structures since no imaginary frequencies have been found. Eight of the structures are enantiomeric to the other and were determined to show that the enantiomers (e.g. **A** and **A'**) possess the same energies. In addition, all the expected isomeric minimum structures are present in two different geometries with different helicities, which have different energies. They are denoted with *P* and *M* stereo assignments. All structures are shown schematically in Supporting Figure 49. The helical structures are in rapid equilibrium with each other at 20 °C as well as at lower temperatures since in the low temperature experiments no line broadening or signal splitting could be observed in the NMR spectra. Therefore, the calculated thermodynamic equilibrium between the two helices was used to describe the properties of the isomers. If this thermodynamically equilibrated mixture was used, we omitted the helix stereo labels. All other structures were shown to be first order saddle points on the potential energy surface since only one imaginary vibrational mode has been found and confirmed them to be transition state structures.

TD-B3LYP/6-331G(d,p) calculations were conducted with the same parameters and number of states = 30 to obtain electronic excitation spectra. To obtain the ECD spectra the following isomeric ratios were used, resulting from the calculated minimum energies in Supplementary Table 3 and the Boltzmann distribution at 20°C:

	Isomer 1	Isomer 2
A	0.070 (<i>M-A</i>)	0.930 (<i>P-A</i>)
B	0.185 (<i>M-B</i>)	0.815 (<i>P-B</i>)
C	0.110 (<i>M-C</i>)	0.890 (<i>P-C</i>)
D	0.065 (<i>P-D</i>)	0.935 (<i>M-D</i>)
A'	0.070 (<i>P-A'</i>)	0.930 (<i>M-A'</i>)
B'	0.185 (<i>P-B'</i>)	0.815 (<i>M-B'</i>)
C'	0.110 (<i>P-C'</i>)	0.890 (<i>M-C'</i>)
D'	0.065 (<i>M-D'</i>)	0.935 (<i>P-D'</i>)
C/D	0.253 (<i>D</i>)	0.747 (<i>C</i>)
C'/D'	0.253 (<i>D'</i>)	0.747 (<i>C'</i>)



Supplementary Figure 49. All isomeric and enantiomeric states of **1**, which were found to be minimum structures. The corresponding energies are given in Supplementary Table 3.



Supplementary Figure 50. Transition state structures between the different isomers of **1**. Only one enantiomeric half of the transition states is shown.

Supplementary Table 3. Calculated minimum and transition state energies for the isomers of HTI 1 and their conversions.

Isomer	G ₀ (Hartree)	ΔG (Hartree)	ΔG (kcal mol ⁻¹)
<i>M-A</i>	-1926.863346	0.004577	2.87211084
<i>M-A'</i>	-1926.8657	0.002185	1.37110819
<i>P-A</i>	-1926.8657	0.002185	1.37110819
<i>P-A'</i>	-1926.863346	0.004577	2.87211084
<i>M-B</i>	-1926.8655	0.002408	1.5110428
<i>M-B'</i>	-1926.8669	0.00103	0.64633475
<i>P-B</i>	-1926.8669	0.00103	0.64633475
<i>P-B'</i>	-1926.8655	0.002408	1.5110428
<i>M-C</i>	-1926.866	0.001936	1.21485833
<i>M-C'</i>	-1926.8679	1E-06	0.00062751
<i>P-C</i>	-1926.8679	0	0
<i>P-C'</i>	-1926.866	0.001936	1.21485833
<i>M-D</i>	-1926.8669	0.001003	0.629392
<i>M-D'</i>	-1926.8645	0.003473	2.17934039
<i>P-D</i>	-1926.8644	0.003476	2.18122291
<i>P-D'</i>	-1926.8669	0.001003	0.629392
TS1	-1926.8115	0.056384	35.3814939
TS2	-1926.8203	0.047614	29.8782359
TS3	-1926.8129	0.055	34.5130208
TS4	-1926.8113	0.056611	35.52393855
TS5	-1926.8313	0.036581	22.9549239
TS6	-1926.8211	0.046818	29.3787383
TS7	-1926.8005	0.067447	42.3236312
TS8	-1926.8065	0.061448	38.5592019

Calculated Ground state geometries - xyz coordinates

<i>M-A</i>				<i>M-A'</i>			
S	-2.199865	0.772639	0.846905	S	2.325543	1.104238	-0.622394
O	-1.034441	-2.251022	-1.322045	O	1.511924	-2.450022	0.764542
C	-3.491379	-0.374401	0.448574	C	3.751193	0.09032	-0.348139
C	-4.828118	-0.257665	0.825353	C	5.074623	0.461003	-0.581556
H	-5.173557	0.583228	1.41448	H	5.322481	1.443268	-0.965231
C	-5.715492	-1.2529	0.421526	C	6.077148	-0.465654	-0.304358
H	-6.758626	-1.176546	0.706408	H	7.111402	-0.191725	-0.478864
C	-5.286261	-2.346076	-0.344666	C	5.774562	-1.740639	0.195308
H	-5.998072	-3.104794	-0.64623	H	6.574146	-2.44112	0.403342
C	-3.952035	-2.451769	-0.714446	C	4.452665	-2.100345	0.421324
H	-3.592339	-3.284716	-1.307584	H	4.188676	-3.078925	0.805574
C	-3.051576	-1.461901	-0.311473	C	3.438181	-1.179423	0.145585
C	-1.609677	-1.436062	-0.618952	C	1.993656	-1.420025	0.315759
C	-0.972047	-0.229298	0.01206	C	1.219609	-0.19916	-0.089784
C	0.332578	0.13056	-0.046158	C	-0.11991	0.008897	0.023913
C	1.418309	-0.810949	-0.458916	C	-1.110757	-1.086435	0.19096
C	2.372963	-0.49183	-1.443724	C	-1.175572	-2.204585	-0.67152
C	3.411916	-1.39037	-1.723323	C	-2.214794	-3.130951	-0.517607
C	3.547102	-2.597032	-1.047365	C	-3.184998	-3.010155	0.470495
C	2.602898	-2.919065	-0.067365	C	-3.118155	-1.915989	1.338841
H	2.697504	-3.855693	0.465508	H	-3.857922	-1.814405	2.121413
C	1.550954	-2.054034	0.221547	C	-2.105285	-0.972394	1.203717
H	4.126863	-1.13218	-2.49722	H	-2.260539	-3.971785	-1.201969
C	0.740366	1.482974	0.473256	C	-0.62116	1.430568	-0.031805
C	1.502541	1.51708	1.672089	C	-0.281131	2.302034	1.037237
C	0.414377	2.717935	-0.118249	C	-1.416913	1.954581	-1.06714
C	1.926593	2.725403	2.226974	C	-0.740984	3.621051	1.056872
C	0.839207	3.926343	0.449315	C	-1.869637	3.277279	-1.041489
C	1.591707	3.926167	1.611284	C	-1.533502	4.101048	0.021468
H	2.506126	2.735468	3.139112	H	-0.486819	4.274691	1.879089
H	0.584691	4.861457	-0.031823	H	-2.469421	3.656158	-1.856074
H	1.920565	4.862492	2.045273	H	-1.883949	5.125816	0.044854
C	-0.367809	2.910549	-1.401001	C	-1.816352	1.126448	-2.263829
C	2.531513	0.249872	3.433806	C	0.874989	2.602285	3.118559
H	2.603408	-0.807782	3.676666	H	1.483764	1.965986	3.757166
H	3.533837	0.657734	3.276392	H	1.469837	3.456209	2.782017
H	2.039865	0.779496	4.254632	H	0.005336	2.955022	3.680221
O	1.752465	0.313673	2.237268	O	0.48395	1.776635	2.020516
F	-0.751259	1.791281	-2.039151	F	-0.784426	0.410381	-2.771141
F	0.360762	3.625888	-2.299535	F	-2.275605	1.890243	-3.281621
F	-1.494119	3.63383	-1.178297	F	-2.805855	0.244077	-1.985353
C	2.307423	0.773915	-2.266795	C	-0.194063	-2.479208	-1.784812
H	2.479166	1.667396	-1.662057	H	0.351807	-1.594775	-2.102274
H	3.071309	0.753681	-3.045097	H	0.538691	-3.221149	-1.455354
H	1.337553	0.886249	-2.752571	H	-0.717327	-2.890303	-2.650786
C	4.676324	-3.549164	-1.355482	C	-4.287353	-4.029045	0.61869
H	5.320786	-3.158274	-2.144601	H	-4.221363	-4.800647	-0.149947
H	5.294266	-3.726893	-0.469853	H	-4.239583	-4.519269	1.596048
H	4.294348	-4.521953	-1.680104	H	-5.271823	-3.55725	0.544516
O	0.617891	-2.33675	1.166347	O	-1.977468	0.08955	2.04068
C	0.692522	-3.571876	1.873541	C	-2.964295	0.314135	3.045833
H	0.607291	-4.426022	1.195042	H	-3.958086	0.444338	2.607552
H	1.621281	-3.650656	2.446873	H	-2.986748	-0.505296	3.77031
H	-0.153589	-3.568533	2.5581	H	-2.666119	1.231913	3.548693

<i>P-A</i>				<i>P-A'</i>			
S	2.325544	-1.104232	-0.622406	S	-2.199865	-0.772637	0.846907
O	1.511922	2.450026	0.764532	O	-1.034438	2.251027	-1.322037
C	3.751193	-0.090315	-0.348147	C	-3.491379	0.374403	0.448575
C	5.074624	-0.460997	-0.581563	C	-4.828119	0.257667	0.825352
H	5.322483	-1.443261	-0.96524	H	-5.173558	-0.583227	1.414479
C	6.077149	0.465659	-0.30436	C	-5.715492	1.252901	0.421523
H	7.111403	0.191731	-0.478865	H	-6.758627	1.176547	0.706402
C	5.774562	1.740643	0.195308	C	-5.286261	2.346077	-0.344668
H	6.574145	2.441123	0.403346	H	-5.998071	3.104794	-0.646235
C	4.452664	2.100348	0.421323	C	-3.952034	2.451771	-0.714445
H	4.188674	3.078927	0.805575	H	-3.592337	3.284718	-1.307582
C	3.438181	1.179427	0.14558	C	-3.051575	1.461903	-0.311471
C	1.993655	1.420028	0.315752	C	-1.609675	1.436065	-0.618947
C	1.21961	0.199162	-0.089793	C	-0.972047	0.2293	0.012064
C	-0.119909	-0.008897	0.023912	C	0.332578	-0.130559	-0.046156
C	-1.110756	1.086433	0.190962	C	1.41831	0.810948	-0.458915
C	-1.175577	2.204582	-0.671518	C	2.372964	0.491827	-1.443723
C	-2.214801	3.130946	-0.517602	C	3.41192	1.390366	-1.72332
C	-3.185003	3.010147	0.470502	C	3.547107	2.597027	-1.047363
C	-3.118154	1.915982	1.338848	C	2.602903	2.919062	-0.067362
H	-3.857918	1.814397	2.121422	H	2.697512	3.855689	0.465511
C	-2.105283	0.97239	1.203721	C	1.550958	2.054034	0.221549
H	-2.260548	3.971781	-1.201964	H	4.126867	1.132174	-2.497217
C	-0.621157	-1.430568	-0.031806	C	0.740366	-1.482975	0.473256
C	-0.281119	-2.302035	1.037233	C	1.502541	-1.517083	1.672088
C	-1.416915	-1.95458	-1.067137	C	0.414372	-2.717935	-0.11825
C	-0.740967	-3.621054	1.056866	C	1.92659	-2.725408	2.226973
C	-1.869636	-3.27728	-1.041487	C	0.839199	-3.926343	0.449314
C	-1.533491	-4.101051	0.021465	C	1.591699	-3.92617	1.611283
H	-0.486795	-4.274697	1.879079	H	2.506121	-2.735474	3.139113
H	-2.469425	-3.656158	-1.856068	H	0.584681	-4.861457	-0.031824
H	-1.883933	-5.125821	0.04485	H	1.920553	-4.862497	2.045271
C	-1.816367	-1.126445	-2.263821	C	-0.367811	-2.910545	-1.401003
C	0.875008	-2.602287	3.11855	C	2.531513	-0.249878	3.433807
H	1.483779	-1.965987	3.757159	H	2.603414	0.807776	3.676666
H	0.005356	-2.955029	3.680211	H	2.039858	-0.779499	4.254631
H	1.469859	-3.456208	2.782006	H	3.533837	-0.657746	3.276399
O	0.483965	-1.776637	2.020508	O	1.752471	-0.313676	2.237265
F	-0.784448	-0.41037	-2.771137	F	-0.751268	-1.791278	-2.03915
F	-2.805872	-0.244082	-1.985335	F	-1.494117	-3.633834	-1.178303
F	-2.275621	-1.89024	-3.281613	F	0.360764	-3.625876	-2.29954
C	-0.19407	2.479208	-1.784811	C	2.307423	-0.773918	-2.266793
H	0.351803	1.594777	-2.102272	H	2.47917	-1.667399	-1.662057
H	-0.717335	2.890301	-2.650784	H	1.33755	-0.886253	-2.752564
H	0.538681	3.221153	-1.455353	H	3.071303	-0.753681	-3.0451
C	-4.287366	4.029029	0.618692	C	4.676326	3.54916	-1.355484
H	-4.221328	4.800679	-0.149891	H	5.320826	3.15824	-2.144557
H	-5.271831	3.557237	0.544424	H	4.294346	4.521926	-1.680173
H	-4.23966	4.519188	1.596086	H	5.294229	3.726948	-0.46984
O	-1.97746	-0.089554	2.040684	O	0.617896	2.336749	1.16635
C	-2.964273	-0.314132	3.045852	C	0.692518	3.571884	1.87353
H	-2.986719	0.505307	3.77032	H	1.621275	3.650674	2.446865
H	-3.95807	-0.444341	2.607585	H	0.607287	4.426022	1.195021
H	-2.666089	-1.231904	3.548717	H	-0.153594	3.568546	2.558086

<i>M-B</i>				<i>M-B'</i>			
S	2.22683	1.136323	-0.631427	S	2.292532	0.847491	-0.81952
O	1.395013	-2.222547	1.161721	O	1.260117	-2.473538	0.952846
C	3.622471	0.066004	-0.416493	C	3.65841	-0.169998	-0.331794
C	4.930728	0.342685	-0.80947	C	5.006154	0.127204	-0.527332
H	5.184391	1.277257	-1.295074	H	5.313005	1.044201	-1.015636
C	5.910689	-0.615403	-0.558326	C	5.954619	-0.786782	-0.074032
H	6.933221	-0.415009	-0.857421	H	7.006923	-0.569547	-0.217542
C	5.599988	-1.82822	0.073051	C	5.57513	-1.977159	0.563122
H	6.38177	-2.554891	0.257711	H	6.334006	-2.669463	0.906696
C	4.292713	-2.092976	0.460069	C	4.229847	-2.2639	0.751052
H	4.023517	-3.021271	0.950856	H	3.906909	-3.176035	1.239516
C	3.300778	-1.141183	0.210014	C	3.268799	-1.355386	0.298547
C	1.872586	-1.278062	0.553384	C	1.809252	-1.525648	0.411871
C	1.118037	-0.057802	0.105888	C	1.106965	-0.345281	-0.197333
C	-0.205357	0.199116	0.270113	C	-0.224218	-0.09266	-0.211596
C	-1.200653	-0.857645	0.609822	C	-1.271285	-1.117922	0.06178
C	-2.138167	-0.706779	1.652793	C	-1.368194	-2.314858	-0.680043
C	-3.099836	-1.69981	1.874344	C	-2.435974	-3.187283	-0.438839
C	-3.180608	-2.840795	1.083454	C	-3.40902	-2.927328	0.521476
C	-2.254759	-2.998472	0.048483	C	-3.317597	-1.74372	1.25836
H	-2.302524	-3.885212	-0.569042	H	-4.066265	-1.528324	2.008507
C	-1.272199	-2.039379	-0.183039	C	-2.272407	-0.85078	1.031663
H	-3.797837	-1.572164	2.694981	H	-2.505892	-4.094465	-1.030185
C	-0.685017	1.612097	0.061107	C	-0.700232	1.271179	-0.638989
C	-0.251414	2.613191	0.970456	C	-1.291453	1.37905	-1.923017
C	-1.541653	2.016926	-0.982908	C	-0.600399	2.441144	0.131115
C	-0.677101	3.937752	0.838889	C	-1.784716	2.597456	-2.392022
C	-1.961111	3.343098	-1.107858	C	-1.09216	3.661862	-0.347408
C	-1.530482	4.295622	-0.195726	C	-1.684941	3.734221	-1.597095
H	-0.349336	4.688698	1.543466	H	-2.237156	2.666774	-3.371062
H	-2.608105	3.626958	-1.924908	H	-1.012952	4.548543	0.267748
H	-1.855879	5.324268	-0.292141	H	-2.068244	4.679331	-1.962025
C	-2.033914	1.049495	-2.03388	C	0.016141	2.537674	1.510199
C	1.080602	3.164907	2.894956	C	-1.931039	0.240557	-3.941057
H	1.72313	2.603349	3.569328	H	-1.845958	-0.779525	-4.308611
H	1.670778	3.925466	2.376941	H	-2.986623	0.516899	-3.871516
H	0.279424	3.64103	3.466777	H	-1.41372	0.918874	-4.625143
O	0.560465	2.200991	1.974843	O	-1.312884	0.235332	-2.651873
F	-3.014841	0.234215	-1.575051	F	0.48822	1.402709	2.03994
F	-1.05229	0.256549	-2.512621	F	-0.878103	3.041358	2.405003
F	-2.557916	1.689786	-3.10603	F	1.054659	3.418511	1.501887
C	-2.138853	0.481929	2.585863	C	-0.378019	-2.712949	-1.747131
H	-2.606823	1.355047	2.120842	H	0.066163	-1.851224	-2.241317
H	-2.70853	0.248365	3.486739	H	0.429255	-3.307877	-1.310865
H	-1.130931	0.771056	2.882322	H	-0.869664	-3.329285	-2.50254
C	-4.231386	-3.895026	1.329547	C	-4.535413	-3.897668	0.779294
H	-4.859097	-3.638249	2.184405	H	-4.57819	-4.669989	0.009449
H	-4.880189	-4.014133	0.45622	H	-4.407883	-4.395787	1.746077
H	-3.774033	-4.869867	1.524293	H	-5.50153	-3.386149	0.806348
O	-0.356129	-2.168316	-1.174367	O	-2.130921	0.306107	1.734094
C	-0.451323	-3.26568	-2.078383	C	-3.112894	0.652395	2.711353
H	-0.308312	-4.221132	-1.564878	H	-4.10442	0.753933	2.260597
H	-1.412889	-3.26925	-2.600477	H	-3.149004	-0.088356	3.515438
H	0.351051	-3.120991	-2.799272	H	-2.794911	1.610683	3.113508

<i>P-B</i>				<i>P-B'</i>			
S	2.292531	-0.847478	-0.819545	S	-2.226831	1.136324	-0.631426
O	1.260118	2.47354	0.952844	O	-1.395015	-2.222546	1.161719
C	3.65841	0.170007	-0.331811	C	-3.622473	0.066006	-0.416492
C	5.006154	-0.127193	-0.527351	C	-4.93073	0.342689	-0.809468
H	5.313005	-1.044186	-1.015665	H	-5.184393	1.277261	-1.295071
C	5.954619	0.786787	-0.074041	C	-5.910691	-0.615398	-0.558323
H	7.006923	0.569552	-0.217553	H	-6.933223	-0.415002	-0.857418
C	5.57513	1.977157	0.563125	C	-5.599992	-1.828216	0.073052
H	6.334007	2.669457	0.906708	H	-6.381774	-2.554886	0.257713
C	4.229848	2.263897	0.751057	C	-4.292717	-2.092973	0.46007
H	3.90691	3.176028	1.239531	H	-4.023521	-3.021269	0.950856
C	3.2688	1.355389	0.298543	C	-3.300781	-1.141181	0.210014
C	1.809253	1.525652	0.411867	C	-1.872589	-1.278061	0.553383
C	1.106966	0.345288	-0.197342	C	-1.118039	-0.057802	0.105886
C	-0.224217	0.092662	-0.211596	C	0.205356	0.199115	0.270111
C	-1.271285	1.117922	0.061787	C	1.200651	-0.857646	0.609822
C	-1.368201	2.314857	-0.680038	C	2.138165	-0.706778	1.652792
C	-2.435985	3.187277	-0.438831	C	3.099836	-1.699807	1.874344
C	-3.409028	2.927316	0.521486	C	3.18061	-2.840792	1.083454
C	-3.317597	1.743709	1.25837	C	2.254762	-2.998471	0.048483
H	-4.066264	1.52831	2.008518	H	2.302529	-3.885211	-0.569043
C	-2.272402	0.850776	1.031673	C	1.272199	-2.03938	-0.183039
H	-2.505911	4.094458	-1.030178	H	3.797838	-1.572158	2.69498
C	-0.700233	-1.271177	-0.638985	C	0.685017	1.612095	0.061106
C	-1.291467	-1.379049	-1.923008	C	0.251416	2.61319	0.970455
C	-0.600388	-2.441143	0.131116	C	1.541654	2.016923	-0.982911
C	-1.78473	-2.597456	-2.392009	C	0.677105	3.937751	0.838888
C	-1.09215	-3.661862	-0.347403	C	1.961113	3.343095	-1.10786
C	-1.684943	-3.734222	-1.597085	C	1.530486	4.295619	-0.195727
H	-2.237181	-2.666774	-3.371044	H	0.34934	4.688697	1.543464
H	-1.012933	-4.548543	0.267751	H	2.608107	3.626955	-1.92491
H	-2.068247	-4.679332	-1.962012	H	1.855884	5.324265	-0.292143
C	0.016163	-2.537672	1.510196	C	2.033912	1.049493	-2.033883
C	-1.931076	-0.240555	-3.941041	C	-1.080585	3.164905	2.894965
H	-1.846	0.779528	-4.308593	H	-1.723106	2.603348	3.569343
H	-1.413762	-0.91887	-4.625131	H	-0.279398	3.641024	3.466776
H	-2.986659	-0.516899	-3.871491	H	-1.670766	3.925467	2.37696
O	-1.31291	-0.235329	-2.651861	O	-0.560463	2.200991	1.974842
F	-0.878068	-3.041366	2.405005	F	1.052289	0.256546	-2.512622
F	0.48824	-1.402705	2.039936	F	3.014842	0.234214	-1.575056
F	1.054689	-3.418502	1.501871	F	2.557912	1.689784	-3.106034
C	-0.378032	2.712952	-1.747129	C	2.138848	0.481931	2.585863
H	0.066145	1.851229	-2.241321	H	2.606808	1.355053	2.120839
H	-0.869681	3.329292	-2.502533	H	1.130926	0.771049	2.882328
H	0.429247	3.307875	-1.310865	H	2.708532	0.248371	3.486735
C	-4.535421	3.897655	0.779309	C	4.231385	-3.895025	1.329552
H	-4.578282	4.669903	0.009395	H	4.859146	-3.638207	2.184362
H	-5.501524	3.386119	0.806498	H	3.774027	-4.869847	1.524382
H	-4.407815	4.395871	1.746032	H	4.880138	-4.014194	0.456197
O	-2.130906	-0.306108	1.734109	O	0.356128	-2.168319	-1.174366
C	-3.1129	-0.652423	2.711336	C	0.451324	-3.265684	-2.07838
H	-3.149034	0.088311	3.515437	H	1.412889	-3.269252	-2.600477
H	-4.104414	-0.753957	2.260554	H	0.308317	-4.221136	-1.564874
H	-2.79492	-1.610717	3.113479	H	-0.351053	-3.120999	-2.799267

<i>M-C</i>				<i>M-C'</i>			
S	1.610025	-1.910654	0.50396	S	-1.575797	-2.021892	-0.510173
O	2.148577	1.690476	-0.881584	O	-2.179781	1.463638	1.132375
C	3.297186	-1.530894	0.112791	C	-3.286769	-1.615489	-0.28051
C	4.379209	-2.399248	0.244901	C	-4.367768	-2.424315	-0.626268
H	4.246674	-3.40767	0.617757	H	-4.21828	-3.397169	-1.078719
C	5.642937	-1.937957	-0.118315	C	-5.653041	-1.949816	-0.373336
H	6.494489	-2.601669	-0.020782	H	-6.50417	-2.56739	-0.63657
C	5.832835	-0.637595	-0.607079	C	-5.865602	-0.694452	0.214296
H	6.826097	-0.305739	-0.883712	H	-6.87588	-0.351313	0.400753
C	4.747365	0.219071	-0.735639	C	-4.781477	0.103186	0.555084
H	4.863539	1.228724	-1.112581	H	-4.915425	1.0774	1.011041
C	3.476264	-0.231087	-0.369716	C	-3.487474	-0.361016	0.303533
C	2.231209	0.553629	-0.444047	C	-2.241178	0.365442	0.600991
C	1.075867	-0.263054	0.068197	C	-1.054002	-0.45819	0.181074
C	-0.205239	0.152532	0.218231	C	0.247008	-0.096354	0.256654
C	-1.283422	-0.820953	0.590792	C	1.343038	-1.076138	-0.019858
C	-2.029759	-0.710255	1.782	C	1.534177	-2.236165	0.759452
C	-3.020941	-1.656521	2.069407	C	2.601434	-3.094842	0.459145
C	-3.312806	-2.709807	1.208556	C	3.483604	-2.847579	-0.585988
C	-2.582911	-2.820891	0.022787	C	3.300352	-1.694577	-1.357061
H	-2.801753	-3.632381	-0.658238	H	3.978889	-1.491546	-2.174597
C	-1.584495	-1.899338	-0.286976	C	2.253663	-0.82021	-1.079387
H	-3.570573	-1.564289	3.000162	H	2.744706	-3.975694	1.076607
C	-0.552508	1.613478	0.106494	C	0.660347	1.29916	0.634726
C	-0.007498	2.514084	1.058675	C	1.309774	1.46889	1.882086
C	-1.420625	2.152338	-0.862841	C	0.500362	2.437488	-0.169683
C	-0.379107	3.85929	1.072477	C	1.803564	2.711109	2.281831
C	-1.776689	3.504367	-0.852203	C	0.992448	3.683349	0.237563
C	-1.267318	4.347743	0.122476	C	1.645054	3.815591	1.452
H	0.025802	4.5295	1.817158	H	2.300765	2.823544	3.234812
H	-2.436923	3.8915	-1.61411	H	0.863911	4.544512	-0.404972
H	-1.549028	5.393603	0.137053	H	2.028584	4.780286	1.761281
C	-1.949552	1.32298	-2.009827	C	-0.207945	2.483244	-1.504981
C	1.493057	2.852472	2.90653	C	2.085939	0.417554	3.899683
H	2.167523	2.216279	3.475405	H	2.040774	-0.588601	4.310479
H	2.065787	3.641906	2.412464	H	3.130612	0.705686	3.753065
H	0.755064	3.295796	3.58096	H	1.602993	1.114361	4.590487
O	0.87318	1.990582	1.948999	O	1.387425	0.355026	2.654693
F	-0.967772	0.652497	-2.651251	F	-1.277926	3.32271	-1.443296
F	-2.558112	2.085544	-2.950193	F	-0.672043	1.321992	-1.987209
F	-2.873899	0.408268	-1.628234	F	0.604571	3.001356	-2.468379
C	-1.79072	0.384241	2.794938	C	0.660701	-2.606523	1.936202
H	-2.222944	1.333514	2.464245	H	0.119893	-1.752756	2.335566
H	-2.258881	0.123959	3.745355	H	-0.07033	-3.368717	1.650613
H	-0.728643	0.556001	2.968155	H	1.275901	-3.028611	2.734234
C	-4.387468	-3.716981	1.5363	C	4.61897	-3.791968	-0.895984
H	-4.852434	-3.502104	2.499751	H	4.668731	-4.60504	-0.17
H	-5.17202	-3.716603	0.773432	H	4.500665	-4.233664	-1.890409
H	-3.978113	-4.730969	1.575154	H	5.579968	-3.269234	-0.889254
O	-0.868256	-1.957698	-1.437887	O	2.017583	0.304451	-1.806876
C	-1.200897	-2.93486	-2.420823	C	2.89643	0.635978	-2.882556
H	-1.040509	-3.950889	-2.047942	H	3.920712	0.783191	-2.527903
H	-2.237215	-2.824414	-2.753656	H	2.882882	-0.136531	-3.656909
H	-0.53014	-2.747941	-3.257033	H	2.513976	1.567953	-3.290666

<i>P-C</i>				<i>P-C'</i>			
S	-1.575796	2.02189	-0.510173	S	1.610023	-1.91066	-0.50396
O	-2.179784	-1.463643	1.132368	O	2.148581	1.69047	0.881578
C	-3.286768	1.615488	-0.280513	C	3.297185	-1.530903	-0.11279
C	-4.367766	2.424315	-0.626271	C	4.379206	-2.39926	-0.244899
H	-4.218278	3.39717	-1.07872	H	4.246668	-3.407682	-0.617751
C	-5.65304	1.949817	-0.37334	C	5.642935	-1.937971	0.118317
H	-6.504169	2.567392	-0.636573	H	6.494485	-2.601686	0.020786
C	-5.865602	0.694452	0.214291	C	5.832835	-0.637609	0.607079
H	-6.875881	0.351314	0.400747	H	6.826098	-0.305754	0.883712
C	-4.781478	-0.103187	0.555077	C	4.747367	0.21906	0.735637
H	-4.915427	-1.077403	1.011033	H	4.863544	1.228713	1.112577
C	-3.487474	0.361014	0.303528	C	3.476266	-0.231095	0.369714
C	-2.241179	-0.365446	0.600985	C	2.231212	0.553623	0.444044
C	-1.054002	0.458186	0.181072	C	1.075868	-0.263061	-0.068198
C	0.247008	0.096352	0.256654	C	-0.205237	0.152529	-0.218233
C	1.343037	1.076138	-0.019854	C	-1.283423	-0.820951	-0.590795
C	1.534174	2.236163	0.759458	C	-2.02976	-0.710248	-1.782003
C	2.60143	3.094844	0.459151	C	-3.020947	-1.656507	-2.069411
C	3.483598	2.847584	-0.585984	C	-3.312817	-2.709794	-1.208562
C	3.300345	1.694585	-1.357062	C	-2.582921	-2.820885	-0.022794
H	3.97888	1.49156	-2.1746	H	-2.801763	-3.632377	0.658227
C	2.253659	0.820215	-1.079388	C	-1.584501	-1.899336	0.28697
H	2.7447	3.975695	1.076614	H	-3.57058	-1.564271	-3.000165
C	0.660347	-1.299162	0.634727	C	-0.552503	1.613476	-0.106495
C	1.309768	-1.468891	1.882091	C	-0.007493	2.514082	-1.058675
C	0.500367	-2.437491	-0.16968	C	-1.420618	2.152335	0.862841
C	1.803556	-2.71111	2.28184	C	-0.379103	3.859287	-1.072478
C	0.992452	-3.683351	0.237569	C	-1.776685	3.504363	0.852203
C	1.64505	-3.815592	1.452009	C	-1.267316	4.34774	-0.122477
H	2.300752	-2.823543	3.234824	H	0.025804	4.529497	-1.817161
H	0.863917	-4.544515	-0.404966	H	-2.436918	3.891496	1.61411
H	2.028579	-4.780287	1.761294	H	-1.549026	5.3936	-0.137055
C	-0.207926	-2.483249	-1.504986	C	-1.949543	1.322978	2.009829
C	2.085913	-0.417555	3.899696	C	1.493082	2.852478	-2.906511
H	2.04074	0.588599	4.310494	H	2.16756	2.216289	-3.475377
H	1.602959	-1.114365	4.590492	H	0.755102	3.295807	-3.580952
H	3.130588	-0.705685	3.753091	H	2.065802	3.641909	-2.412429
O	1.387415	-0.355026	2.654697	O	0.873187	1.990581	-1.948998
F	-0.672041	-1.322	-1.987208	F	-0.967761	0.652491	2.651247
F	-1.277896	-3.322733	-1.443316	F	-2.873895	0.40827	1.628241
F	0.604605	-3.001339	-2.46838	F	-2.558093	2.085545	2.950198
C	0.660701	2.606518	1.936211	C	-1.790716	0.384249	-2.79494
H	0.119871	1.752758	2.335557	H	-2.222941	1.333522	-2.464248
H	1.275908	3.028579	2.734253	H	-0.728639	0.556007	-2.968155
H	-0.07031	3.368735	1.650631	H	-2.258876	0.123968	-3.745358
C	4.618973	3.791966	-0.895969	C	-4.387488	-3.716959	-1.536306
H	4.668642	4.605117	-0.170066	H	-4.852418	-3.502107	-2.49978
H	5.579983	3.269253	-0.889081	H	-3.978152	-4.730957	-1.575109
H	4.500764	4.23355	-1.890454	H	-5.172066	-3.716536	-0.773464
O	2.01758	-0.304444	-1.806879	O	-0.868261	-1.957704	1.437881
C	2.896411	-0.635951	-2.882577	C	-1.200941	-2.934832	2.420836
H	2.882853	0.136572	-3.656915	H	-2.237265	-2.82436	2.753643
H	3.920698	-0.783172	-2.527941	H	-1.040561	-3.950875	2.047989
H	2.513951	-1.567919	-3.2907	H	-0.5302	-2.747901	3.257057

<i>M-D</i>				<i>M-D'</i>			
S	-1.791115	1.946003	0.260081	S	-1.252801	-2.022026	-0.709468
O	-2.165457	-1.788339	-0.790945	O	-2.176655	1.192362	1.291507
C	-3.471476	1.416144	0.055915	C	-2.967063	-1.909692	-0.272467
C	-4.601848	2.214676	0.220032	C	-3.948219	-2.852955	-0.572788
H	-4.515968	3.25819	0.497873	H	-3.70911	-3.75536	-1.122388
C	-5.852666	1.635957	0.015311	C	-5.251393	-2.607792	-0.144944
H	-6.741492	2.243947	0.139605	H	-6.025364	-3.332443	-0.370806
C	-5.982644	0.28812	-0.34896	C	-5.579166	-1.447084	0.570342
H	-6.967534	-0.135314	-0.503573	H	-6.600359	-1.28284	0.891866
C	-4.849495	-0.497852	-0.511292	C	-4.594096	-0.51353	0.86387
H	-4.919286	-1.541771	-0.794758	H	-4.817415	0.392676	1.415093
C	-3.589822	0.070382	-0.303582	C	-3.284343	-0.747288	0.436771
C	-2.299065	-0.627936	-0.435093	C	-2.135286	0.146317	0.66175
C	-1.170569	0.309503	-0.105636	C	-0.898369	-0.437621	0.035616
C	0.147332	-0.003962	-0.043339	C	0.337252	0.115757	0.00465
C	1.178936	1.066216	0.112172	C	1.522943	-0.686926	-0.442028
C	1.338565	2.113757	-0.819923	C	2.314112	-0.324244	-1.550884
C	2.34215	3.071411	-0.612563	C	3.416534	-1.112516	-1.903489
C	3.194268	3.032319	0.483143	C	3.772994	-2.250118	-1.186303
C	3.04167	1.994974	1.410407	C	2.99732	-2.610415	-0.081875
H	3.692669	1.956777	2.273383	H	3.269498	-3.487894	0.489037
C	2.05617	1.030167	1.232411	C	1.889787	-1.849895	0.291274
H	2.459583	3.861272	-1.347454	H	4.003628	-0.825491	-2.769296
C	0.586474	-1.443924	-0.005204	C	0.583701	1.532575	0.442221
C	0.181237	-2.237299	1.101076	C	1.437591	1.72652	1.560207
C	1.424391	-2.048164	-0.95822	C	0.075054	2.68681	-0.181151
C	0.64977	-3.542387	1.255059	C	1.778056	3.005049	2.004823
C	1.877757	-3.363562	-0.805826	C	0.415953	3.966145	0.274271
C	1.499102	-4.09891	0.304812	C	1.264516	4.122267	1.357424
H	0.351774	-4.131385	2.110812	H	2.431269	3.132478	2.856311
H	2.511935	-3.804251	-1.560992	H	0.018652	4.836233	-0.231473
H	1.853732	-5.114816	0.430451	H	1.528116	5.114316	1.703322
C	1.842758	-1.3328	-2.21844	C	-0.86592	2.720545	-1.366187
C	-1.100887	-2.395077	3.123957	C	2.764935	0.690667	3.273341
H	-1.760707	-1.724778	3.670666	H	2.974866	-0.335732	3.565629
H	-1.655148	-3.291096	2.829908	H	3.696266	1.186541	2.985323
H	-0.257863	-2.6752	3.7621	H	2.307359	1.221488	4.11302
O	-0.666395	-1.655733	1.982559	O	1.86428	0.595613	2.169155
F	0.801881	-0.72097	-2.833876	F	-2.058123	3.27032	-1.025501
F	2.372284	-2.176508	-3.13438	F	-1.145912	1.537663	-1.945236
F	2.784466	-0.381231	-2.005753	F	-0.362369	3.50838	-2.354831
C	0.52364	2.261042	-2.085913	C	2.002129	0.873689	-2.417758
H	-0.132696	1.417892	-2.274655	H	2.124447	1.813806	-1.874892
H	-0.089717	3.165195	-2.039472	H	2.673694	0.899037	-3.276769
H	1.195137	2.366847	-2.942019	H	0.978536	0.842525	-2.793215
C	4.263225	4.077319	0.686432	C	4.960453	-3.090677	-1.58704
H	4.284128	4.790139	-0.139384	H	5.518148	-2.62687	-2.402246
H	4.094028	4.636129	1.612139	H	5.643698	-3.235921	-0.745294
H	5.252928	3.617701	0.765461	H	4.643112	-4.084535	-1.918442
O	1.842703	0.022793	2.118381	O	1.124009	-2.158097	1.368671
C	2.699599	-0.104467	3.252016	C	1.418249	-3.332687	2.121483
H	3.740984	-0.249885	2.950275	H	1.348167	-4.232461	1.502835
H	2.625028	0.76915	3.906321	H	2.411427	-3.277487	2.577294
H	2.350403	-0.986064	3.785629	H	0.664381	-3.373365	2.90526

<i>P-D</i>				<i>P-D'</i>			
S	1.252804	-2.022022	-0.709476	S	-1.791119	-1.946002	0.260084
O	2.176654	1.192362	1.291507	O	-2.165456	1.78833	-0.79098
C	2.967065	-1.90969	-0.27247	C	-3.471479	-1.416144	0.055911
C	3.948221	-2.852952	-0.572792	C	-4.601852	-2.214671	0.220038
H	3.709113	-3.755355	-1.122395	H	-4.515973	-3.258182	0.49789
C	5.251395	-2.607791	-0.144943	C	-5.852669	-1.635953	0.015311
H	6.025365	-3.332442	-0.370805	H	-6.741497	-2.24394	0.139612
C	5.579166	-1.447086	0.570348	C	-5.982645	-0.288119	-0.348975
H	6.600358	-1.282843	0.891875	H	-6.967536	0.135314	-0.503593
C	4.594095	-0.513532	0.863875	C	-4.849496	0.497849	-0.511316
H	4.817414	0.392673	1.415101	H	-4.919285	1.541764	-0.794794
C	3.284343	-0.747288	0.436771	C	-3.589823	-0.070384	-0.3036
C	2.135287	0.146317	0.661749	C	-2.299065	0.627931	-0.435114
C	0.898371	-0.437621	0.035611	C	-1.170572	-0.309504	-0.105644
C	-0.337251	0.115757	0.004649	C	0.147329	0.003961	-0.043342
C	-1.522942	-0.686926	-0.442029	C	1.178932	-1.066215	0.112178
C	-2.314111	-0.324244	-1.550886	C	1.338563	-2.113761	-0.819911
C	-3.416532	-1.112517	-1.903491	C	2.342149	-3.071413	-0.612544
C	-3.772993	-2.250118	-1.186305	C	3.194265	-3.032313	0.483163
C	-2.997317	-2.610417	-0.081878	C	3.041664	-1.994964	1.410422
H	-3.269492	-3.487898	0.489031	H	3.692661	-1.956762	2.273399
C	-1.889786	-1.849896	0.291272	C	2.056162	-1.03016	1.232419
H	-4.003625	-0.825494	-2.7693	H	2.459583	-3.861278	-1.34743
C	-0.583702	1.532574	0.442222	C	0.586472	1.443923	-0.005208
C	-1.437591	1.726516	1.560208	C	0.181223	2.237304	1.101063
C	-0.075054	2.686811	-0.181147	C	1.424406	2.048155	-0.958214
C	-1.778059	3.005044	2.004826	C	0.649759	3.542391	1.255046
C	-0.415955	3.966144	0.274278	C	1.877774	3.363552	-0.805821
C	-1.264519	4.122263	1.35743	C	1.499106	4.098906	0.304808
H	-2.431272	3.132471	2.856314	H	0.351757	4.131394	2.110793
H	-0.018653	4.836234	-0.231462	H	2.511965	3.804235	-1.56098
H	-1.52812	5.114311	1.70333	H	1.853737	5.114812	0.430447
C	0.865919	2.72055	-1.366183	C	1.842791	1.332783	-2.218424
C	-2.764943	0.690657	3.273334	C	-1.100957	2.395111	3.123906
H	-2.97488	-0.335744	3.565613	H	-1.760806	1.724827	3.670596
H	-2.307375	1.221471	4.113021	H	-0.257959	2.675239	3.762083
H	-3.69627	1.186534	2.985309	H	-1.655196	3.291129	2.829814
O	-1.864277	0.595607	2.169156	O	-0.666417	1.655744	1.982541
F	1.145917	1.537669	-1.945231	F	0.80193	0.720931	-2.833862
F	2.05812	3.270331	-1.025498	F	2.784513	0.38123	-2.005718
F	0.362364	3.508381	-2.354827	F	2.372315	2.176489	-3.134367
C	-2.002127	0.873689	-2.417759	C	0.523641	-2.261054	-2.085903
H	-2.12446	1.813806	-1.874896	H	-0.132706	-1.417912	-2.274643
H	-0.97853	0.842533	-2.793204	H	1.195142	-2.366846	-2.942008
H	-2.673683	0.899029	-3.276778	H	-0.089701	-3.165216	-2.039465
C	-4.960463	-3.090668	-1.587029	C	4.263225	-4.077309	0.686457
H	-5.518043	-2.626959	-2.402369	H	4.284117	-4.790146	-0.139345
H	-4.643154	-4.084603	-1.918229	H	5.252929	-3.617689	0.765462
H	-5.643806	-3.235724	-0.74533	H	4.094042	-4.636101	1.612178
O	-1.124006	-2.158099	1.368667	O	1.842689	-0.022783	2.118384
C	-1.418243	-3.332694	2.121473	C	2.699582	0.104487	3.25202
H	-2.411423	-3.277499	2.577283	H	2.625014	-0.769128	3.90633
H	-1.348158	-4.232465	1.502822	H	3.740966	0.249911	2.950282
H	-0.664377	-3.373373	2.905251	H	2.35038	0.986085	3.785629

TS1				TS2			
S	-2.576824	0.788658	-0.403234	S	-2.624626	1.430337	0.232785
O	-0.826564	-2.628321	0.200921	O	-1.435345	-2.229475	-0.369742
C	-3.674002	-0.543044	-0.046552	C	-3.92039	0.249617	0.032343
C	-5.064193	-0.459908	0.01611	C	-5.286712	0.529635	0.062018
H	-5.579597	0.479857	-0.141346	H	-5.650454	1.538147	0.219282
C	-5.775562	-1.625295	0.292775	C	-6.176301	-0.527017	-0.115927
H	-6.857252	-1.582922	0.350022	H	-7.242268	-0.330522	-0.094254
C	-5.119181	-2.84769	0.4983	C	-5.718695	-1.837403	-0.321679
H	-5.696661	-3.738677	0.712928	H	-6.432149	-2.641019	-0.458473
C	-3.733514	-2.913184	0.42687	C	-4.355405	-2.100075	-0.349698
H	-3.199887	-3.844015	0.579568	H	-3.972645	-3.101385	-0.509047
C	-3.013174	-1.748426	0.150121	C	-3.45812	-1.043554	-0.169147
C	-1.54574	-1.65798	0.036488	C	-1.989981	-1.160198	-0.178688
C	-1.108552	-0.217093	-0.260686	C	-1.319347	0.20032	0.058117
C	0.211268	0.185687	-0.324024	C	0.053772	0.374858	0.054412
C	1.175541	-0.982827	-0.300541	C	0.834039	-0.888691	-0.227339
C	1.757795	-1.363738	0.920679	C	1.078199	-1.817459	0.802863
C	2.643524	-2.439203	0.982956	C	1.777047	-2.992834	0.548984
C	2.949757	-3.167157	-0.171189	C	2.202174	-3.295429	-0.750025
C	2.357946	-2.790382	-1.376029	C	1.905415	-2.404435	-1.776153
H	2.595064	-3.342683	-2.279966	H	2.208651	-2.639919	-2.791205
C	1.471809	-1.711781	-1.455966	C	1.224312	-1.204202	-1.535394
H	3.092643	-2.726687	1.92487	H	1.982887	-3.692502	1.348505
C	1.924072	-0.969266	3.287228	C	0.85072	-2.340399	3.133896
O	1.379519	-0.632817	2.013491	O	0.570747	-1.490561	2.024771
H	1.656076	-1.989386	3.579291	H	0.428111	-3.339698	2.990158
H	3.013243	-0.861157	3.299205	H	1.927648	-2.421137	3.311482
H	1.48472	-0.265232	3.991576	H	0.377103	-1.870113	3.993828
C	0.871311	1.52835	-0.19363	C	0.884002	1.620228	0.034077
C	2.314457	1.551593	-0.241147	C	0.339017	2.943258	-0.040512
C	0.333917	2.79233	0.256103	C	2.318273	1.609547	-0.129775
C	3.067912	2.405059	0.57453	C	0.988594	3.97642	-0.724452
C	1.098984	3.660645	1.030994	C	2.976888	2.663284	-0.759257
C	2.443737	3.413953	1.283313	C	2.292584	3.807285	-1.152516
H	4.141487	2.294141	0.622521	H	0.483442	4.917328	-0.886782
H	0.654536	4.583285	1.378439	H	4.047805	2.612645	-0.89381
H	3.013797	4.069558	1.929357	H	2.800614	4.596174	-1.692632
C	0.870044	-1.33473	-2.787503	C	0.883391	-0.305838	-2.701457
H	1.297722	-1.937897	-3.590275	H	1.227247	-0.747547	-3.637922
H	-0.214042	-1.482741	-2.798336	H	-0.196621	-0.148723	-2.779327
H	1.052984	-0.281234	-3.017197	H	1.343599	0.681493	-2.607998
C	-0.921286	3.459172	-0.260353	C	3.283954	0.635786	0.532789
F	-0.68716	4.774669	-0.515371	F	4.411171	1.302281	0.919331
F	-1.972794	3.456832	0.591778	F	3.733742	-0.36975	-0.2456
F	-1.322394	2.939971	-1.442164	F	2.790464	0.105838	1.667575
C	3.895044	-4.343214	-0.097875	C	2.976283	-4.564181	-1.01703
H	4.134873	-4.721448	-1.093365	H	3.006919	-4.793553	-2.083943
H	4.832051	-4.071208	0.396904	H	4.010459	-4.472433	-0.667681
H	3.45683	-5.16679	0.475473	H	2.53536	-5.418203	-0.49572
C	4.319477	0.504903	-1.075741	C	-1.469125	4.429012	0.542809
H	4.875677	1.415794	-1.310679	H	-0.827647	5.213518	0.948396
H	4.615196	0.123725	-0.095718	H	-1.75565	4.664368	-0.48463
H	4.514257	-0.248777	-1.834499	H	-2.360018	4.328212	1.157659
O	2.906827	0.737647	-1.130237	O	-0.812189	3.156153	0.619751

TS3				TS4			
S	2.171838	0.60136	0.952262	S	-2.237501	-0.797075	0.633812
O	1.243028	-2.900367	1.281799	O	-1.867204	2.838475	1.131047
C	3.424175	-0.481839	0.306932	C	-3.641452	0.110728	0.043163
C	4.748613	-0.152476	0.032263	C	-4.89164	-0.411727	-0.280958
H	5.123598	0.850919	0.194058	H	-5.095468	-1.472787	-0.201684
C	5.581872	-1.154383	-0.465904	C	-5.877499	0.472962	-0.715843
H	6.612649	-0.915695	-0.701827	H	-6.853058	0.085214	-0.986135
C	5.111886	-2.458373	-0.664674	C	-5.632334	1.849766	-0.806769
H	5.779787	-3.217733	-1.053065	H	-6.417081	2.514597	-1.146699
C	3.79338	-2.781483	-0.354099	C	-4.388735	2.362112	-0.451716
H	3.4206	-3.792257	-0.473586	H	-4.187095	3.426371	-0.488507
C	2.948466	-1.775994	0.110872	C	-3.388917	1.477216	-0.048557
C	1.564869	-1.927847	0.635938	C	-2.053814	1.823985	0.487042
C	0.833044	-0.586309	0.512496	C	-1.111257	0.636107	0.375834
C	-0.378192	-0.053958	0.145592	C	0.221849	0.359215	0.182365
C	-1.660722	-0.646969	-0.375268	C	1.426013	1.153878	-0.264837
C	-1.986321	-2.027027	-0.201634	C	2.56367	0.431524	-0.783729
C	-3.241992	-2.559494	-0.498617	C	3.803583	1.03168	-1.003076
C	-4.241235	-1.765834	-1.044469	C	3.992985	2.39277	-0.807116
C	-3.920511	-0.4417	-1.318516	C	2.878813	3.134396	-0.439912
H	-4.664172	0.181117	-1.802241	H	2.97589	4.209742	-0.344164
C	-2.679855	0.132822	-1.018111	C	1.622998	2.568536	-0.194128
H	-3.437615	-3.605346	-0.310864	H	4.627365	0.432985	-1.363066
C	-1.24208	-4.194912	0.514849	C	3.525916	-1.682387	-1.454202
O	-1.004965	-2.808476	0.273878	O	2.3991	-0.87226	-1.11371
H	-2.016096	-4.33657	1.274694	H	3.970624	-1.364237	-2.401174
H	-1.529575	-4.711991	-0.405026	H	4.281225	-1.663096	-0.664379
H	-0.297155	-4.583908	0.880627	H	3.132094	-2.689167	-1.562714
C	-0.459351	1.434545	0.455637	C	0.531667	-1.068272	0.636417
C	-1.104295	1.76735	1.671899	C	0.997401	-1.184314	1.966508
C	0.09126	2.484807	-0.29598	C	0.318794	-2.252443	-0.084845
C	-1.203535	3.094883	2.095694	C	1.238715	-2.437001	2.538109
C	-0.005099	3.811319	0.134459	C	0.549296	-3.503004	0.492864
C	-0.651303	4.111068	1.32369	C	1.007891	-3.59142	1.799179
H	-1.703209	3.339263	3.022437	H	1.598522	-2.515489	3.554294
H	0.418799	4.603297	-0.469063	H	0.377801	-4.401388	-0.08612
H	-0.728569	5.13926	1.655519	H	1.190439	-4.560863	2.246722
C	-2.561235	1.563321	-1.511221	C	0.555855	3.576617	0.112108
H	-2.533259	2.301582	-0.710328	H	-0.256054	3.526661	-0.615188
H	-1.685408	1.709226	-2.137819	H	0.111904	3.43284	1.092243
H	-3.430528	1.790983	-2.128708	H	0.97596	4.581406	0.065081
C	0.797871	2.313724	-1.62205	C	-0.124542	-2.298405	-1.529359
F	0.78759	1.060936	-2.113141	F	-0.329491	-1.103699	-2.106167
F	2.091913	2.708122	-1.56459	F	-1.276637	-3.006069	-1.672342
F	0.223635	3.0996	-2.57659	F	0.787415	-2.950881	-2.301683
C	-5.611356	-2.323046	-1.331837	C	5.342215	3.031816	-1.006227
H	-6.225543	-2.323417	-0.424701	H	5.250249	4.102089	-1.20029
H	-6.133655	-1.727082	-2.082624	H	5.961344	2.910389	-0.110629
H	-5.556042	-3.355226	-1.685713	H	5.88238	2.573421	-1.837927
O	-1.600182	0.719442	2.377197	O	1.182344	-0.01212	2.63017
C	-2.26355	0.968672	3.6191	C	1.641727	-0.046057	3.983057
H	-3.149553	1.593646	3.476559	H	2.630335	-0.508485	4.055044
H	-2.564904	-0.008971	3.988566	H	1.705142	0.994105	4.295117
H	-1.58967	1.439206	4.340536	H	0.93682	-0.577716	4.628612

TS5				TS6			
S	-1.569631	2.157278	-0.209798	S	-2.036437	2.08921	0.479444
O	-1.987051	-1.513358	1.015297	O	-2.064881	-1.747555	-0.161568
C	-3.226917	1.680647	0.156551	C	-3.630623	1.403405	0.189383
C	-4.34803	2.50953	0.08497	C	-4.833239	2.110491	0.17485
H	-4.261627	3.545963	-0.219744	H	-4.859541	3.179703	0.347317
C	-5.587135	1.968166	0.415774	C	-6.004949	1.39931	-0.069048
H	-6.469855	2.595444	0.362738	H	-6.950884	1.928642	-0.085108
C	-5.71401	0.628682	0.816206	C	-5.983356	0.01406	-0.293681
H	-6.690281	0.233087	1.06922	H	-6.910122	-0.51459	-0.481076
C	-4.590047	-0.182839	0.888259	C	-4.777605	-0.673728	-0.275743
H	-4.656003	-1.218825	1.199657	H	-4.729986	-1.742847	-0.446463
C	-3.343968	0.353418	0.549373	C	-3.59656	0.033343	-0.031228
C	-2.064501	-0.370953	0.588024	C	-2.246583	-0.55288	0.014253
C	-0.911989	0.501492	0.08576	C	-1.18583	0.511464	0.304274
C	0.380987	0.026708	-0.057471	C	0.168066	0.245403	0.39416
C	1.701839	0.705021	-0.245237	C	1.388442	1.107686	0.581703
C	1.846754	2.128353	-0.344998	C	2.680849	0.458211	0.649899
C	3.032704	2.793977	-0.046143	C	3.867333	1.098455	0.291148
C	4.19621	2.080385	0.219946	C	3.885531	2.454339	-0.000472
C	4.139344	0.699702	0.060684	C	2.69965	3.153556	0.208204
H	5.06179	0.13307	0.118975	H	2.717894	4.236326	0.148144
C	2.959114	0.000013	-0.20762	C	1.489524	2.542941	0.539186
H	3.06162	3.874021	-0.060115	H	4.792111	0.540013	0.278107
C	0.806745	4.239147	-0.893278	C	3.922499	-1.577609	1.049773
O	0.777805	2.81165	-0.806775	O	2.724163	-0.802997	1.127208
H	0.966615	4.693884	0.087476	H	4.279631	-1.653666	0.019632
H	1.579735	4.567563	-1.591322	H	4.70613	-1.157837	1.686123
H	-0.172342	4.523868	-1.271926	H	3.647712	-2.564917	1.414515
C	0.475605	-1.462575	0.192547	C	0.465286	-1.217645	0.092885
C	0.820208	-1.90697	1.485283	C	0.399703	-2.150271	1.150826
C	0.196275	-2.421145	-0.78695	C	0.760395	-1.68815	-1.188584
C	0.905256	-3.269128	1.770182	C	0.656646	-3.498264	0.931743
C	0.276185	-3.787136	-0.502303	C	1.011016	-3.050908	-1.412492
C	0.633825	-4.201747	0.772474	C	0.963267	-3.942409	-0.355241
H	1.174515	-3.610008	2.760175	H	0.618679	-4.207729	1.746779
H	0.06839	-4.513799	-1.274793	H	1.238171	-3.399398	-2.409634
H	0.702113	-5.259468	0.9971	H	1.161326	-4.994155	-0.525185
C	3.205049	-1.46069	-0.556705	C	0.428025	3.545752	0.941617
H	3.002608	-2.15855	0.25472	H	-0.204087	3.862467	0.112503
H	2.620897	-1.772509	-1.41843	H	-0.201403	3.179916	1.748697
H	4.258296	-1.569042	-0.820304	H	0.931983	4.438315	1.315299
C	-0.228341	-2.014387	-2.174759	C	0.73951	-0.778482	-2.390671
F	0.5462	-1.031486	-2.699534	F	1.534226	0.311627	-2.266793
F	-1.505347	-1.555254	-2.221215	F	-0.506243	-0.306021	-2.662639
F	-0.171126	-3.044795	-3.04887	F	1.148975	-1.409755	-3.516603
C	5.472399	2.781169	0.60151	C	5.142655	3.147595	-0.451182
H	5.490849	2.980539	1.67871	H	5.196094	3.164697	-1.54546
H	6.346942	2.172434	0.364704	H	5.170655	4.183944	-0.108038
H	5.568783	3.742869	0.09245	H	6.03584	2.635204	-0.088109
O	1.043575	-0.927342	2.399205	C	0.006423	-2.495603	3.491078
C	1.388125	-1.295781	3.736225	H	-0.259777	-1.86165	4.33441
H	2.325888	-1.858104	3.764634	H	-0.763676	-3.260556	3.354006
H	1.511547	-0.358802	4.27504	H	0.970219	-2.975153	3.686304
H	0.591341	-1.882224	4.202721	O	0.079089	-1.625338	2.361936

TS7				TS8			
TS7				TS8			
S	-1.501893	-1.823295	0.496143	S	1.882929	-1.309213	-0.909554
O	-2.530518	1.756427	0.88429	O	2.751964	2.262541	-0.936335
C	-3.211817	-1.554574	0.112252	C	3.477646	-0.991315	-0.199961
C	-4.185424	-2.535657	-0.06235	C	4.482126	-1.925108	0.042915
H	-3.943314	-3.588612	0.017688	H	4.345802	-2.972735	-0.197438
C	-5.486984	-2.12417	-0.347136	C	5.672955	-1.473649	0.611942
H	-6.256419	-2.872912	-0.497319	H	6.46146	-2.186999	0.823037
C	-5.818119	-0.76577	-0.439661	C	5.867584	-0.119775	0.912952
H	-6.837363	-0.47406	-0.661964	H	6.801385	0.204504	1.356089
C	-4.84154	0.204174	-0.238583	C	4.868174	0.808124	0.633136
H	-5.078285	1.260993	-0.282559	H	5.01164	1.864248	0.830349
C	-3.532477	-0.202592	0.018879	C	3.664038	0.356814	0.095897
C	-2.390666	0.670874	0.363234	C	2.543743	1.18913	-0.414722
C	-1.076775	-0.070759	0.210997	C	1.259522	0.34953	-0.438565
C	0.247599	0.229535	0.010293	C	-0.091102	0.446406	-0.19061
C	1.131018	-0.969921	0.349266	C	-0.833069	-0.842308	-0.499741
C	1.295866	-2.066212	-0.530252	C	-0.758996	-1.966342	0.35811
C	2.050813	-3.172127	-0.147339	C	-1.415759	-3.150236	0.029984
C	2.66168	-3.219962	1.111727	C	-2.141799	-3.257649	-1.160133
C	2.491544	-2.14372	1.975611	C	-2.181751	-2.163702	-2.019632
H	2.94832	-2.171418	2.95943	H	-2.719461	-2.242624	-2.958774
C	1.731922	-1.020304	1.616177	C	-1.538418	-0.959438	-1.710002
H	2.176377	-4.006098	-0.825403	H	-1.362732	-4.003378	0.693188
C	0.661044	-3.104218	-2.598436	C	0.073861	-2.899837	2.405319
O	0.679446	-1.96778	-1.73787	O	-0.003018	-1.821794	1.477183
H	1.667441	-3.372092	-2.934543	H	-0.913715	-3.155324	2.80137
H	0.197967	-3.96675	-2.109307	H	0.528521	-3.786796	1.95337
H	0.062994	-2.811477	-3.459408	H	0.707058	-2.544713	3.216189
C	1.063671	1.471857	-0.299758	C	-1.003999	1.599609	0.135972
C	2.372497	1.217489	-0.850363	C	-0.658358	2.958918	-0.134735
C	0.87575	2.856393	0.032545	C	-2.370209	1.43509	0.556473
C	3.457815	2.075472	-0.648148	C	-1.625446	3.948616	-0.361627
C	1.963841	3.714906	0.204886	C	-3.31725	2.44141	0.371559
C	3.263386	3.306179	-0.051327	C	-2.962886	3.674191	-0.159228
H	4.443327	1.785865	-0.982216	H	-1.319157	4.934176	-0.679508
H	1.779126	4.737456	0.499539	H	-4.336667	2.271626	0.685355
H	4.097968	3.971842	0.129738	H	-3.714492	4.43201	-0.342099
C	1.572511	0.103719	2.615327	C	-1.607874	0.180266	-2.700295
H	0.530776	0.421609	2.704418	H	-2.271997	0.975889	-2.349542
H	1.918274	-0.21121	3.600914	H	-0.626871	0.631534	-2.867984
H	2.151431	0.985529	2.325072	H	-1.989636	-0.17213	-3.659579
C	-0.437899	3.605203	0.066341	C	-2.919486	0.27947	1.375907
F	-0.981254	3.717865	1.292702	F	-1.992363	-0.282126	2.170683
F	-1.32842	3.088798	-0.801207	F	-3.510259	-0.701126	0.655755
F	-0.266267	4.895191	-0.352188	F	-3.892767	0.718672	2.224272
C	3.480369	-4.424413	1.510072	C	-2.872278	-4.536839	-1.490293
H	2.880987	-5.339186	1.473765	H	-3.143786	-4.577933	-2.546757
H	4.326549	-4.568213	0.831028	H	-2.264325	-5.414891	-1.257382
H	3.87459	-4.318749	2.522183	H	-3.795636	-4.61929	-0.906939
O	2.499561	0.113221	-1.606381	O	0.644885	3.23922	-0.166917
C	3.789825	-0.324679	-2.040625	C	1.091343	4.556086	-0.504925
H	4.24209	0.401488	-2.720868	H	0.797297	4.82203	-1.523591
H	4.453795	-0.506975	-1.19198	H	0.699018	5.291294	0.202148

References

1. Lee, W.-H.; Zhu, J.; Hu, C.-M. Small molecule modifiers of the HEC1-NEK2 interaction in G2/M. *U.S. Patent No. 9,422,275*. 23 Aug. **2016**.
2. Moinet, G.; Leriche, C.; Kergoat, M. New 2-acyl-3-alkoxybenzo-furan or -thiophene derivatives, useful as hypoglycemics, particularly for treating diabetes and its complications, stimulate secretion of insulin. *Patent No. FR2862646* **2015**.
3. Jehle, B. G. Synthesis and Characterization of HTI Photoswitches with Eight States. *Bachelor thesis*, Ludwig-Maximilians-Universität, Munich, 2018.
4. Megerle, U.; Lechner, R.; König, B.; Riedle, E., Laboratory apparatus for the accurate, facile and rapid determination of visible light photoreaction quantum yields. *Photochem. Photobiol. Sci.* **2010**, *9* (10), 1400-1406.
5. Geertsema, E. M.; van der Molen, S. J.; Martens, M.; Feringa, B. L., Optimizing rotary processes in synthetic molecular motors. *Proc. Natl. Acad. Sci. U. S. A.* **2009**, *106* (40), 16919-16924.
6. Gerwien, A.; Schildhauer, M.; Thumser, S.; Mayer, P.; Dube, H., Direct evidence for hula twist and single-bond rotation photoproducts. *Nat. Commun.* **2018**, *9* (1), 2510.
7. Gerwien, A.; Mayer, P.; Dube, H., Photon-Only Molecular Motor with Reverse Temperature-Dependent Efficiency. *J. Am. Chem. Soc.* **2018**, *140* (48), 16442-16445.
8. Gerwien, A.; Mayer, P.; Dube, H., Green light powered molecular state motor enabling eight-shaped unidirectional rotation. *Nat. Commun.* **2019**, *10* (1), 4449.
9. Bruker (2012), SAINT. Bruker-AXS Inc., Madison, Wisconsin, USA.
10. Sheldrick, G. M. (1996), SADABS, University of Göttingen, Germany.
11. Sheldrick, G., Crystal structure refinement with SHELXL. *Acta Crystallogr., Sect. C: Cryst. Struct. Commun.* **2015**, *71* (1), 3-8.
12. Spek, A. L., PLATON SQUEEZE: a tool for the calculation of the disordered solvent contribution to the calculated structure factors. *Acta Cryst.* **2015**, *C71* (1), 9-18.
13. Farrugia, L. J., WinGX and ORTEP for Windows: an update. *J. Appl. Cryst.* **2012**, *45* (4), 849-854.
14. Frisch, M. J.; Trucks, G. W.; Schlegel, H. B.; Scuseria, G. E.; Robb, M. A.; Cheeseman, J. R.; Scalmani, G.; Barone, V.; Mennucci, B.; Petersson, G. A.; Nakatsuji, H.; Caricato, M.; Li, X.; Hratchian, H. P.; Izmaylov, A. F.; Bloino, J.; Zheng, G.; Sonnenberg, J. L.; Hada, M.; Ehara, M.; Toyota, K.; Fukuda, R.; Hasegawa, J.; Ishida, M.; Nakajima, T.; Honda, Y.; Kitao, O.; Nakai, H.; Vreven, T.; Montgomery, J., J. A.; Peralta, J. E.; Ogliaro, F.; Bearpark, M.; Heyd, J. J.; Brothers, E.; Kudin, K. N.; Staroverov, V. N.; Kobayashi, R.; Normand, J.; Raghavachari,

K.; Rendell, A.; Burant, J. C.; Iyengar, S. S.; Tomasi, J.; Cossi, M.; Rega, N.; Millam, J. M.; Klene, M.; Knox, J. E.; Cross, J. B.; Bakken, V.; Adamo, C.; Jaramillo, J.; Gomperts, R.; Stratmann, R. E.; Yazyev, O.; Austin, A. J.; Cammi, R.; Pomelli, C.; Ochterski, J. W.; Martin, R. L.; Morokuma, K.; Zakrzewski, V. G.; Voth, G. A.; Salvador, P.; Dannenberg, J. J.; Dapprich, S.; Daniels, A. D.; Farkas, Ö.; Foresman, J. B.; Ortiz, J. V.; Cioslowski, J.; Fox, D. J. *Gaussian 09, Revision A.02*, Gaussian, Inc.: Wallingford CT, 2009.